

BRAID VARIETY CLUSTER STRUCTURES, I: 3D PLABIC GRAPHS

PAVEL GALASHIN, THOMAS LAM, MELISSA SHERMAN-BENNETT, AND DAVID SPEYER

ABSTRACT. We introduce 3-dimensional generalizations of Postnikov's plabic graphs and use them to establish cluster structures for type A braid varieties. Our results include known cluster structures on open positroid varieties and double Bruhat cells, and establish new cluster structures for type A open Richardson varieties.

CONTENTS

1. Introduction	1
2. Open Richardson varieties	3
3. Double braid quivers	7
4. Invariance under moves	19
5. Cluster algebras associated to 3D plabic graphs	26
6. Double braid varieties	31
7. Deodhar geometry and seeds	41
8. Moves preserve the cluster algebra	46
9. Proof of Theorem 7.14	52
10. Applications	55
References	57

1. INTRODUCTION

Braid varieties $\mathring{R}_{u,\beta}$ are smooth, affine, complex algebraic varieties associated to a permutation u and a braid word β , that is, a word representing an element of the positive braid monoid. The purpose of this work is to construct a cluster algebra structure [FZ02] on the coordinate ring of a braid variety.

Theorem 1.1. *The coordinate ring $\mathbb{C}[\mathring{R}_{u,\beta}]$ of a braid variety is a cluster algebra.*

Date: October 11, 2022.

2020 Mathematics Subject Classification. Primary: 13F60. Secondary: 14M15, 05E99.

Key words and phrases. Plabic graph, cluster algebra, open Richardson variety, conjugate surface, local acyclicity, Deodhar hypersurface.

P.G. was supported by an Alfred P. Sloan Research Fellowship and by the National Science Foundation under Grants No. DMS-1954121 and No. DMS-2046915. T.L. was supported by Grant No. DMS-1953852 from the National Science Foundation. M.S.B. was supported by the National Science Foundation under Award No. DMS-2103282. D.E.S was supported by Grants No. DMS-1854225 and No. DMS-1855135. Any opinions, findings, and conclusions or recommendations expressed in this material are those of the authors and do not necessarily reflect the views of the National Science Foundation.

The braid varieties we consider were studied, rather recently, in [Mel19, CGGS20], generalizing varieties considered previously in [Deo85, MR04, WY07]. Theorem 1.1 resolves conjectures of [Lec16, CGGS21].

Certain special cases of braid varieties, namely open Richardson varieties and open positroid varieties, have played a key role in the combinatorial geometry of flag varieties and Grassmannians. *Open Richardson varieties* $\mathring{R}_{u,w}$ are subvarieties of the variety SL_n/B_+ of complete flags in \mathbb{C}^n , arising in the study of total positivity and Poisson geometry [Deo85, Lus98, MR04, Pos06, BGY06, KLS13]. An explicit cluster structure for open Richardson varieties was conjectured by Leclerc [Lec16]. Ménard [Mé22] gave an alternative conjectural cluster structure, which was proved by Cao and Keller [CK22] to be an upper cluster structure; Ménard’s and Leclerc’s cluster structures are expected to coincide. Another upper cluster structure was constructed by Ingermanson [Ing19]. The cluster structure of Theorem 1.1, in the case of open Richardson varieties, agrees with that of Ingermanson. It is related to the cluster structure of Leclerc [Lec16] by the twist automorphism [GL22b, SSB].

We also prove that the cluster varieties in Theorem 1.1 are locally acyclic [Mul13]; in the case of open Richardson varieties we use this to establish a variant of a conjecture of Lam and Speyer [LS16]. In particular, the cohomology of braid varieties satisfies the curious Lefschetz phenomenon (Theorem 10.1).

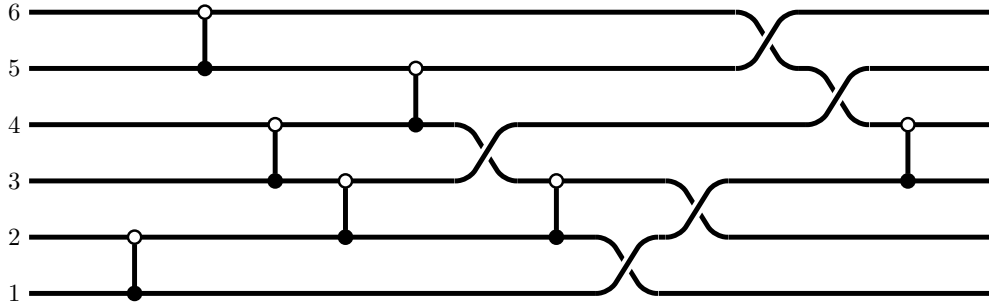
Theorem 1.1 generalizes the (type A) results of [FZ99, GY20] on double Bruhat cells and [SW21] on double Bott–Samelson cells, and also the results of Ingermanson [Ing19] and Cao and Keller [CK22], who found upper cluster structures on open Richardson varieties (see also [Mé22]). Furthermore, Theorem 1.1 generalizes the main result of [GL19] (see also [Sco06, MS16, SSBW19]), where the same statement was proved for *open positroid varieties* [KLS13], which are special cases of open Richardson varieties. Positroid varieties are parametrized by *plabic graphs* [Pos06], whose planar dual quivers describe the cluster algebra structure on the associated open positroid varieties.

Ever since the completion of [GL19], it has been our hope that constructing a cluster structure for open Richardson varieties would lead to a meaningful generalization of Postnikov’s plabic graphs; indeed, discovering such a generalization turned out to be a crucial step in our proof of Theorem 1.1. We associate a *3D plabic graph* to each pair (u, β) consisting of a permutation u and a (double) braid word β , and use the combinatorics of this graph to construct our cluster structure. The reader is invited to look forward at the examples in Figures 1–5.

An important geometric ingredient in our approach is the study of the Deodhar geometry of braid varieties, originally used by Deodhar [Deo85] in the flag variety setting. We define an open Deodhar torus $T_{u,\beta} \subset \mathring{R}_{u,\beta}$, and our cluster variables are interpreted as characters of $T_{u,\beta}$ that have certain orders of vanishing along the Deodhar hypersurfaces in the complement of the Deodhar torus. We expect this geometric approach to have applications to other settings where cluster structures are expected to make an appearance.

Our work has a number of applications. Our cluster structure implies, via [LS16], a curious Lefschetz phenomenon for the cohomology of braid varieties. Our approach is closely related to the combinatorics of *braid Richardson links* that are associated to a braid variety; in particular, we relate certain quiver point counts to the HOMFLY polynomial of these links.

We learned at the final stages of completing this manuscript that a cluster structure for braid varieties was independently announced in a recent preprint [CGG⁺22]. It would be interesting to investigate the relation between our 3D plabic graphs and the approach


 FIGURE 1. A 3D plabic graph $G_{u,w}$.

of [CGG⁺22]. The results of [CGG⁺22] apply more generally to braid varieties of arbitrary Lie type, while in the present paper we focus on varieties of type A . Our results and methods will be extended to include braid varieties of arbitrary type in a separate paper [GLSBS].

Overview. In Section 2, we give a synopsis of our main results in the setting of open Richardson varieties. In the rest of the paper we work in the setting of braid varieties. We define 3D plabic graphs and the associated quivers $\tilde{Q}_{u,\beta}$ in Section 3. Next, we develop the combinatorics of 3D plabic graphs and show that the quivers $\tilde{Q}_{u,\beta}$ are invariant under braid moves on the word β , naturally extending *square moves* from Postnikov’s plabic graphs to 3D plabic graphs; see Section 4. We discuss cluster algebras associated to 3D plabic graphs in Section 5 and show that they are *locally acyclic* in the sense of [Mul13]. In Sections 6 and 7, we study the Deodhar geometry of $\mathring{R}_{u,\beta}$ and construct a seed in $\mathbb{C}(\mathring{R}_{u,\beta})$ for each 3D plabic graph. We then show that the seeds are related by mutation in Section 8. Finally, in Section 9, we prove Theorem 7.14 by induction on the length of β . We conclude with some applications of our approach in Section 10.

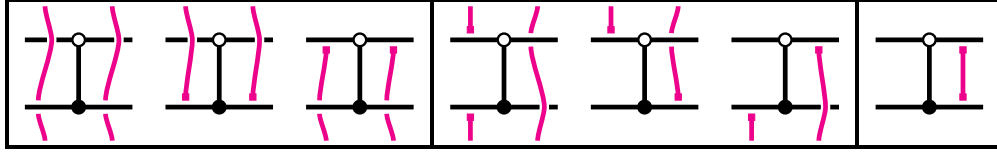
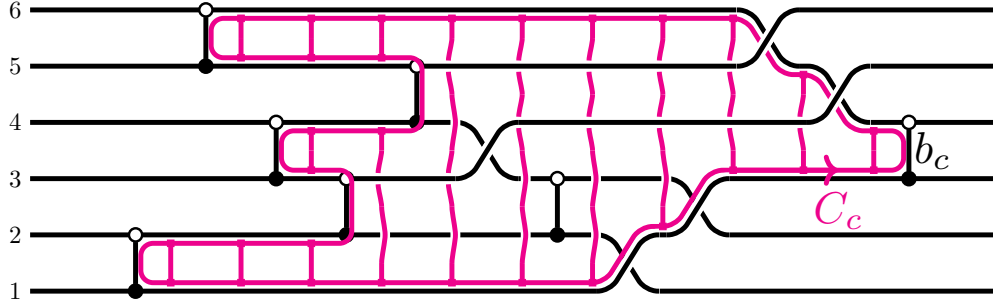
Acknowledgments. T.L. and D.E.S. thank our students Ray Karpman and Gracie Ingermanson for helping us understand the relationship between Deodhar’s positive subexpressions and Postnikov’s combinatorics and for the other ideas discussed in Section 2.6. M.S.B. thanks Daping Weng for illuminating conversations on [SW21]. We also appreciate many conversations with Allen Knutson about Richardson and Bott–Samelson varieties, and Deodhar tori. We thank Roger Casals, Eugene Gorsky, and Anton Mellit for conversations related to this project. We also thank the authors of [CGG⁺22] for sharing their exciting results with us.

2. OPEN RICHARDSON VARIETIES

In this section, we give a more detailed explanation of Theorem 1.1 in the case of open Richardson varieties.

2.1. Open Richardson varieties. Let $G = \mathrm{SL}_n$, and let B_+ , B_- be the opposite Borel subgroups of upper and lower triangular matrices, respectively. For two permutations $u, w \in S_n$ such that $u \leq w$ in the Bruhat order, the *open Richardson variety* $\mathring{R}_{u,w}$ is defined as

$$\mathring{R}_{u,w} := (B_- u B_+ \cap B_+ w B_+) / B_+.$$

FIGURE 2. Propagation rules (right to left) for the relative cycles in $G_{u,w}$.FIGURE 3. Applying propagation rules to find one relative cycle C_c of $G_{u,w}$.

To each pair $u \leq w$ and to each reduced word \mathbf{w} for w we associate an *ice quiver* $\tilde{Q}_{u,\mathbf{w}}$ (Section 2.3). Let $\mathcal{A}(\tilde{Q}_{u,\mathbf{w}})$ be the associated cluster algebra; see Section 5.1 for background.

Theorem 2.1. *For all $u \leq w$ in S_n , we have an isomorphism*

$$\mathbb{C}[\mathring{R}_{u,w}] \cong \mathcal{A}(\tilde{Q}_{u,\mathbf{w}}).$$

Moreover, the cluster algebra $\mathcal{A}(\tilde{Q}_{u,\mathbf{w}})$ is locally acyclic and really full rank.

The cluster algebra terminology in Theorem 2.1 will be introduced in Section 5.1. We now describe the 3D plabic graph $G_{u,\mathbf{w}}$, the quiver $\tilde{Q}_{u,\mathbf{w}}$, and the associated cluster algebra $\mathcal{A}(\tilde{Q}_{u,\mathbf{w}})$.

2.2. 3D plabic graphs. Let $\mathbf{w} = (i_1, i_2, \dots, i_m)$ be a reduced word for w . Consider the unique rightmost subexpression \mathbf{u} for u inside \mathbf{w} , and let $J_{u,\mathbf{w}} \subset [m] := \{1, 2, \dots, m\}$ be the set of indices *not* used in \mathbf{u} . The 3D plabic graph $G_{u,\mathbf{w}}$ is obtained from the wiring diagram for w by replacing all crossings in $[m] \setminus J_{u,\mathbf{w}}$ by overcrossings and replacing each crossing $c \in J_{u,\mathbf{w}}$ by a *black-white bridge edge* b_c ; see Figure 1. We place a *marked point* on each of the n leftmost boundary vertices of $G_{u,\mathbf{w}}$, and denote by \mathbf{M} the set of these marked points.

The number of bridges in $G_{u,\mathbf{w}}$ is $|J_{u,\mathbf{w}}| = \ell(w) - \ell(u)$, which is the dimension of $\mathring{R}_{u,w}$. To each index $c \in J_{u,\mathbf{w}}$ we will associate an (oriented) *relative cycle* C_c in $G_{u,\mathbf{w}}$, which by definition is either a cycle in $G_{u,\mathbf{w}}$ or a union of oriented paths in $G_{u,\mathbf{w}}$ with endpoints in \mathbf{M} .

Each relative cycle C_c will naturally bound a disk D_c .¹ For instance, in Figure 3, the vertical sections of D_c are shown in wavy pink lines. We indicate the relative position of D_c in \mathbb{R}^3 with respect to the edges of $G_{u,\mathbf{w}}$ by over/under-crossings. We will compute D_c , and therefore its boundary C_c , starting from the bridge b_c and proceeding to the left using the *propagation rules* in Figure 2. We choose the counterclockwise orientation of C_c , so that as

¹More precisely, when C_c is a cycle, $\partial D_c = C_c$, and when C_c is a union of paths with marked endpoints, ∂D_c is the union of C_c together with several straight line segments connecting pairs of marked points.

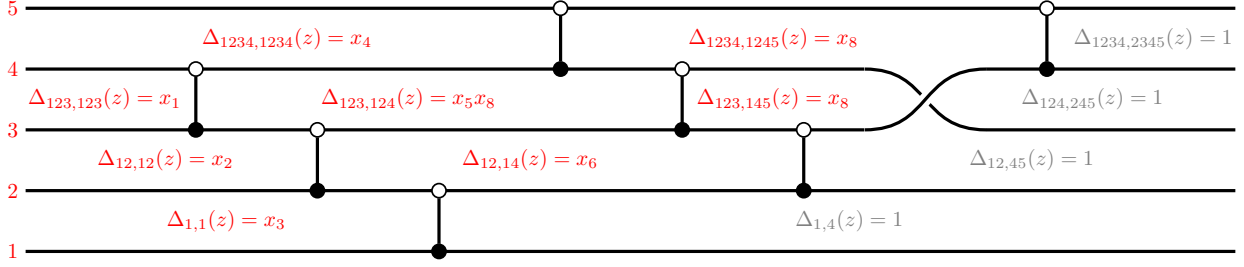


FIGURE 4. Factorization of chamber minors into cluster variables.

one traverses C_c , the disk D_c is to the left. See Section 3.4 for a description of relative cycles in the case of double braid varieties.

2.3. The quiver. A *quiver* Q is a directed graph without directed cycles of length 1 and 2. An *ice quiver* \tilde{Q} is a quiver whose vertex set $V = V(\tilde{Q})$ is partitioned into *frozen* and *mutable* vertices: $\tilde{V} = V^{\text{fro}} \sqcup V^{\text{mut}}$. The arrows between pairs of frozen vertices are automatically omitted.

The procedure in Section 2.2 yields a bicolored graph $G_{u,w}$ decorated with a family $(C_c)_{c \in J_{u,w}}$ of relative cycles. To this data, we associate an ice quiver $\tilde{Q}_{u,w}$. Our construction will rely on the results of [FG09, GK13]. The vertex set $V(\tilde{Q}_{u,w}) := J_{u,w}$ is in bijection with the set of relative cycles. If a relative cycle C_c is actually a cycle in $G_{u,w}$ then c is a mutable vertex of $\tilde{Q}_{u,w}$; otherwise, if C_c is a union of paths with endpoints in \mathbf{M} , c is a frozen vertex of $\tilde{Q}_{u,w}$.

To compute the arrows of $\tilde{Q}_{u,w}$, we consider $G_{u,w}$ as a *ribbon graph*, with counterclockwise half-edge orientations around white vertices and clockwise half-edge orientations around black vertices. Let $\mathbf{S}_{u,w}$ be the surface with boundary obtained by replacing every edge of $G_{u,w}$ by a thin ribbon and gluing the ribbons together according to the local orientations at the vertices of $G_{u,w}$. See Figure 6(d) for an example of $\mathbf{S}_{u,w}$. The n marked points of $G_{u,w}$ give rise to n marked points on $\partial\mathbf{S}_{u,w}$, the set of which is also denoted by \mathbf{M} .

We view each relative cycle C_c as an element of the relative homology $\Lambda_{u,w} := H_1(\mathbf{S}_{u,w}, \mathbf{M})$. It turns out that each mutable relative cycle can be also viewed as an element of the dual lattice $\Lambda_{u,w}^*$; see Section 3.3. The (signed) number of arrows between two vertices $c, d \in J_{u,w}$ in $\tilde{Q}_{u,w}$, where d is mutable, is defined to be the (signed) intersection number $\langle C_c, C_d \rangle$ of the relative cycles C_c and C_d . These intersection numbers can be computed explicitly using simple pictorial rules; see Algorithm 3.8.

2.4. The seed. To each $c \in J_{u,w}$ we associate a *cluster variable* $x_c \in \mathbb{C}[\mathring{R}_{u,w}]$. Let \mathbf{Ch}_c be the *chamber* (i.e., a connected component of the complement of $G_{u,w}$ in the plane) located immediately to the left of the bridge b_c . To this data, one can associate a regular function on $\mathring{R}_{u,w}$ called a *chamber minor* $\Delta_c \in \mathbb{C}[\mathring{R}_{u,w}]$. Variants of these functions appear in [MR04, Lec16, Ing19].

Specifically, given an element $gB_+ \in \mathring{R}_{u,w}$, one can find a unique matrix $z \in B_+$ such that $gB_+ = zwB_+$ and $\Delta_{u[i],w[i]}(z) = 1$ for all $i = 1, 2, \dots, n$. Here we write $v[i] := \{v(1), \dots, v(i)\}$ for $v \in S_n$, and $\Delta_{A,B}$ denotes the matrix minor with row set A and column set B . The wiring diagram of w is obtained from $G_{u,w}$ by replacing every bridge with a crossing, and the wiring

diagram of u is obtained by erasing all bridges from $G_{u,\mathbf{w}}$. Given any chamber \mathbf{Ch} , let A be the set of left endpoints of u -strands (i.e., the strands in the wiring diagram of u) passing below \mathbf{Ch} , and let B be the set of left endpoints of w -strands passing below \mathbf{Ch} . The chamber minor for \mathbf{Ch} is then given by $\Delta_{A,B}(z)$.

For $d \in J_{u,\mathbf{w}}$, we say that \mathbf{Ch}_c is *inside* C_d if it is contained inside the projection of the disk D_d to the plane. Then the cluster variables $(x_c)_{c \in J_{u,\mathbf{w}}}$ are uniquely defined by the invertible monomial transformation

$$(2.1) \quad \Delta_c = \prod_{d \in J_{u,\mathbf{w}}: \mathbf{Ch}_c \text{ is inside } C_d} x_d.$$

See Figure 4 for an example when $w = s_3s_2s_1s_4s_3s_2s_3s_4$ and $u = s_3$, and see Section 6.6.1 for further details.

The cluster $\{x_c\}_{c \in J_{u,\mathbf{w}}}$ together with the quiver $\tilde{Q}_{u,\mathbf{w}}$ is a seed $\Sigma_{u,\mathbf{w}}$ in $\mathbb{C}(\mathring{R}_{u,w})$. To prove Theorem 2.1, we show that $\mathbb{C}[\mathring{R}_{u,w}] = \mathcal{A}(\Sigma_{u,\mathbf{w}})$.

2.5. Deodhar geometry. In [Deo85], Deodhar constructed a stratification of $\mathring{R}_{u,w}$ for each reduced word \mathbf{w} of w . The strata are of the form $\mathbb{C}^a \times (\mathbb{C}^*)^b$. The dense open stratum in Deodhar's stratification is called the *Deodhar torus*, and denoted $T_{u,\mathbf{w}} \subset \mathring{R}_{u,w}$. The Deodhar torus is the initial cluster torus in our cluster structure. We show in Proposition 7.4 that the chamber minors $\{\Delta_c\}_{c \in J_{u,\mathbf{w}}}$ are a basis of characters for $T_{u,\mathbf{w}}$.

We show that the cluster variables $\{x_d\}_{d \in J_{u,\mathbf{w}}}$ are certain distinguished characters on $T_{u,\mathbf{w}}$. Namely, the complement $\mathring{R}_{u,w} \setminus T_{u,\mathbf{w}}$ is a union of irreducible components called (*mutable*) *Deodhar hypersurfaces* V_d . We deduce from (2.1) that the mutable cluster variable x_d is the unique character of $T_{u,\mathbf{w}}$ which vanishes to order one along V_d and has no zeroes along other Deodhar hypersurfaces. Frozen Deodhar hypersurfaces and frozen cluster variables are constructed using a slightly different geometric approach.

2.6. Comparison to known cluster structures. Our construction simultaneously includes several known cluster structures.

When w is a k -Grassmannian permutation, the open Richardson variety $\mathring{R}_{u,w}$ is an open positroid variety in the sense of [Pos06, KLS13]. In this case, Karpman [Kar17] showed that the graph $G_{u,\mathbf{w}}$ is one of Postnikov's reduced plabic graphs [Pos06] with n extra leaves attached. In particular, in this case $G_{u,\mathbf{w}}$ is planar and each cycle C_c bounds a single face of $G_{u,\mathbf{w}}$, which is not usually true for general $w \in S_n$. In this case, the first two authors [GL19] showed that the open positroid variety is a cluster variety, with quiver coming from the plabic graph; this gives the quiver $\tilde{Q}_{u,\mathbf{w}}$.

Many of our ideas appeared in the unpublished Ph.D. dissertation of Ingermanson [Ing19], which constructs an upper cluster structure on $\mathring{R}_{u,w}$. The fourth author was Ingermanson's advisor and is grateful for the ideas he learned from her. We summarize the constructions in our paper that appear in [Ing19]. Ingermanson writes down the same monomial transformation as (2.1), but defines it via a much more involved recursion. Ingermanson constructs a bridge diagram (in the case that \mathbf{w} is a particular reduced word called the "unipeak word") which is isomorphic to our graph $G_{u,\mathbf{w}}$ but is defined as an abstract graph rather than embedded in \mathbb{R}^3 . Ingermanson's quiver is identical to our $\tilde{Q}_{u,\mathbf{w}}$, but it is described in a very different way, along the lines of Section 3.7.

2.7. Braid Richardson varieties. Open Richardson varieties generalize to *braid Richardson varieties*. We say that two flags $B_1, B_2 \in G/B_+$ are in *relative position* $w \in S_n$ if there exists a matrix $g \in G$ such that $(gB_1, gB_2) = (B_+, wB_+)$. In this case, we write $B_1 \xrightarrow{w} B_2$. Consider a (not necessarily reduced) word $\beta = (i_1, i_2, \dots, i_m) \in [n-1]^m$ and let $u \in S_n$. Following the nomenclature of [GLTW22], define the *braid Richardson variety*

$$(2.2) \quad \mathring{R}_{u,\beta} = \left\{ (B_1, B_2, \dots, B_m) \in (G/B_+)^m \mid B_+ \xrightarrow{s_{i_1}} B_1 \xrightarrow{s_{i_2}} \dots \xrightarrow{s_{i_m}} B_m \xleftarrow{w_0 u} B_- \right\}.$$

This variety is nonempty whenever $u \leq \beta$ in the sense of Definition 3.1. In the case $u = w_0$, the definition (2.2) is the same as the definition of the braid variety $X(\beta)$ considered in [CGG⁺22], and is isomorphic to the braid variety $X(\beta, w_0)$ in [CGGS20]. We shall show that braid Richardson varieties are isomorphic to the braid varieties we study in Section 6.

When β is a reduced word for some $w \in S_n$ then using a variant of Lemma 6.2(2–3), we see that $\mathring{R}_{u,\beta}$ is isomorphic to the space $\left\{ B \in G/B_+ \mid B_+ \xrightarrow{w} B \xleftarrow{w_0 u} B_- \right\}$ which can be identified with the Richardson variety $\mathring{R}_{u,w} \subset G/B_+$. Thus, braid Richardson varieties generalize open Richardson varieties. Theorem 2.1 extends to the setting of braid Richardson varieties.

In Section 3.1, we describe our construction in the most general setting of double braid varieties, and define a 3D plabic graph $G_{u,\beta}$ and a quiver $\tilde{Q}_{u,\beta}$ for a pair (u, β) consisting of a permutation u and a *double braid word* β (Section 3.1). If β is a double braid word and $u = \text{id}$, then $G_{u,\beta}$ is again planar. In this case, if we impose that the double word β is reduced, we recover the classical cluster structure on type A double Bruhat cells [FZ99, BFZ05, GY20]. If we allow β to be non-reduced, then we recover the type A results of [SW21] on double Bott–Samelson varieties. We note that the fact that our graphs are non-planar indicates that our construction gives a non-trivial 3-dimensional extension of the combinatorics of [FZ99, Pos06, SW21].

3. DOUBLE BRAID QUIVERS

The goal of this section is to define 3D plabic graphs, conjugate surfaces, relative cycles, and the associated quivers in the extended generality of *double braid words*.

3.1. Double braid words. Let $I := [n-1]$. A *double braid word* is a word $\beta = (i_1, i_2, \dots, i_m) \in (\pm I)^m$ in the alphabet

$$\pm I := \{-1, -2, \dots, -(n-1)\} \sqcup \{1, 2, \dots, n-1\}.$$

We denote the set of double braid words by $(\pm I)^m$. We will usually abbreviate $\beta = (i_1, i_2, \dots, i_m)$ as $\beta = i_1 i_2 \dots i_m$. For $\beta \in (\pm I)^m$, we write $\ell(\beta) := m$. The goal of this section is to associate a quiver $\tilde{Q}_{u,\beta}$ to a pair (u, β) , where $u \in S_n$ and $\beta \in (\pm I)^m$.

The word $\beta \in (\pm I)^m$ should be considered as a *shuffle* of two positive braid words in the commuting alphabets $I, -I$. We emphasize that the letter $-i$ does *not* correspond to σ_i^{-1} , the inverse of the braid group generator σ_i . We call elements of I *red* and elements of $-I$ *blue*.

For $i \in \pm I$, let

$$s_i^+ := \begin{cases} s_i, & \text{if } i > 0, \\ \text{id}, & \text{if } i < 0, \end{cases} \quad s_i^- := \begin{cases} \text{id}, & \text{if } i > 0, \\ s_{-i}, & \text{if } i < 0. \end{cases}$$

We use the convention that the positive indices act on the right while the negative indices act on the left; for a permutation $u \in S_n$ and $i \in \pm I$, we write this action as $u \mapsto s_i^- u s_i^+$. For a double braid word β , its *Demazure product* is defined by

$$\pi(\beta) := s_{i_m}^- * s_{i_{m-1}}^- * \cdots * s_{i_1}^- * s_{i_1}^+ * s_{i_2}^+ * \cdots * s_{i_m}^+ \in S_n,$$

where $*$ denotes the standard Demazure product on S_n .

Definition 3.1. For $u \in S_n$ and a double braid word β , we write $u \leq \beta$ if $u \leq \pi(\beta)$ in the Bruhat order on S_n .

Let $\beta = (i_1, i_2, \dots, i_m) \in (\pm I)^m$ and $u \in S_n$. A u -subexpression of β is a sequence $\mathbf{u} = (u_{(0)}, u_{(1)}, \dots, u_{(m)}) \in S_n^{m+1}$ such that $u_{(0)} = \text{id}$, $u_{(m)} = u$, and such that for each $c \in [m]$, we have either $u_{(c)} = u_{(c-1)}$ or $u_{(c)} = s_{i_c}^- u_{(c-1)} s_{i_c}^+$. It is clear that β contains a u -subexpression if and only if $u \leq \beta$.

Suppose that $u \leq \beta$. Out of all u -subexpressions of β , there exists a unique ‘‘rightmost’’ one, called the u -positive distinguished subexpression (u -PDS). It can be computed explicitly using the following operation which we call *Demazure quotient*: for $u \in S_n$ and $i \in I$, set

$$s_i \triangleright u = \begin{cases} s_i u, & \text{if } s_i u < u, \\ u, & \text{otherwise,} \end{cases} \quad \text{and} \quad u \triangleleft s_i = \begin{cases} u s_i, & \text{if } u s_i < u, \\ u, & \text{otherwise.} \end{cases}$$

By convention, we set $\text{id} \triangleright u = u = u \triangleleft \text{id}$. The u -PDS $\mathbf{u} = (u_{(0)}, u_{(1)}, \dots, u_{(m)})$ is computed iteratively starting from $u_{(m)} = u$. For $c = m, m-1, \dots, 1$, we set

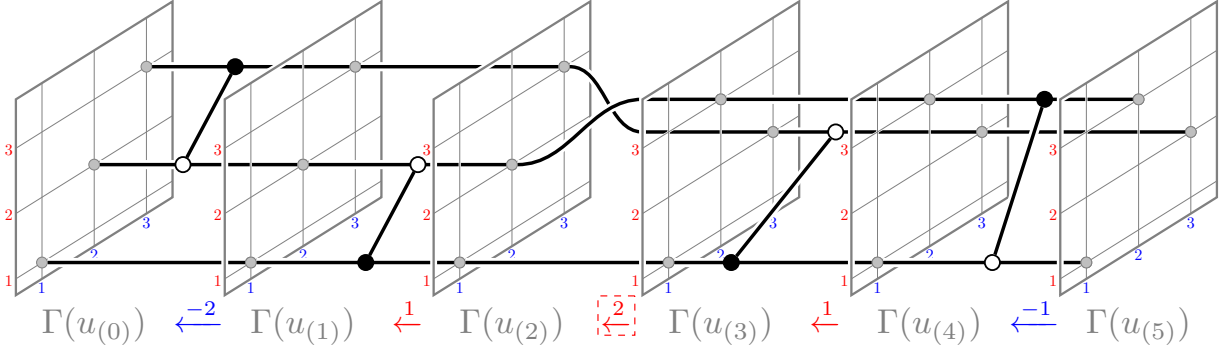
$$(3.1) \quad u_{(c-1)} := s_{i_c}^- \triangleright u_{(c)} \triangleleft s_{i_c}^+.$$

Since $u \leq \beta$, we have $u_{(0)} = \text{id}$. We set $J_{u,\beta} := \{c \in [m] \mid u_{(c)} = u_{(c-1)}\}$. We refer to the indices in $J_{u,\beta}$ as *solid crossings* and to the indices in $[m] \setminus J_{u,\beta}$ as *hollow crossings*. The indices in $[m] \setminus J_{u,\beta}$ form a reduced word for u , i.e., we have $|J_{u,\beta}| = \ell(\beta) - \ell(u)$.

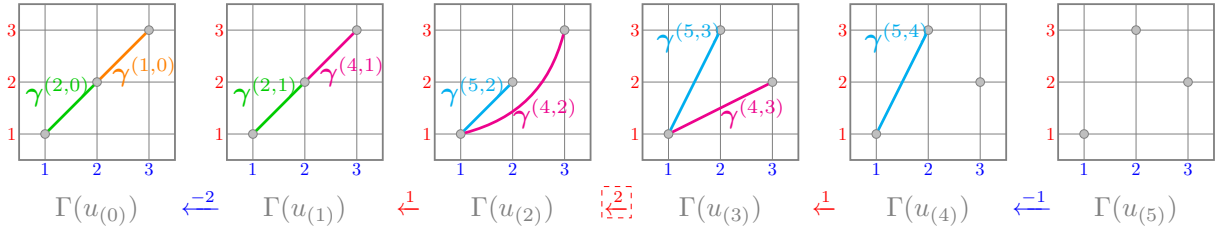
Remark 3.2. When $\beta \in I^m$ is a reduced word for a permutation and $u \leq \beta$, the sequence $(u_{(0)}, \dots, u_{(m)})$ is a positive distinguished subexpression in the sense of [MR04, Definition 3.4]. The terminology of ‘‘solid’’ and ‘‘hollow’’ crossings is drawn from [MR04], who draw wiring diagrams in this way. When the positive and negative subwords of β are both reduced and $u \leq \beta$, $(u_{(0)}, \dots, u_{(m)})$ is a positive double distinguished subexpression in the sense of [WY07].

For the rest of this section, we fix a pair $(u, \beta) \in S_n \times (\pm I)^m$ satisfying $u \leq \beta$, and let \mathbf{u} be the u -PDS of β .

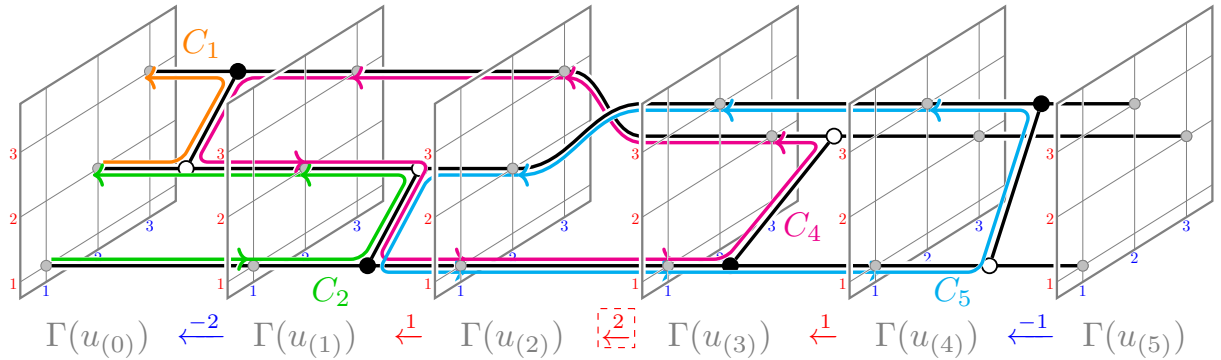
Remark 3.3. All our constructions (including quivers, 3D plabic graphs, cluster algebra structures, and braid varieties) will be invariant under the following operation of appending hollow crossings on the right: if $i \in \pm I$ is such that $u < u' := s_i^- u s_i^+$ then we are allowed to replace (u, β) with $(u', \beta i)$. In particular, starting with any pair (u, β) satisfying $u \leq \beta$, we can append hollow crossings to obtain a pair (w_0, β') for some double braid word $\beta' \in (\pm I)^{m+\ell(w_0)-\ell(u)}$.



(a) 3D plabic graph $G_{u,\beta}$



(b) monotone curves in $G_{u,\beta}$



(c) relative cycles in $G_{u,\beta}$

FIGURE 5. A 3D plabic graph $G_{u,\beta}$ for $u = s_2$ and $\beta = (-2, 1, 2, 1, -1)$; see Example 3.10.

3.2. 3D plabic graphs. We view permutations $z \in S_n$ as bijections $[n] \rightarrow [n]$, with multiplication given by composition. Thus, if $z = xy$ then we have $z(i) = x(y(i))$ for $i \in [n]$. The *permutation diagram* $\Gamma(z) \subset \mathbb{Z}^2$ of $z \in S_n$ is the set of dots $(i, z(i))$ for $i \in [n]$. We use Cartesian coordinates for permutation diagrams.² Thus, the dot (i, j) is located in column i and row j , with the dot $(1, 1)$ located in the bottom-left corner. We let \preceq be the partial order on $\mathbb{Z}^2 \subset \mathbb{R}^2$ given by $(x, y) \preceq (x', y')$ whenever $x \leq x'$ and $y \leq y'$.

²The reader who likes permutation *matrices* should therefore flip our permutation diagrams upside down, and should also remember that the convention for matrices is to list the vertical coordinate first and the horizontal coordinate second.

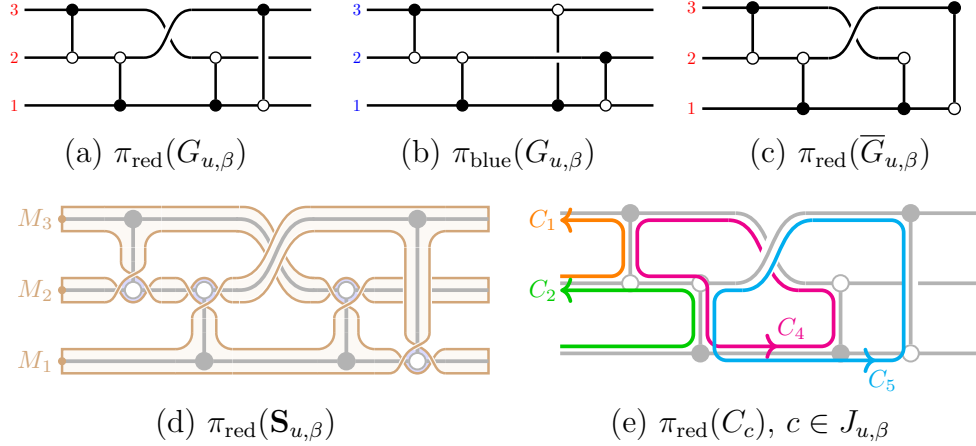


FIGURE 6. Projections of objects associated to 3D plabic graphs (cf. Figure 5 and Example 3.10).

We consider \mathbb{Z}^3 with coordinates (i, j, t) , where the third coordinate t is referred to as the *time*. For each $c = 0, 1, \dots, m$, place the permutation diagram $\Gamma(u_{(c)})$ in the $t = c$ plane.

We now define the 3D plabic graph $G_{u,\beta}$; see Example 3.10 and Figure 5(a). We first give an informal description; see below for an explicit description in coordinates in \mathbb{Z}^3 .

Definition 3.4. Start by drawing n strands in $\mathbb{R}^3 \supset \mathbb{Z}^3$ whose time coordinate is monotone increasing, so that for $c = 0, 1, \dots, m$, each of the n dots of $\Gamma(u_{(c)})$ belongs to exactly one strand. For each $c \in [m]$, the permutation diagrams $\Gamma(u_{(c-1)})$ and $\Gamma(u_{(c)})$ either are identical or differ by a row (if $i_c > 0$) or by a column (if $i_c < 0$) transposition. The strands of $G_{u,\beta}$ connect each dot of $\Gamma(u_{(c-1)})$ to the corresponding dot of $\Gamma(u_{(c)})$. In addition, for each solid crossing $c \in J_{u,\beta}$, we add a *bridge edge* b_c at time $t = c - \frac{1}{2}$ between the two strands $S_1 \prec S_2$ participating in the solid crossing, where the partial order \preceq is extended from the dots of $\Gamma(u_{(c-1)}) = \Gamma(u_{(c)})$ to the strands passing through them. If $i_c > 0$ (resp., $i_c < 0$), the strands S_1, S_2 are located in adjacent rows (resp., columns), and the bridge b_c is black at S_1 and white at S_2 (resp., white at S_1 and black at S_2). The vertex of b_c on S_1 (resp., on S_2) is called the *start* (resp., the *end*) of b_c .

For $0 < c < m$, we do not view the dots in $\Gamma(u_{(c)})$ as vertices of $G_{u,\beta}$. The dots in $\Gamma(u_{(0)})$ are viewed as degree 1 *marked boundary vertices* of $G_{u,\beta}$. The dots in $\Gamma(u_{(m)})$ are viewed as unmarked degree 1 vertices of $G_{u,\beta}$. We let $\bar{G}_{u,\beta}$ be obtained from $G_{u,\beta}$ by deleting these n vertices and the n edges incident to them; see Figure 6(c).

It is convenient to project 3D plabic graphs to the plane. There are two natural choices for such projections. The *red projection* of $G_{u,\beta}$ is its image under the map $\pi_{\text{red}} : \mathbb{R}^3 \rightarrow \mathbb{R}^2$, $(i, j, t) \mapsto (t, j)$. Similarly, the *blue projection* of $G_{u,\beta}$ is obtained by applying the map $\pi_{\text{blue}} : \mathbb{R}^3 \rightarrow \mathbb{R}^2$, $(i, j, t) \mapsto (t, i)$. We will mostly work with the red projection $\pi_{\text{red}}(G_{u,\beta})$; see Figures 6 and 7. We sometimes mention the *faces* of $\pi_{\text{red}}(G_{u,\beta})$ and $\pi_{\text{blue}}(G_{u,\beta})$; by this we mean connected components of the complement.

We now give a formal description of $G_{u,\beta}$. Suppose first that $c \in J_{u,\beta}$ is a solid crossing. Then $u_{(c-1)} = u_{(c)}$, and we connect each dot $(i, j, c-1)$ in $\Gamma(u_{(c-1)})$ to the corresponding dot (i, j, c) of $\Gamma(u_{(c)})$, where $j = u_{(c-1)}(i) = u_{(c)}(i)$. Suppose now that $c \in [m] \setminus J_{u,\beta}$ is a hollow

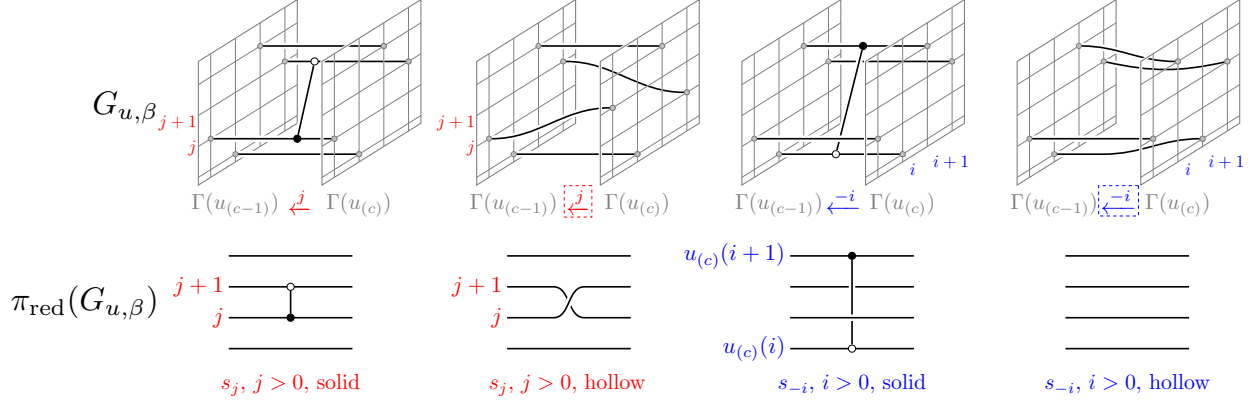


FIGURE 7. Applying the red projection to a 3D plabic graph.

crossing. If $i_c > 0$, then $\Gamma(u_{(c-1)})$ and $\Gamma(u_{(c)})$ differ by a row transposition, and we connect the dots accordingly. Specifically, letting $j := i_c$, we connect:

- $(i, j, c-1) \in \Gamma(u_{(c-1)})$ to $(i, j+1, c) \in \Gamma(u_{(c)})$,
- $(i', j+1, c-1) \in \Gamma(u_{(c-1)})$ to $(i', j, c) \in \Gamma(u_{(c)})$, and
- $(i'', j'', c-1) \in \Gamma(u_{(c-1)})$ to $(i'', j'', c) \in \Gamma(u_{(c)})$ for $j'' \neq j, j+1$.

Similarly, if $i_c < 0$, then $\Gamma(u_{(c-1)})$ and $\Gamma(u_{(c)})$ differ by a column transposition. Letting $i := |i_c|$, we connect:

- $(i, j, c-1) \in \Gamma(u_{(c-1)})$ to $(i+1, j, c) \in \Gamma(u_{(c)})$,
- $(i+1, j', c-1) \in \Gamma(u_{(c-1)})$ to $(i, j', c) \in \Gamma(u_{(c)})$, and
- $(i'', j'', c-1) \in \Gamma(u_{(c-1)})$ to $(i'', j'', c) \in \Gamma(u_{(c)})$ for $i'' \neq i, i+1$.

We add $|J_{u, \beta}|$ -many bridges to $G_{u, \beta}$. Consider a solid crossing $c \in J_{u, \beta}$. Suppose first that $i_c > 0$ and let $j := i_c$. Then $G_{u, \beta}$ contains strands connecting the dots $(i, j, c-1)$ to (i, j, c) and $(i', j+1, c-1)$ to $(i', j+1, c)$, for some $i, i' \in [n]$. In order for c to be solid, we must have $i < i'$. We put a black vertex on the segment connecting $(i, j, c-1)$ to (i, j, c) , and a white vertex on the segment connecting $(i', j+1, c-1)$ to $(i', j+1, c)$, and connect these two vertices by an edge, which we call a *bridge* and denote b_c . Suppose now that $i_c < 0$ and let $i := |i_c|$. Then $G_{u, \beta}$ contains strands connecting the dots $(i, j, c-1)$ to (i, j, c) and $(i+1, j', c-1)$ to $(i+1, j', c)$, for some $j, j' \in [n]$, and again we must have $j < j'$. We put a black vertex on the segment connecting $(i, j, c-1)$ to (i, j, c) , and a white vertex on the segment connecting $(i+1, j', c-1)$ to $(i+1, j', c)$, and connect these two vertices by a bridge b_c .

3.3. Conjugate surfaces. Continuing Section 2.3, we endow the graph $G_{u, \beta}$ with the structure of a *marked ribbon graph* in the language of [FG06, Section 3]. A *ribbon graph* is a graph together with a choice, for each vertex v , of a cyclic orientation on the half-edges emanating from v . Taking the red projection of $G_{u, \beta}$, we choose the counterclockwise (resp., clockwise) orientation for each white (resp., black) vertex of $G_{u, \beta}$. The marked degree 1 vertices of $G_{u, \beta}$ are the n dots in $\Gamma(u_{(0)})$.³

³In [FG06], all degree 1 vertices of a ribbon graph are considered automatically marked, but we do not mark the n dots in $\Gamma(u_{(m)})$. Removing the dots in $\Gamma(u_{(m)})$ yields the graph $\overline{G}_{u, \beta}$, which is truly a marked ribbon graph in the language of [FG06].

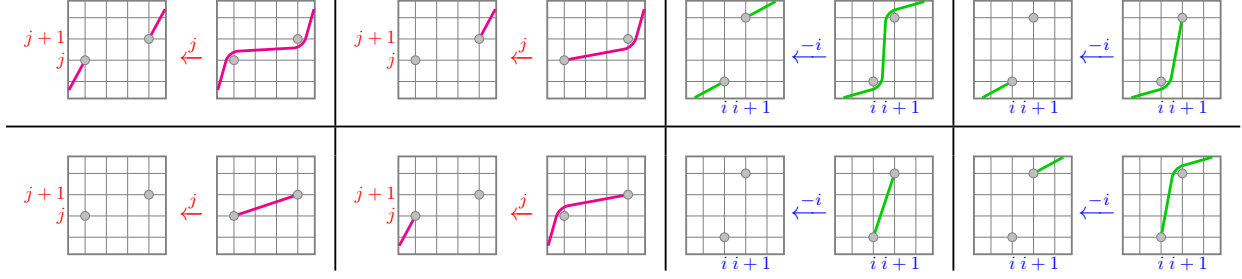


FIGURE 8. Propagation rules for monotone curves; see Section 3.4. In any case not depicted here, the monotone curve is unchanged by the action of a solid crossing.

Remark 3.5. From now on, we view $G_{u,\beta}$ as a ribbon graph, not as a bicolored graph. When projecting a ribbon graph $G_{u,\beta}$ to the plane, we choose the color of each vertex to be white (resp., black) if its local half-edge orientation is counterclockwise (resp., clockwise). Thus, for example, we can change the color of a given vertex q by altering the drawing of G ; see Figure 9(left). In this case, we label the resulting vertex by \bar{q} , emphasizing that q and \bar{q} represent the same vertex of G .

We let $\mathbf{S}_{u,\beta} = \mathbf{S}(G_{u,\beta})$ be the marked surface with boundary associated to $G_{u,\beta}$ in a standard way: we replace every edge of $G_{u,\beta}$ by a thin rectangle, every vertex of $G_{u,\beta}$ by a disk, and glue the rectangles to the boundaries of the disks according to the local orientation around each vertex. Thus, $\partial\mathbf{S}_{u,\beta}$ has several connected components, and we stress that we do *not* glue disks to them. The surface $\mathbf{S}_{u,\beta}$ can be drawn using the red projection of $G_{u,\beta}$ as shown in Figure 6(d). In particular, $\mathbf{S}_{u,\beta}$ is orientable, with black and white vertices in the red projection of $G_{u,\beta}$ corresponding to the different sides of $\mathbf{S}_{u,\beta}$.

We apply a similar construction to $\bar{G}_{u,\beta}$, and it is clear that the resulting surface $\mathbf{S}(\bar{G}_{u,\beta})$ is homeomorphic to $\mathbf{S}_{u,\beta}$.

Let \mathbf{M} be the set of marked points on $\partial\mathbf{S}_{u,\beta}$; thus, $|\mathbf{M}| = n$. Let $\Lambda_{u,\beta} := H_1(\mathbf{S}_{u,\beta}, \mathbf{M})$. (All relative homology groups we consider are with integer coefficients.) The elements of $\Lambda_{u,\beta}$, called *relative cycles*, are represented by \mathbb{Z} -linear combinations of *arcs*, where an arc is either an oriented closed curve embedded into the interior of $\mathbf{S}_{u,\beta}$ or an oriented curve embedded into $\mathbf{S}_{u,\beta}$ with both endpoints marked. Let $\Lambda_{u,\beta}^* := H_1(\mathbf{S}_{u,\beta} \setminus \mathbf{M}, \partial\mathbf{S}_{u,\beta} \setminus \mathbf{M})$. We have an *intersection form* on $(\mathbf{S}_{u,\beta}, \mathbf{M})$ which gives rise to a perfect pairing

$$(3.2) \quad \langle \cdot, \cdot \rangle : \Lambda_{u,\beta} \otimes \Lambda_{u,\beta}^* \rightarrow \mathbb{Z};$$

see e.g. [CW22, Proposition 3.48] or [Mel19, Section 6.1]. For $C \in \Lambda_{u,\beta}$, $C' \in \Lambda_{u,\beta}^*$, the *intersection number* $\langle C, C' \rangle$ is the integer obtained by counting signed intersection points between two generic relative cycles representing C and C' .

Remark 3.6. An oriented cycle in $G_{u,\beta}$ can be naturally lifted to an element of $\Lambda_{u,\beta}$ as well as to an element of $\Lambda_{u,\beta}^*$. On the other hand, an oriented path with both endpoints marked can only be naturally lifted to an element of $\Lambda_{u,\beta}$.

3.4. Relative cycles. Fix a solid crossing $c \in J_{u,\beta}$. Our goal is to associate to it a relative cycle $C_c \in \Lambda_{u,\beta}$. As in Section 2.2, we will obtain C_c as the boundary of a certain 2-dimensional disk D_c inside \mathbb{R}^3 .

A *monotone curve* inside a permutation diagram $\Gamma(z) \subset \mathbb{R}^2$ is a curve $\gamma : [0, 1] \rightarrow \mathbb{R}^2$ whose endpoints are dots in $\Gamma(z)$, with no other dots of $\Gamma(z)$ on γ , and such that both coordinates of γ are strictly monotone increasing. Recall that we write $(x, y) \preceq (x', y')$ if $x \leq x'$ and $y \leq y'$. Write $(x, y) \prec (x', y')$ if $(x, y) \preceq (x', y')$ and $(x, y) \neq (x', y')$. Thus, $\gamma(0) \prec \gamma(1)$. A *monotone multicurve* is a collection $\boldsymbol{\gamma} = (\gamma_1, \gamma_2, \dots, \gamma_k)$ of monotone curves inside $\Gamma(z)$ such that

$$\gamma_1(0) \prec \gamma_1(1) \prec \gamma_2(0) \prec \gamma_2(1) \prec \dots \prec \gamma_k(0) \prec \gamma_k(1).$$

The intersection of the disk D_c with each plane $t = r$, $0 \leq r \leq c - 1$, will be a monotone multicurve inside $\Gamma(u_{(r)})$ denoted $\boldsymbol{\gamma}^{(c,r)}$. For $r = c - 1$, $\boldsymbol{\gamma}^{(c,c-1)}$ consists of a single monotone curve connecting the two dots on the strands which are connected by b_c . We then compute $\boldsymbol{\gamma}^{(c,r)}$ iteratively for $r = c - 2, \dots, 1, 0$, using the following *propagation rules*. When passing from $\boldsymbol{\gamma}^{(c,r)}$ to $\boldsymbol{\gamma}^{(c,r-1)}$ for a solid crossing r , each monotone curve γ in $\boldsymbol{\gamma}^{(c,r)}$ either is preserved or *gets cut*. The cutting moves are shown in Figure 8, and all other curves not shown in Figure 8 are preserved. When the crossing r is hollow, each monotone curve γ changes “smoothly” so that a dot \mathfrak{d} of $\Gamma(u_{(r)})$ is above (resp., below) γ if and only if the dot \mathfrak{d}' of $\Gamma(u_{(r-1)})$ that is on the same strand as \mathfrak{d} is above (resp., below) the image of γ in $\Gamma(u_{(r-1)})$; see e.g. Figure 5(b).

To give a coordinate description in the case of a solid crossing, let $r \in J_{u,\beta}$ be such that $i_r > 0$ and let $j := i_r$. Let $\mathfrak{d} := (i, j)$ and $\mathfrak{d}' := (i', j + 1)$ be the dots in $\Gamma(u_{(r)}) = \Gamma(u_{(r-1)})$, for some $i, i' \in [n]$. Then the curve γ *gets cut* if and only if it passes weakly above \mathfrak{d} and weakly below \mathfrak{d}' . Assume now that $i_r < 0$ and let $i := |i_r|$. Let $\mathfrak{d} := (i, j)$ and $\mathfrak{d}' := (i + 1, j')$ be the dots in $\Gamma(u_{(r)}) = \Gamma(u_{(r-1)})$, for some $j, j' \in [n]$. Then γ *gets cut* if and only if it passes weakly to the right of \mathfrak{d} and weakly to the left of \mathfrak{d}' . In both cases, the cutting move consists of removing the part of γ passing between \mathfrak{d} and \mathfrak{d}' . (In particular, if neither \mathfrak{d} nor \mathfrak{d}' was an endpoint of γ then we split γ into two monotone curves γ', γ'' satisfying $\gamma'(1) = \mathfrak{d}$ and $\gamma''(0) = \mathfrak{d}'$. On the other hand, if both \mathfrak{d} and \mathfrak{d}' were endpoints of γ then the whole of γ disappears.)

Definition 3.7. If $\boldsymbol{\gamma}^{(c,0)}$ is empty, then we declare c to be *mutable*, otherwise, we declare c to be *frozen*. We let $J_{u,\beta}^{\text{fro}}$ and $J_{u,\beta}^{\text{mut}}$ denote the sets of frozen and mutable indices, respectively.

Thus, we have a decomposition $J_{u,\beta} = J_{u,\beta}^{\text{fro}} \sqcup J_{u,\beta}^{\text{mut}}$.

If c is mutable, we obtain a disk D_c inside \mathbb{R}^3 whose boundary ∂D_c is a cycle C_c in $G_{u,\beta}$ that does not pass through any marked points. If c is frozen, we treat $\boldsymbol{\gamma}^{(c,0)}$ as part of the boundary of the disk D_c , and denote the rest of ∂D_c by $C_c := \partial D_c \setminus \boldsymbol{\gamma}^{(c,0)}$. In both cases, ∂D_c passes through the bridge b_c , and we orient ∂D_c so that it is directed from the start to the end of b_c ; cf. Definition 3.4. This induces an orientation on each arc in C_c , and therefore we obtain a relative cycle $C_c \in \Lambda_{u,\beta}$. See Figures 5(c) and 6(e).

3.5. The quiver. Our goal is to associate an ice quiver $\tilde{Q}_{u,\beta}$ to the pair (u, β) .

The vertex set of $\tilde{Q}_{u,\beta}$ is $\tilde{V} := J_{u,\beta}$, with frozen vertices $V^{\text{fro}} := J_{u,\beta}^{\text{fro}}$ and mutable vertices $V^{\text{mut}} := J_{u,\beta}^{\text{mut}}$ (cf. Definition 3.7). Let $c \in \tilde{V}$ and $d \in V^{\text{mut}}$, and consider the corresponding relative cycles C_c, C_d . By Remark 3.6, we may view C_d as an element of $\Lambda_{u,\beta}^*$. The *cluster exchange matrix* $\tilde{B}(\tilde{Q}_{u,\beta}) = (\tilde{b}_{c,d})_{c \in \tilde{V}, d \in V^{\text{mut}}}$ of $\tilde{Q}_{u,\beta}$ is given by

$$(3.3) \quad \tilde{b}_{c,d} = \#\{\text{arrows } c \rightarrow d \text{ in } \tilde{Q}\} - \#\{\text{arrows } d \rightarrow c \text{ in } \tilde{Q}\} := \langle C_c, C_d \rangle.$$

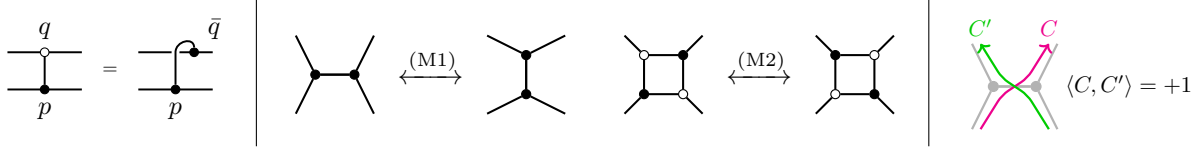


FIGURE 9. Left: switching the color of a vertex. Middle: contraction-uncontraction move (M1) and square move (M2). Right: sign convention for the intersection form of $\mathbf{S}_{u,\beta}$.

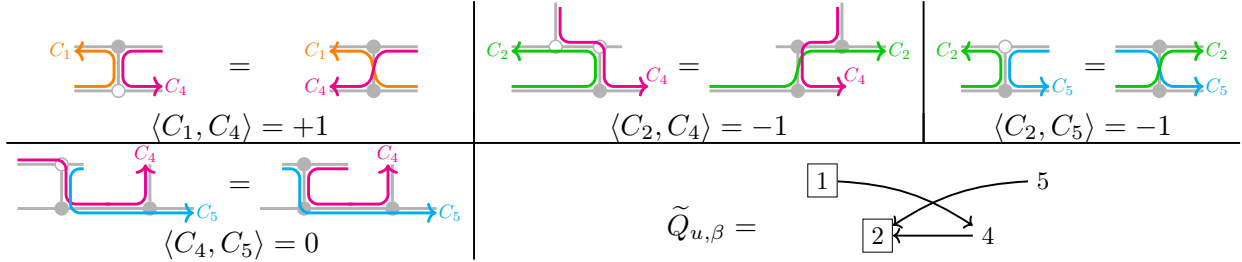


FIGURE 10. Computing the quiver $\tilde{Q}_{u,\beta}$ corresponding to Figures 5 and 6 and Example 3.10; see Algorithm 3.8.

In other words, the (signed) number of arrows from c to d in $\tilde{Q}_{u,\beta}$ is given by the intersection number $\langle C_c, C_d \rangle$. We give an explicit algorithm for computing intersection numbers.

Algorithm 3.8. The intersection form $\langle C, C' \rangle$ of the surface $\mathbf{S}_{u,\beta} = \mathbf{S}(G_{u,\beta})$ may be computed as follows. See Figure 10 and the top row of Figure 13(right) for examples.

- Viewing C, C' as subgraphs of $G_{u,\beta}$, decompose $C \cap C'$ into a union of disjoint paths.
- For each of these paths P , we will have a contribution $\langle C, C' \rangle|_P \in \{-1, 0, 1\}$; the intersection number $\langle C, C' \rangle$ will be the sum of $\langle C, C' \rangle|_P$ over the components P of $C \cap C'$.
- Let $P = (p_0, p_1, \dots, p_r)$ be one of the paths. The contribution $\langle C, C' \rangle|_P$ will depend only on which neighbors of p_0 and p_r are visited by C and C' , and in which order.
- Draw P in the plane with all vertices black (cf. Remark 3.5) and perturb C, C' slightly so that they have either zero or one intersection point.
- If C, C' have zero intersection points, we have $\langle C, C' \rangle|_P = 0$.
- If C, C' have one intersection point p , we have $\langle C, C' \rangle|_P = +1$ if the tangent vectors of (C, C') at p form a positively oriented basis of the plane and $\langle C, C' \rangle|_P = -1$ otherwise; see Figure 9(right).

Remark 3.9. As we pointed out in Section 3.3, the surface $\mathbf{S}_{u,\beta}$ is orientable. It follows that we have $\langle C_d, C_d \rangle = 0$ for all mutable $d \in J_{u,\beta}$.

Example 3.10. Let $u := s_2 \in S_3$ and $\beta := (-2, 1, 2, 1, -1)$. Thus, $J_{u,\beta} = \{1, 2, 4, 5\}$. The graph $G_{u,\beta}$ is given in Figure 5(a), and its red and blue projections are shown in Figure 6(a,b), respectively. The monotone (multi)curves are computed in Figure 5(b) using the propagation rules from Figure 8. The relative cycles $(C_c)_{c \in J_{u,\beta}}$ are shown in Figures 5(c) and 6(e), and the surface $\mathbf{S}_{u,\beta}$ is shown in Figure 6(d). In Figure 10, we use this data to compute the intersection numbers $\langle C_c, C_d \rangle$ and the quiver $\tilde{Q}_{u,\beta}$ via Algorithm 3.8. The frozen vertices of $\tilde{Q}_{u,\beta}$ are boxed in Figure 10.

Remark 3.11. The simplified propagation rules shown in Figure 2 are obtained from the rules in Figure 8 by applying the red projection. It is therefore important to distinguish between over/under-crossings when applying the rules in Figure 2 to the red projection of a 3D plabic graph in Figure 3. However, the ribbon graph $G_{u,\beta}$ and the associated surface $\mathbf{S}_{u,\beta}$ are most naturally considered as abstract objects without a fixed choice of an embedding in \mathbb{R}^3 . Thus, in the rest of our figures, e.g., when drawing the boundary of $\mathbf{S}_{u,\beta}$ in Figure 6(d) or the graphs in Figures 23–25, the over/under-crossings are irrelevant, and are chosen arbitrarily.

Definition 3.12. Given an ice quiver \tilde{Q} and a mutable vertex $d \in V^{\text{mut}}$, one can *mutate* \tilde{Q} in direction d to obtain another quiver $\tilde{Q}' = \mu_d(\tilde{Q})$, the *mutation* of \tilde{Q} at d . Mutation preserves the sets of mutable and frozen vertices, and changes the arrows as follows:

- for each directed path $c \rightarrow d \rightarrow e$ in \tilde{Q} of length 2, add an arrow $c \rightarrow e$ to \tilde{Q}' ;
- reverse all arrows in \tilde{Q} incident to d ;
- remove all directed 2-cycles in the resulting directed graph, one at a time.

This operation may create arrows between pairs of frozen vertices; such pairs are omitted.

Recall that the quiver $\tilde{Q}_{u,\beta}$ is obtained from the collection $(C_c)_{c \in J_{u,\beta}}$ of relative cycles in $\Lambda_{u,\beta}$ via (3.3). Following [GK13, Section 4.1.2] and [FG09, Section 1.2], we explain how for each $d \in J_{u,\beta}^{\text{mut}}$, the quiver $\mu_d(\tilde{Q}_{u,\beta})$ is obtained in the same way via (3.3) from another collection $(\mu_d(C_c))_{c \in J_{u,\beta}}$ of relative cycles in $\Lambda_{u,\beta}$. Namely, we set

$$(3.4) \quad \mu_d(C_c) := \begin{cases} C_c + \max(\langle C_c, C_d \rangle, 0) C_d, & \text{if } c \neq d, \\ -C_d, & \text{if } c = d. \end{cases}$$

Since d is mutable, we see that for each mutable c , the relative cycle $\mu_d(C_c)$ is still naturally an element of both $\Lambda_{u,\beta}$ and $\Lambda_{u,\beta}^*$.

Lemma 3.13 ([FG09, Lemma 1.7]). *The exchange matrix of $\mu_d(\tilde{Q}_{u,\beta})$ is given via (3.3) by the intersection numbers of the relative cycles $(\mu_d(C_c))_{c \in J_{u,\beta}}$.*

Remark 3.14. We will show in Section 5.3 that $(C_c)_{c \in J_{u,\beta}}$ is a \mathbb{Z} -basis of $\Lambda_{u,\beta}$. It follows that $(\mu_d(C_c))_{c \in J_{u,\beta}}$ is a \mathbb{Z} -basis of $\Lambda_{u,\beta}$ as well.

3.6. Distinguished subexpressions. The goal of this section is to explain how the propagation rules for monotone curves from Section 3.4 reflect the combinatorics of *almost positive subexpressions*. These results will be used in Section 7 for comparison to geometry.

Let $\beta \in (\pm I)^m$ be a double braid word and $u \leq \beta$. A u -subexpression \mathbf{u} of β is called *distinguished* if $u_{(c)} \leq s_{i_c}^- u_{(c-1)} s_{i_c}^+$ for each $c \in [m]$. This notion originated in the study of the geometry of open Richardson varieties [Deo85, MR04, WY07].

Definition 3.15. Let $d \in J_{u,\beta}$. Let $v_{(m)}^{(d)} := u$, and for $c = m, m-1, \dots, 1$, define

$$v_{(c-1)}^{(d)} := \begin{cases} s_{i_d}^- * v_{(d)}^{(d)} * s_{i_d}^+, & \text{if } c = d, \\ s_{i_c}^- \triangleright v_{(c)}^{(d)} \triangleleft s_{i_c}^+, & \text{otherwise.} \end{cases}$$

We call the sequence $(v_{(0)}^{(d)}, \dots, v_{(m)}^{(d)})$ the (u, d) -almost positive sequence $((u, d)$ -APS).

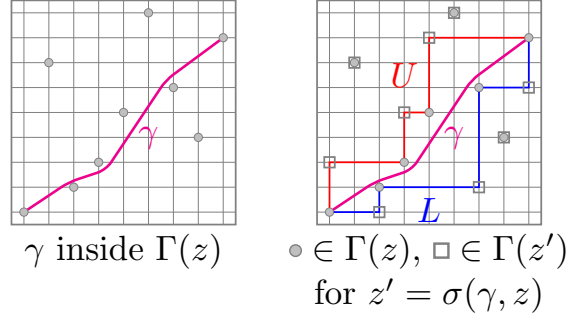


FIGURE 11. Recovering the almost positive subexpression from the corresponding monotone curve.

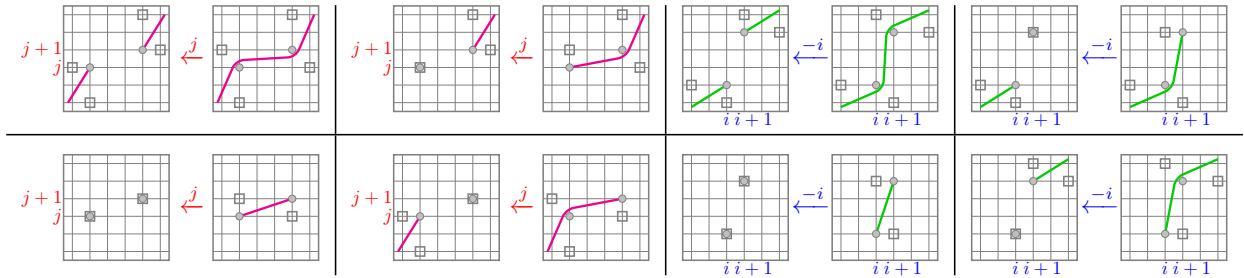


FIGURE 12. Propagation rules (Figure 8) shown together with the corresponding almost positive subexpressions.

In other words, the u -PDS is obtained by starting with u and taking successive Demazure quotients according to the letters of β . The (u, d) -APS is obtained by taking Demazure quotients up to crossing d ; then making a “mistake” at crossing d and taking Demazure product rather than Demazure quotient; then continuing to take Demazure quotients.

Consider a monotone curve γ inside a permutation diagram $\Gamma(z)$ for $z \in S_n$. Take the smallest skew shape λ/μ containing γ whose inner corners are at the dots of $\Gamma(z)$, and let L and U be its lower and upper boundaries, respectively; see Figure 11. Let \mathfrak{D}_γ be the set of dots of $\Gamma(z)$ contained in $U \cup L$. Let \mathfrak{D}'_γ be the set of outer corners of λ/μ , i.e., the set of lattice points where L turns left or U turns right. We define $z' := \sigma(\gamma, z) \in S_n$ to be the permutation such that $\Gamma(z')$ is obtained from $\Gamma(z)$ by replacing the dots in \mathfrak{D}_γ with the dots in \mathfrak{D}'_γ . Given a monotone multicurve $\boldsymbol{\gamma} = (\gamma_1, \gamma_2, \dots, \gamma_k)$, we let $\sigma(\boldsymbol{\gamma}, z) := \sigma(\gamma_1, \sigma(\gamma_2, \dots, \sigma(\gamma_k, z) \dots))$. The following result explains the relation between monotone curves and almost positive subexpressions.

Proposition 3.16. *Let $d \in J_{u, \beta}$. Then for all $c \leq d - 1$, we have*

$$(3.5) \quad v_{(c)}^{(d)} = \sigma(\boldsymbol{\gamma}^{d,c}, u_{(c)}).$$

Proof. For $c = d - 1$, the permutations $v_{(c)}^{(d)}$ and $u_{(c)}$ differ by a single transposition which corresponds to creating the monotone curve $\boldsymbol{\gamma}^{(d, d-1)}$. For $c = d - 2, \dots, 0$, we check (3.5) by induction, since the propagation rules of Figure 8 turn out to exactly reflect the application of Demazure quotient to pairs $(u_{(c)}, v_{(c)}^{(d)})$; see Figure 12. \square

Corollary 3.17. *A solid index $d \in J_{u, \beta}$ is mutable if and only if $v_{(0)}^{(d)} = \text{id}$.*

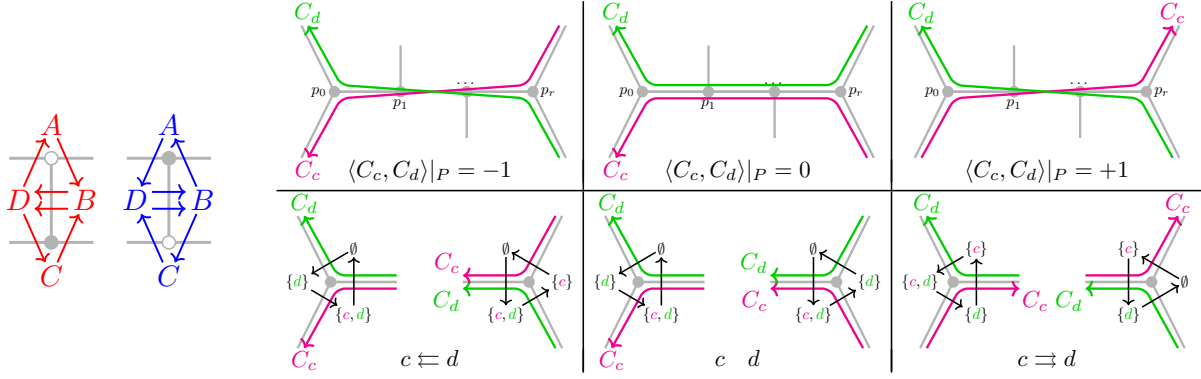


FIGURE 13. The half-arrow description of $\tilde{Q}_{u,\beta}$; see Section 3.7.

3.7. Half-arrow description of $\tilde{Q}_{u,\beta}$. We give an alternative description of $\tilde{Q}_{u,\beta}$ that will be useful in Proposition 7.17. For each red crossing $c \in J_{u,\beta}$, $i_c > 0$, consider the four faces A, B, C, D around the red projection of the bridge b_c as shown in Figure 13(left). To each face $X \in \{A, B, C, D\}$ we associate a collection $\nabla^+(X)$ of indices $d \in J_{u,\beta}$ such that X is inside the red projection of the disk D_d ; cf. (2.1). Then for each pair $(X, Y) = (A, B), (B, D), (D, A), (C, B), (B, D), (D, C)$ (note that (B, D) is listed twice), we draw a half-arrow from each element of $\nabla^+(X)$ to each element of $\nabla^+(Y)$. Similarly, for each blue crossing $c \in J_{u,\beta}$, $i_c < 0$, we consider the four faces A, B, C, D in the blue projection, and then for each $(X, Y) = (A, B), (B, D), (D, A), (C, B), (B, D), (D, C)$, we draw a half-arrow from each element of $\nabla^-(Y)$ to each element of $\nabla^-(X)$. Here, $\nabla^-(X)$ is the set of indices $d \in J_{u,\beta}$ such that X is inside the blue projection of D_b . We obtain a collection of half-arrows between the elements of $J_{u,\beta}$.

Proposition 3.18. *For $c, d \in J_{u,\beta}$, the difference between the number of half-arrows $c \rightarrow d$ and the number of half-arrows $d \rightarrow c$ equals $2\langle C_c, C_d \rangle$.*

In other words, by (3.3), the quiver $\tilde{Q}_{u,\beta}$ is obtained by just summing up the signed half-arrow contributions and dividing the result by 2.

Proof. The above half-arrow description can be replaced by the following local description. Consider a vertex p of $G_{u,\beta}$, and draw the neighborhood of $\mathbf{S}_{u,\beta}$ around p so that p is black. Label the faces around p by A, B, C in counterclockwise order. For $X \in \{A, B, C\}$, let $\nabla_p(X)$ denote the set of indices $c \in J_{u,\beta}$ such that C_c passes through p with X to the left of C_c . Then for each $(X, Y) = (A, B), (B, C), (C, A)$, draw a half-arrow from each element of $\nabla_p(X)$ to each element of $\nabla_p(Y)$.

Consider two relative cycles C_c, C_d , for $c, d \in J_{u,\beta}$. Recall from Algorithm 3.8 that the intersection number $\langle C_c, C_d \rangle$ may be computed as a sum of local contributions $\langle C_c, C_d \rangle|_P$ from maximal by inclusion paths in $C_c \cap C_d$. Such contributions are shown in the top row of Figure 13(right). On the other hand, as shown in the bottom row of Figure 13(right), the (signed) contribution to the number of half-arrows $c \rightarrow d$ is ± 1 for p_0 and p_r (and zero for each of p_1, \dots, p_{r-1}) so that the combined half-arrow contribution from p_0 and p_r is exactly $2\langle C_c, C_d \rangle|_P$. Summing over all such paths P , the result follows. \square

3.8. Postnikov’s plabic graphs. We explain how our 3D plabic graphs generalize the plabic graphs of [Pos06]. A permutation $w \in S_n$ is called k -Grassmannian if $w(1) < \dots <$

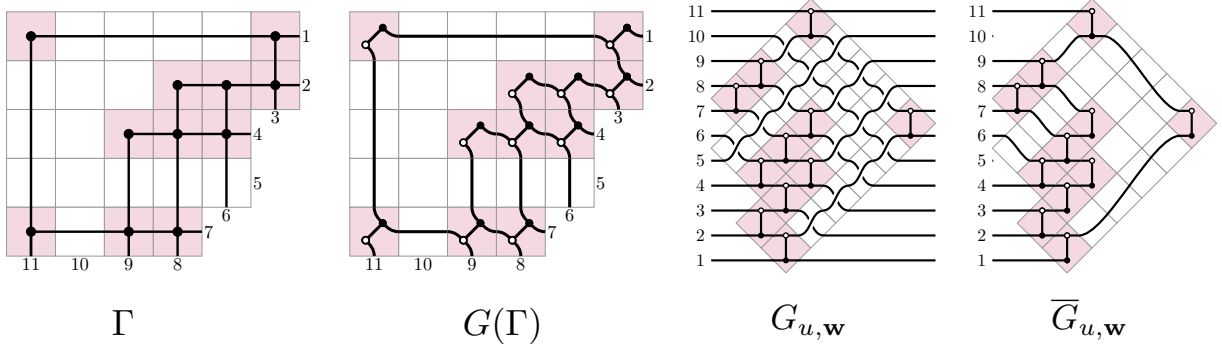
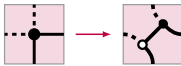


FIGURE 14. Left: converting a Le-diagram Γ into a plabic graph $G(\Gamma)$. Right: the graphs $G_{u,w}$ and $\overline{G}_{u,w}$ for (u, w) corresponding to Γ .

$w(n-k)$ and $w(n-k+1) < \dots < w(n)$. We denote by $S_n^{(k)}$ the set of k -Grassmannian permutations. Thus, any reduced word for $w \in S_n^{(k)}$ ends with s_{n-k} , and all reduced words for w are related by commutation moves. It is well known that k -Grassmannian permutations are in bijection with Young diagrams that fit inside a $k \times (n-k)$ rectangle. We draw Young diagrams in English notation. A *Le-diagram* is a way of placing a dot in some of the boxes of λ so that whenever a box of λ has a dot above it in the same column and to the left of it in the same row, it must also contain a dot. For each dot, we draw horizontal and vertical line segments connecting it to the southeastern boundary of λ . An example of a Le-diagram Γ is shown in Figure 14(left). One can convert a Le-diagram Γ into a plabic graph $G(\Gamma)$ using

the local rule . The graph $G(\Gamma)$ is drawn in a disk which we identify with

the Young diagram λ . Thus, $G(\Gamma)$ has n boundary vertices on the southeastern boundary of λ , and it has a unique northwestern boundary face which we denote F_0 . Rotating Γ by 135° clockwise, replacing all empty boxes with crossings, and all dots with black-white bridges, we obtain a graph $G_{u,w}$, where \mathbf{w} is a reduced word for w and $u \leq w$ in the Bruhat order on S_n ; see Figure 14.

Proposition 3.19. *Let Γ be a Le-diagram and let $u \leq w$ be the corresponding pair of permutations. Then we have*

$$G(\Gamma) = \overline{G}_{u,w}.$$

Moreover, each relative cycle C_c of $\overline{G}_{u,w}$ traverses the boundary of a face of $G(\Gamma)$ in the counterclockwise direction, and this gives a bijection between the relative cycles $(C_c)_{c \in J_{u,w}}$ and all faces of $G(\Gamma)$ except F_0 .

Proof. It follows from the definition of a Le-diagram that once a strand in $G_{u,w}$ participates in a hollow crossing, it never participates in a solid crossing to the right of that hollow crossing. In particular, all hollow crossings disappear when we pass from $G_{u,w}$ to $\overline{G}_{u,w}$, and thus it follows that $G(\Gamma) = \overline{G}_{u,w}$; see also [Kar16, Figure 5] and [GL19, Figure 7]. An example is given in Figure 14(right).

To compute the relative cycles in $G_{u,w}$, we may use the propagation rules in Figure 2. From here, the statement that the relative cycles correspond to the faces of $G(\Gamma)$ follows immediately. \square

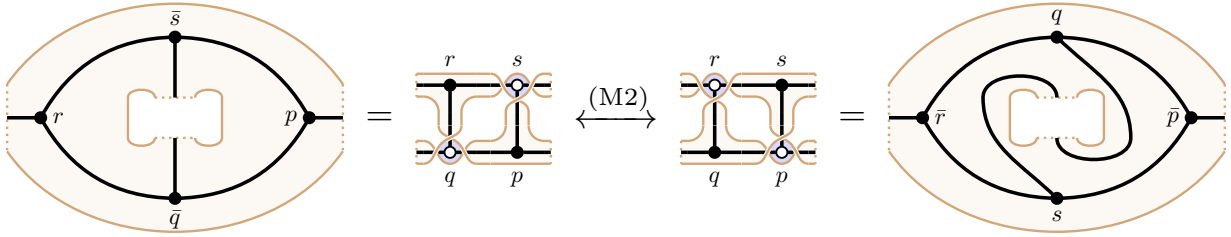


FIGURE 15. Applying a square move (M2) to $G_{u,\beta}$ preserves the surface $\mathbf{S}_{u,\beta}$ but changes the embedding of $G_{u,\beta}$ in $\mathbf{S}_{u,\beta}$. See also [GK13, Figure 20].

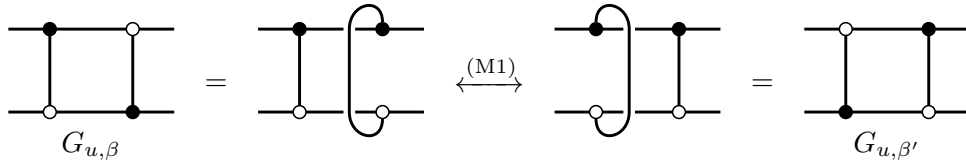


FIGURE 16. Representing the square move (M2) as a composition of two contraction-uncontraction moves (M1).

4. INVARIANCE UNDER MOVES

In this section, we show that the mutation class of the quiver $\tilde{Q}_{u,\beta}$ defined above is invariant under applying *double braid moves* to β .

4.1. Moves for 3D plabic graphs. Just as in Postnikov's theory [Pos06], our two main moves for 3D plabic graphs are the *contraction-uncontraction move* (M1) and the *square move* (M2), shown in Figure 9(middle). The move (M1) can be performed on any edge $e = \{p, q\}$ of a 3D plabic graph G . Specifically, we draw G in the plane so that p and q are of the same color, and then we apply the usual contraction-uncontraction move, producing two other vertices of the same color as p and q . The move (M2) can be performed on any 4-cycle (p, q, r, s) in G , as shown in Figure 15. The moves (M1)–(M2) preserve the conjugate surface $\mathbf{S} = \mathbf{S}(G)$ but change the embedding of G inside of \mathbf{S} . In particular, it will be important later that as one applies the various *double braid moves* to the double braid word β , the surface $\mathbf{S}_{u,\beta}$ stays unchanged throughout the process.

Remark 4.1. Surprisingly, the square move (M2) can be obtained by performing two contraction-uncontraction moves (M1) on G ; see Figure 16. We still distinguish (M2) as a separate transformation, for the following reason. We have associated three kinds of objects to a pair (u, β) : a 3D plabic graph $G_{u,\beta}$, a marked surface $\mathbf{S}_{u,\beta}$, and a collection $(C_c)_{c \in J_{u,\beta}}$ of relative cycles in $\mathbf{S}_{u,\beta}$. While $G_{u,\beta}$ determines $\mathbf{S}_{u,\beta}$, neither $G_{u,\beta}$ nor $\mathbf{S}_{u,\beta}$ determines $(C_c)_{c \in J_{u,\beta}}$. Thus, if one applies moves (M1)–(M2) to $G_{u,\beta}$, one has to specify additional rules for how the tuple $(C_c)_{c \in J_{u,\beta}}$ changes. These rules are given in Theorem 4.3 below: the tuple $(C_c)_{c \in J_{u,\beta}}$ changes according to (3.4) when we apply *mutation braid moves* corresponding to (M2), and is preserved when we apply *non-mutation braid moves* corresponding to other sequences of moves (M1).

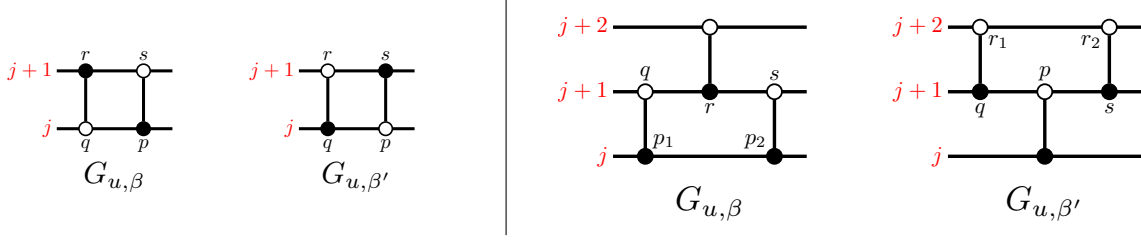


FIGURE 17. Applying braid moves from part (1) of Theorem 4.3 results in applying a square move to $G_{u, \beta}$.

4.2. Moves for double braid words. Two double braid words are (*double braid*) *equivalent* if they are related by a sequence of the following double braid moves:

- (B1) $ij \leftrightarrow ji$ if $i, j \in \pm I$ have different signs;
- (B2) $ij \leftrightarrow ji$ if $i, j \in \pm I$ have the same sign and $|i - j| > 1$;
- (B3) $iji \leftrightarrow jij$ if $i, j \in \pm I$ have the same sign and $|i - j| = 1$.

Definition 4.2. We say that a double braid move is *fully solid* if all of the indices involved are solid. Suppose that $i_{d-1} = -j$ and $i_d = i$ for some $i, j \in I$ and $2 \leq d \leq m$. Then we say that the move (B1) swapping these two indices is *special* if $u_{(d-1)}s_i = s_ju_{(d-1)}$, and *solid-special* if it is special and fully solid. Motivated by the following theorem, we call (B1) (solid-special) and (B3) (fully solid) *mutation moves*. All other braid moves are *non-mutation moves*.

Theorem 4.3. *The mutation type of $\tilde{Q}_{u, \beta}$ is invariant under double braid moves (B1)–(B3) on β . More precisely:*

- (1) *Under mutation moves, the quiver $\tilde{Q}_{u, \beta}$ changes by a mutation. The relative cycles $(C_c)_{c \in J_{u, \beta}}$ change according to (3.4). The graph $G_{u, \beta}$ changes by a square move (M2).*
- (2) *Under non-mutation moves, the quiver $\tilde{Q}_{u, \beta}$ and the relative cycles $(C_c)_{c \in J_{u, \beta}}$ are unchanged, up to relabeling. The graph $G_{u, \beta}$ changes by a sequence of contraction-uncontraction moves (M1).*

In both cases, the surface $\mathbf{S}_{u, \beta}$ is unchanged.

We prove Theorem 4.3 in the next two subsections. Throughout, we let β and β' be two braids related by one of the moves in Theorem 4.3. We denote the 3D plabic graphs by $G_{u, \beta}$ and $G_{u, \beta'}$, the surfaces by $\mathbf{S}_{u, \beta}$ and $\mathbf{S}_{u, \beta'}$, and the relative cycles by $(C_c)_{c \in J_{u, \beta}}$ and $(C'_c)_{c \in J_{u, \beta'}}$, respectively.

4.3. Mutation moves. We prove part (1) of Theorem 4.3. Assume that we are applying a mutation move involving either the indices i_{d-1}, i_d or i_{d-2}, i_{d-1}, i_d for some $d \in J_{u, \beta}$. By Lemma 3.13, it suffices to show that the relative cycles change according to (3.4), i.e., that $C'_c = \mu_d(C_c)$ for all $c \in J_{u, \beta}$.

4.3.1. Applying (B1) (solid-special). We would like to swap two solid crossings $i_{d-1} = -i$ and $i_d = j$ (with $i, j \in I$) such that $u_{(d-1)}s_i = s_ju_{(d-1)}$. Since $d-1, d$ are both solid, we have $u_{(d-2)} = u_{(d-1)} = u_{(d)}$. In addition, using $u_{(d)}s_i = s_ju_{(d)}$, we find that $u_{(d)}(i) = j$ and $u_{(d)}(i+1) = j+1$. The graph $G_{u, \beta}$ therefore contains a 4-cycle spanned by the pair (b_{d-1}, b_d) of bridges of opposite color; see Figure 17(left). It follows that the graph $G_{u, \beta'}$ is

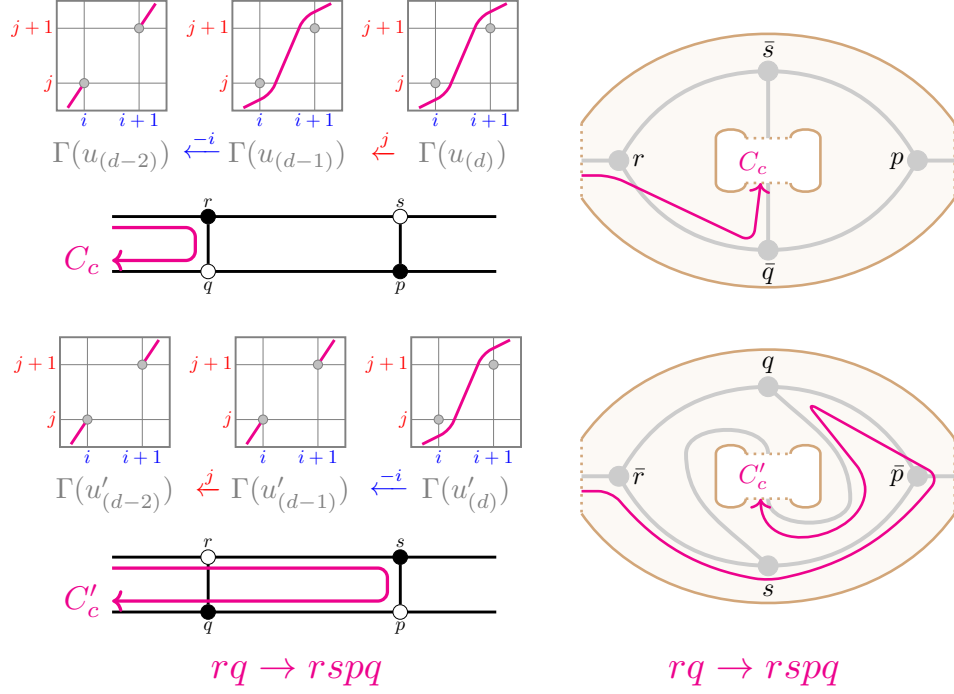


FIGURE 18. An example of computing the signature $rq \rightarrow rspq$ of a relative cycle C_c under the move (B1) (solid-special).

obtained from $G_{u,\beta}$ by applying a square move (M2). In particular, we have $\mathbf{S}_{u,\beta} = \mathbf{S}_{u,\beta'}$; see Figure 15.

We will show that $C'_c = \mu_d(C_c)$ by classifying all possible cases of how a relative cycle C_c can look around the square $psrq$. This amounts to classifying the behavior of the monotone multicurves $\gamma^{(c,d)}, \gamma^{(c,d-1)}, \gamma^{(c,d-2)}$ around the dots $\mathfrak{d} := (i, j)$ and $\mathfrak{d}' := (i+1, j+1)$ of $\Gamma(u_{(d)})$. Note that, with the exception of the relative cycles C_d and C_{d-1} , the monotone multicurve $\gamma^{(c,d)}$ determines $\gamma^{(c,d-1)}$ and $\gamma^{(c,d-2)}$. Moreover, it suffices to consider the behavior of each monotone curve of $\gamma^{(c,d)}$ separately; cf. Remark 4.4 below.

For a relative cycle C_c in $G_{u,\beta}$, its *signature* is the ordered list of vertices of the square $psrq$ that C_c passes through. For example, let us consider a monotone curve γ inside $\Gamma(u_{(d)})$ passing below \mathfrak{d} and above \mathfrak{d}' , as in Figure 18. Using the rules in Figure 8, we propagate γ to $\Gamma(u_{(d-1)})$ and $\Gamma(u_{(d-2)})$, and find that the relevant part of C_c passes first through r and then through q in $G_{u,\beta}$. Therefore, the signature of this relative cycle is rq . Repeating the same procedure for the graph $G_{u,\beta'}$, we find that the signature of C_c in $G_{u,\beta'}$ is $rspq$; see Figure 18(left). As shown in Figure 18(right), the cycle with signature rq in $G_{u,\beta}$ is homotopic to the cycle with signature $rspq$ in $G_{u,\beta'}$ when we view them as cycles in the ambient surface $\mathbf{S}_{u,\beta} = \mathbf{S}_{u,\beta'}$.

In Figure 19, we list all possible relative cycles that pass through at least one vertex of the square $psrq$, given together with their monotone curves γ inside $\Gamma(u_{(d)})$ and the signatures in $G_{u,\beta}$ and $G_{u,\beta'}$. For example, C_d is shown in Figure 19(a), and the curve γ from Figure 18 is shown in Figure 19(d).

We will want to understand how C_c and C'_c relate, not as drawn in the planar projections in Figure 19, but as drawn on the surface $\mathbf{S}_{u,\beta} = \mathbf{S}_{u,\beta'}$. Comparing the signatures to Figure 15, we see that for all $c \in J_{u,\beta}$, the following are equivalent:

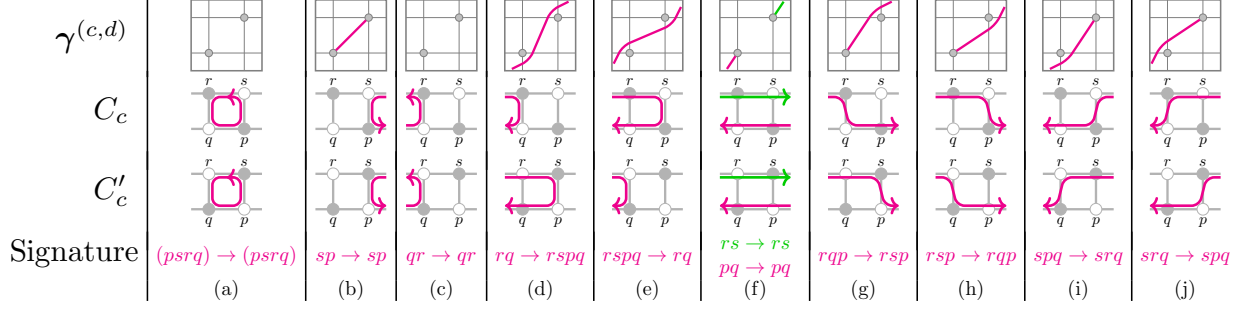


FIGURE 19. The possible relative cycles and their signatures for the proof in Section 4.3.1.

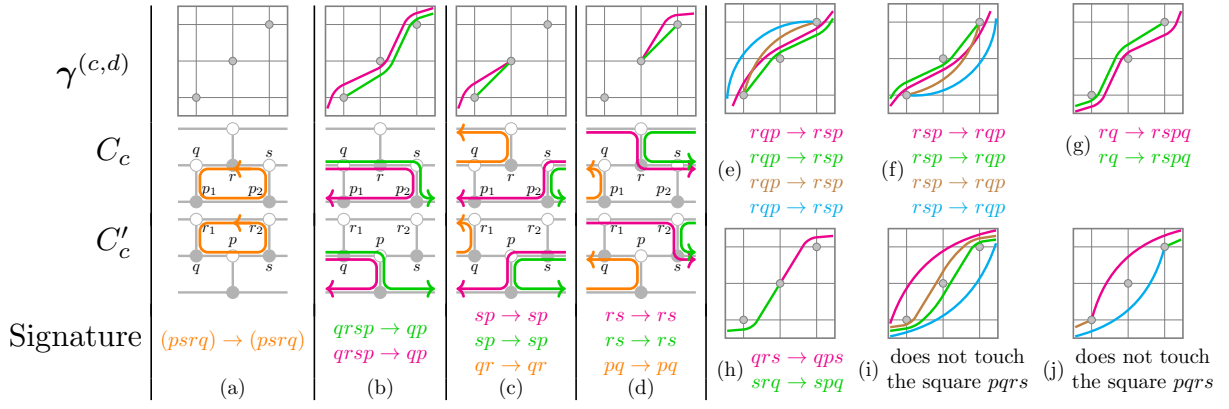


FIGURE 20. The possible signatures for the proof in Section 4.3.2.

- $C_c \neq C'_c$ (as elements of $\Lambda_{u,\beta} = \Lambda_{u,\beta'}$);
- either $c = d$ or $\langle C_c, C_d \rangle > 0$ (in which case $\langle C_c, C_d \rangle = 1$);
- C_c is shown in Figure 19(a,b,c).

Note that C_d is represented in the notation of Figure 15 as the cycle passing through the vertices of the square $psrq$. Thus, in order to have $\langle C_c, C_d \rangle > 0$, when C_c is drawn in Figure 15(far left), it needs to start inside $psrq$ and end outside of $psrq$. This happens precisely when C_c is one of the relative cycles shown in Figure 19(b,c). We see that indeed in all cases, we have $C'_c = \mu_d(C_c)$.

Remark 4.4. In general, C_c is represented by a monotone *multicurve* inside $\Gamma(u_d)$, and thus, for example, the two monotone curves shown in Figure 19(f) could be parts of a single monotone multicurve. However, this does not affect our analysis because the intersection number $\langle C_c, C_d \rangle$ is additive over all intersection points in $C_c \cap C_d$.

4.3.2. *Applying (B3) (fully solid).* We proceed using a similar strategy. Suppose that $i_{d-2} = j$, $i_{d-1} = j+1$, and $i_d = j$ for some $j \in I$, with all three indices solid. The 3D plabic graphs $G_{u,\beta}$ and $G_{u,\beta'}$ are shown in Figure 17(right). In particular, after applying a contraction-uncontraction move (M1) to the vertices p_1, p_2 of $G_{u,\beta}$ and to the vertices r_1, r_2 of $G_{u,\beta'}$, we obtain two graphs which differ by a square move (M2), where the square has vertices $psrq$. Abusing notation, we denote these two graphs again by $G_{u,\beta}$ and $G_{u,\beta'}$.

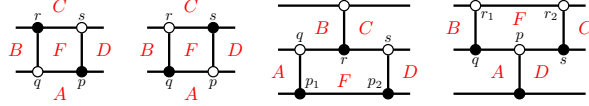


FIGURE 21. Labeling the faces when applying the square move.

Let us now classify the relative cycles. There are a total of 26 options for how a monotone curve can look like inside $\Gamma(u_{(d)})$. In addition, there are 3 more relative cycles C_d, C_{d-1}, C_{d-2} which do not correspond to any monotone curves in $\Gamma(u_{(d)})$, shown in orange in Figure 20(a,c,d). Out of these 29 options, 8 relative cycles shown in Figure 20(i,j) do not pass through any of the vertices of the square $psrq$ (after applying the above contraction-uncontraction moves). The remaining 21 relative cycles, together with their signatures in $G_{u,\beta}$ and $G_{u,\beta'}$, are shown in Figure 20(a–h).

Comparing the signatures to Figure 15, we see that for all $c \in J_{u,\beta}$, the following are equivalent:

- $C_c \neq C'_c$;
- either $c = d$ or $\langle C_c, C_d \rangle > 0$ (in which case $\langle C_c, C_d \rangle = 1$);
- C_c is shown in Figure 20(a,b,c).

We again get that $C'_c = \mu_d(C_c)$ in each case. This completes the proof of part (1) of Theorem 4.3.

4.3.3. Chamber minors. Suppose we are applying one of the mutation moves from part (1) of Theorem 4.3 at C_d for some $d \in J_{u,\beta}^{\text{mut}}$. Then (after possibly applying moves (M1) from Section 4.3.2), the graph $G_{u,\beta}$ contains a square $psrq$. Let G be the portion of the red projection of $G_{u,\beta}$ located in the small neighborhood of $psrq$; thus, G is planar. Let F be the face of G inside this square, and let A, B, C, D be the four faces adjacent to the square in clockwise order; see Figure 21. (We only consider A, B, C, D in a small neighborhood of the square.) For $c \in J_{u,\beta}$ and a face $E \in \{F, A, B, C, D\}$, we will write $\text{ord}_c(E) = 1$ if E is inside C_c and $\text{ord}_c(E) = 0$ otherwise. As in Section 2.4, we say that E is *inside* C_c if E is contained inside the red projection of the disk D_c , or in other words, if E is to the left of the curve representing the red projection of C_c . We define $\text{ord}'_c(E)$ similarly using the graph $G_{u,\beta'}$ and the cycles C'_c in it. It follows from part (1) of Theorem 4.3 that the difference $C_c - C'_c$ in $\Lambda_{u,\beta}$ is always a multiple of C_d . Thus, we have $\text{ord}'_c(E) = \text{ord}_c(E)$ for $E \neq F$. (Alternatively, this can be seen directly from Figures 19 and 20.) The following result will be used in the proof of Proposition 8.11.

Lemma 4.5. *For all $c \in J_{u,\beta} \setminus \{d\}$, we have*

$$(4.1) \quad \text{ord}_c(F) + \text{ord}'_c(F) = \min(\text{ord}_c(A) + \text{ord}_c(C), \text{ord}_c(B) + \text{ord}_c(D)).$$

Proof. Follows by inspection from Figures 19 and 20. For example, if C_c is given in Figure 19(d) then (4.1) becomes $1 + 0 = \min(0 + 1, 1 + 1)$. Similarly, if both monotone curves in Figure 19(f) are parts of the same monotone multicurve corresponding to C_c then (4.1) becomes $0 + 0 = \min(0 + 0, 1 + 1)$. \square

4.4. Non-mutation moves. We prove part (2) of Theorem 4.3. The following result will be convenient to show equalities of the form $C'_c = C_c$ without classifying all possible monotone curves as we did in Section 4.3.

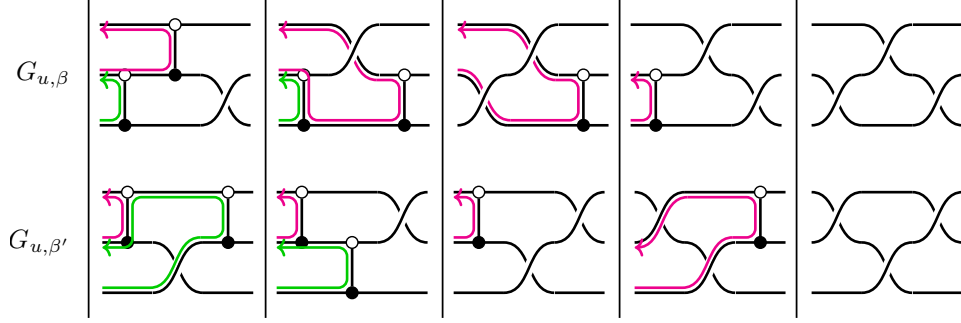


FIGURE 22. Applying move (B3) (not fully solid).

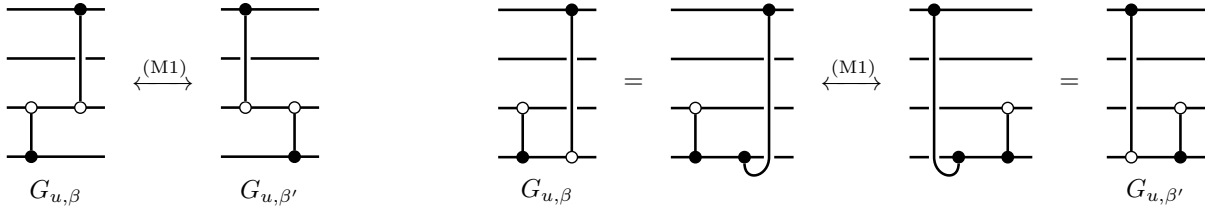


FIGURE 23. Representing the move (B1) (not special) by the moves from Figure 9.

Lemma 4.6. *Suppose that the double braids β, β' are related by one of the moves (B1)–(B3) involving the indices in some interval $(l, r) \subset [m]$ of length 2 or 3. Suppose in addition that the portion $G_{u, \beta}|_{[l, r]}$ of $G_{u, \beta}$ between $\Gamma(u_{(l)})$ and $\Gamma(u_{(r)})$ has no cycles, and that $G_{u, \beta'}|_{[l, r]}$ is obtained from $G_{u, \beta}|_{[l, r]}$ via a sequence of contraction-uncontraction moves (M1). Then, for all $c \in J_{u, \beta} \setminus (l, r]$, we have $C_c = C'_c$.*

Proof. By Proposition 3.16, the monotone multicurves of C_c inside $\Gamma(u_{(l)})$ and $\Gamma(u_{(r)})$ are determined by the combinatorics of *almost positive subexpressions*, specifically, by the pairs $(u_{(l)}, v_{(c)}^{(l)})$ and $(u_{(r)}, v_{(c)}^{(r)})$. One can check (cf. Figure 22) that these pairs are invariant under applying the moves (B1)–(B3) on the interval $(l, r]$. Thus, we see that the monotone multicurves of C_c inside $\Gamma(u_{(l)})$ and $\Gamma(u_{(r)})$ are preserved under the double braid move. Thus, the locations where C_c enters and exits $G_{u, \beta}|_{[l, r]}$ remain unchanged as we apply the move. Since $G_{u, \beta}|_{[l, r]}$ has no cycles, the restriction of C_c to $G_{u, \beta}|_{[l, r]}$ is determined by these locations. It is then clear that as we apply the moves (M1) to $G_{u, \beta}|_{[l, r]}$, the relative cycle C_c is preserved. \square

In order to prove part (2) of Theorem 4.3, it suffices to find a *relabeling bijection* $J_{u, \beta} \xrightarrow{\sim} J_{u, \beta'}$, $c \mapsto c'$, such that $C'_{c'} = C_c$ for all $c \in J_{u, \beta}$.

4.4.1. Applying (B1) (special, not fully solid). Just as in Section 4.3.1, we assume that we have two crossings $i_{d-1} = -i$ and $i_d = j$ (with $i, j \in I$) such that $u_{(d-1)}s_i = s_ju_{(d-1)}$, but now at least one of the two crossings is hollow. In this case, we must have that d is hollow and $d-1$ is solid. Indeed, recall from (3.1) that $u_{(d-1)} = u_{(d)} \triangleleft s_j$ and $u_{(d-2)} = s_i \triangleright u_{(d-1)}$. If $u_{(d-1)} = u_{(d)}s_j < u_{(d)}$ then d is hollow, and then $s_iu_{(d-1)} = u_{(d-1)}s_j = u_{(d)} > u_{(d-1)}$, so $d-1$ must be solid. Otherwise, we have $u_{(d-1)} = u_{(d)} < u_{(d)}s_j$, and then $s_iu_{(d-1)} = u_{(d-1)}s_j > u_{(d-1)}$, so both d and $d-1$ are solid, a contradiction.

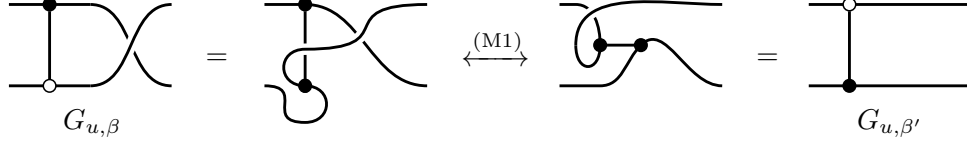


FIGURE 24. Representing the move (B1) (special, not fully solid) by the moves from Figure 9.

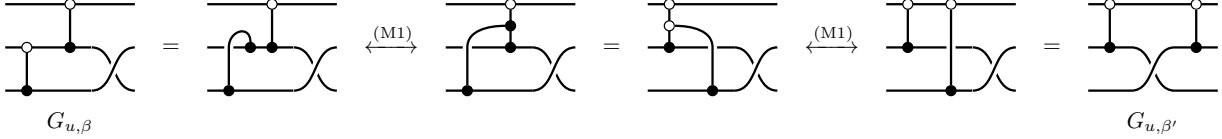


FIGURE 25. Representing the move (B3) (not fully solid) by the moves from Figure 9.

After we swap $-i$ and j in β , the crossing $i'_d = -i$ becomes hollow while $i'_{d-1} = j$ becomes solid. Thus, we have $J_{u,\beta} = J_{u,\beta'}$. We take the relabeling bijection to be the identity map. The graphs $G_{u,\beta}$ and $G_{u,\beta'}$ are related by a single move (M1) shown in Figure 24, and their restrictions to $[d-2, d]$ have no cycles. By Lemma 4.6, we get $C'_c = C_c$ inside $\Lambda_{u,\beta} = \Lambda_{u,\beta'}$ for all $c \in J_{u,\beta}$.

4.4.2. *Applying (B1) (not special)*. We take the relabeling bijection $c \mapsto c'$ to be the transposition of $d-1$ and d . If one or both of the crossings $d-1, d$ is hollow, we have $G_{u,\beta} = G_{u,\beta'}$, and we check using Lemma 4.6 that $C_c = C'_{c'}$ for all $c \in J_{u,\beta}$. Assume now that both crossings $d-1$ and d are solid.

If the bridges b_{d-1}, b_d share two strands in common then the move (B1) is special, a contradiction. If the bridges b_{d-1}, b_d share zero strands in common then $G_{u,\beta} = G_{u,\beta'}$, and we are done by Lemma 4.6. From now on, we assume that the bridges b_{d-1}, b_d share exactly one strand in common.

There are two cases: either the start of one bridge is on the same strand as the end of the other bridge, or the start (resp., the end) of one bridge is on the same strand as the start (resp., the end) of the other bridge. In each case, $G_{u,\beta}$ and $G_{u,\beta'}$ are related by a sequence of moves (M1) shown in Figure 23. We are done by Lemma 4.6.

4.4.3. *Applying (B2)*. We take the relabeling bijection $c \mapsto c'$ to be the transposition of $d-1$ and d . We have $G_{u,\beta} = G_{u,\beta'}$. We are done by Lemma 4.6.

4.4.4. *Applying (B3) (not fully solid)*. Suppose that $i_{d-2} = j$, $i_{d-1} = j+1$, and $i_d = j$ for some $j \in I$. In $\Gamma(u_{(d-3)})$, the dots (i, j) , $(i', j+1)$, $(i'', j+2)$ are located in \prec -increasing order, i.e., we have $i < i' < i''$. The restriction of $\Gamma(u_{(d)})$ to the rows $j, j+1, j+2$ and columns i, i', i'' , however, could be any permutation in S_3 . If this permutation is the identity, then the crossings $d-2, d-1, d$ are all solid, a contradiction. For each of the remaining five permutations in S_3 , the corresponding graphs $G_{u,\beta}$ and $G_{u,\beta'}$ are shown in Figure 22. Observe that their restrictions to $[d-3, d]$ have no cycles. In some cases, we have $G_{u,\beta} = G_{u,\beta'}$. In the remaining two cases (one of which is obtained from the other by a vertical flip), the sequence of moves (M1) relating $G_{u,\beta}$ to $G_{u,\beta'}$ is shown in Figure 25. In each of the five cases, there

is a unique relabeling bijection $J_{u,\beta} \cap \{d-2, d-1, d\} \xrightarrow{\sim} J_{u,\beta'} \cap \{d-2, d-1, d\}$ preserving the monotone multicurve inside $\Gamma(u_{(d-3)})$; it is indicated by colored curves in Figure 22. Extending the relabeling bijection by the identity map outside the interval $\{d-2, d-1, d\}$, we are done by Lemma 4.6. This finishes the proof of Theorem 4.3.

4.5. Color-switching moves. We introduce two more moves, which allow us to switch the color of the first or the last letter of β . For $i \in I = [n-1]$, let $i^* := n-i$, so that $s_i w_0 = w_0 s_{i^*}$.

(B4) (assuming $u = w_0$) $\beta_0 i \leftrightarrow \beta_0(-i^*)$ for $i \in \pm I$ and $\beta_0 \in (\pm I)^{m-1}$.

(B5) $i\beta_0 \leftrightarrow (-i)\beta_0$ for $i \in \pm I$ and $\beta_0 \in (\pm I)^{m-1}$;

Note that the assumption $u = w_0$ in (B4) is not restrictive in view of Remark 3.3.

For an ice quiver \tilde{Q} , its *mutable part* is the induced subquiver of \tilde{Q} with vertex set V^{mut} , where V^{mut} is the set of mutable vertices of \tilde{Q} .

Proposition 4.7.

(1) Under the move (B4), $\tilde{Q}_{u,\beta}$, $G_{u,\beta}$, $\mathbf{S}_{u,\beta}$, and $(C_c)_{c \in J_{u,\beta}}$ are unchanged.

(2) Under the move (B5), the mutable part $Q_{u,\beta}$ of $\tilde{Q}_{u,\beta}$ is unchanged.

Proof. First, let us consider the move (B4). Since $u = w_0$, the index m must be hollow. There are no relative cycles passing through the corresponding strands of $G_{u,\beta}$, since they only pass through the graph $\bar{G}_{u,\beta}$ from Section 3.2. This verifies the first part of the proposition.

Now, consider the move (B5). Without loss of generality, assume that $i := i_1 > 0$. Since we only care about the mutable part of $\tilde{Q}_{u,\beta}$, we may disregard all frozen indices, i.e., indices $c \in J_{u,\beta}$ such that the monotone multicurve $\gamma^{(c,0)}$ is nonempty. The index 1 is either hollow or frozen. For any mutable index $d \in J_{u,\beta}$, if $\gamma^{(d,1)}$ is empty then the intersection number $\langle C_c, C_d \rangle$ clearly stays unchanged under (B5) for all $c \in J_{u,\beta}$. Let $c \in J_{u,\beta}$ be a mutable index such that the monotone multicurve $\gamma^{(c,1)}$ is nonempty (but $\gamma^{(c,0)}$ is empty). Then the index 1 must be solid (and therefore frozen). Using a contraction-uncontraction move similar to the one in Figure 24, we see that the marked surface $\mathbf{S}_{u,\beta'}$ (where β' is obtained by applying (B5) to β) is obtained from $\mathbf{S}_{u,\beta}$ by swapping the labels of the marked points i and $i+1$. Since this swap does not affect the part of $\mathbf{S}_{u,\beta}$ to the right of $\Gamma(u_{(0)})$, we see that for any two mutable relative cycles C_c, C_d that pass through the bridge b_1 , their intersection number is unchanged under (B5). This verifies the second part of the proposition. \square

5. CLUSTER ALGEBRAS ASSOCIATED TO 3D PLABIC GRAPHS

The goal of this section is to show that the cluster algebra defined by $\tilde{Q}_{u,\beta}$ is *locally acyclic* [Mul13] and *really full rank* [LS16].

5.1. Background on cluster algebras. We briefly recall the definition of a cluster algebra and related concepts.

Recall from Section 2.3 the definition of an ice quiver \tilde{Q} , with vertex set $\tilde{V} = V^{\text{mut}} \sqcup V^{\text{fro}}$. We say that \tilde{Q} is *isolated* if its mutable part has no arrows. For a set $S \subset V^{\text{mut}}$, let $\tilde{Q}[S]$ denote the ice quiver obtained from \tilde{Q} by further declaring all vertices in S to be frozen. We write $\tilde{Q} - S$ for the ice quiver obtained from \tilde{Q} by removing the vertices in S .

The associated (*extended*) *exchange matrix* $\tilde{B}(\tilde{Q}) = (b_{v,w})_{v \in \tilde{V}, w \in V^{\text{mut}}}$ is defined by

$$b_{v,w} = \#\{\text{arrows } v \rightarrow w \text{ in } \tilde{Q}\} - \#\{\text{arrows } w \rightarrow v \text{ in } \tilde{Q}\}$$

Definition 5.1. We say that \tilde{Q} is *really full rank* if the rows of its exchange matrix span $\mathbb{Z}^{|V^{\text{mut}}|}$ over \mathbb{Z} .

Let $\mathcal{F} \cong \mathbb{C}(t_1, \dots, t_r)$ be isomorphic to the field of rational functions in r algebraically independent variables. A *seed* in \mathcal{F} is a pair $\Sigma = (\mathbf{x}, \tilde{Q})$ where \tilde{Q} is an ice quiver with r vertices $\tilde{V} = V^{\text{mut}} \sqcup V^{\text{fro}}$ and $\mathbf{x} = \{x_v\}_{v \in \tilde{V}}$ is a transcendence basis of \mathcal{F} . The tuple \mathbf{x} is the *cluster*, its elements are *cluster variables* and x_v is *mutable* if $v \in V^{\text{mut}}$ and *frozen* otherwise.

Given a seed (\mathbf{x}, \tilde{Q}) in \mathcal{F} and $d \in V^{\text{mut}}$, one can *mutate* in direction d to obtain a new seed $\mu_d(\mathbf{x}, \tilde{Q}) = (\mathbf{x}', \mu_d(\tilde{Q}))$. The quiver of the mutated seed is the mutation of \tilde{Q} in direction d (see Definition 3.12). The cluster $\mathbf{x}' = \{x'_v\}_{v \in \tilde{V}}$ of the new seed satisfies $x'_v = x_v$ for $v \neq d$ and

$$x'_d = \frac{\prod_{v \rightarrow d} x_v + \prod_{d \rightarrow v} x_v}{x_d} \in \mathcal{F}.$$

By repeatedly mutating, we generate (possibly infinitely) many seeds and cluster variables. We denote by $\mathcal{A}(\mathbf{x}, \tilde{Q})$ the *cluster algebra* associated to the seed (\mathbf{x}, \tilde{Q}) . This is the \mathbb{C} -subalgebra of \mathcal{F} generated by all cluster variables and the inverses of frozen variables. We call $\mathcal{A}(\mathbf{x}, \tilde{Q})$ *isolated* (resp., *really full rank*) if \tilde{Q} is.

We denote by $\mathcal{U}(\mathbf{x}, \tilde{Q})$ the *upper cluster algebra* associated to the seed (\mathbf{x}, \tilde{Q}) ; see [BFZ05]. It is given by

$$\mathcal{U}(\mathbf{x}, \tilde{Q}) = \bigcap_{(\mathbf{x}', \tilde{Q}')} \mathbb{C}[(x'_v)^{\pm 1} : v \in \tilde{V}] \subset \mathcal{F},$$

where the intersection is taken over all seeds $(\mathbf{x}', \tilde{Q}')$ which can be obtained from (\mathbf{x}, \tilde{Q}) by a sequence of mutations.

Note that we have isomorphisms $\mathcal{A}(\mathbf{x}, \tilde{Q}) \cong \mathcal{A}(\mathbf{y}, \tilde{Q})$ and $\mathcal{U}(\mathbf{x}, \tilde{Q}) \cong \mathcal{U}(\mathbf{y}, \tilde{Q})$ for any two clusters \mathbf{x}, \mathbf{y} . Thus, we may occasionally write $\mathcal{A}(\tilde{Q})$ and $\mathcal{U}(\tilde{Q})$ if the particular choice of initial cluster does not matter.

In general, we have $\mathcal{A}(\mathbf{x}, \tilde{Q}) \subseteq \mathcal{U}(\mathbf{x}, \tilde{Q})$, and the containment may be strict. However, we have equality if $\mathcal{A}(\mathbf{x}, \tilde{Q})$ is *locally acyclic*, a property introduced by Muller [Mul13]. We need a few definitions before defining local acyclicity; we follow the presentation of [Mul14].

Let $\mathcal{A}(\mathbf{x}, \tilde{Q})$ be a cluster algebra and let $S \subset V^{\text{mut}}$. Then the cluster algebra $\mathcal{A}(\mathbf{x}, \tilde{Q}[S])$ obtained by freezing S is a *cluster localization* of $\mathcal{A}(\mathbf{x}, \tilde{Q})$ if

$$(5.1) \quad \mathcal{A}(\mathbf{x}, \tilde{Q}[S]) = \mathcal{A}(\mathbf{x}, \tilde{Q})[x_v^{-1} : v \in S].$$

(In general, the left-hand side is contained in the right.) Lemma 4.3 of [Mul13] states that if $\mathcal{A}(\mathbf{x}, \tilde{Q}[S]) = \mathcal{U}(\mathbf{x}, \tilde{Q}[S])$, then (5.1) automatically holds.

A collection of cluster localizations $\{\mathcal{A}_i\}$ of a cluster algebra \mathcal{A} is a *cover* if for every prime ideal P of \mathcal{A} , there is some \mathcal{A}_i such that $\mathcal{A}_i P \subsetneq \mathcal{A}_i$. A cluster algebra is *locally acyclic* if it has a cover by isolated cluster algebras. We say that \tilde{Q} is *locally acyclic* if $\mathcal{A}(\tilde{Q})$ is.

We will use the following facts about locally acyclic cluster algebras.

Proposition 5.2 ([Mul13, Proposition 3.10]). *Let \tilde{Q} be an ice quiver and let Q denote its mutable part, as usual. Then $\mathcal{A}(\tilde{Q})$ is locally acyclic if and only if $\mathcal{A}(Q)$ is locally acyclic.*

Theorem 5.3 ([Mul13, Theorem 4.1]). *If $\mathcal{A}(\mathbf{x}, \tilde{Q})$ is locally acyclic, then $\mathcal{A}(\mathbf{x}, \tilde{Q}) = \mathcal{U}(\mathbf{x}, \tilde{Q})$.*

One frequently studied class of locally acyclic quivers are *Louise* quivers [LS16]. We focus instead on *sink-recurrent* quivers, defined below, which may not be Louise but are locally acyclic. In the next subsection, we show that our quivers of interest, $\tilde{Q}_{u,\beta}$, are sink-recurrent (see Theorem 5.6).

Let Q be a quiver with no frozen vertices. A vertex s of Q is a *sink* if it has no outgoing arrows. We let $N_s^{\text{in}}(Q)$ be the set of vertices of Q that have an arrow pointing to s . The following notion is analogous to the class of *leaf-recurrent quivers* from [GL22a, Section 5.4]; see also [GL22a, Remark 5.14].

Definition 5.4. The class of *sink-recurrent quivers* is defined recursively as follows.

- Any isolated quiver Q is sink-recurrent.
- Any quiver that is mutation equivalent to a sink-recurrent quiver is sink-recurrent.
- Suppose that a quiver Q has a sink vertex s such that the quivers $Q - \{s\}$ and $Q - (N_s^{\text{in}}(Q) \cup \{s\})$ are sink-recurrent. Then Q is sink-recurrent.

The above definition refers to mutable quivers (without frozen vertices). We say that an ice quiver \tilde{Q} is *sink-recurrent* if its mutable part Q is sink-recurrent.

Proposition 5.5. *If \tilde{Q} is a sink-recurrent quiver, then $\mathcal{A}(\mathbf{x}, \tilde{Q})$ is locally acyclic.*

Proof. If \tilde{Q} is isolated, we are done. Otherwise, since local acyclicity is a property of the cluster algebra rather than the quiver, we may assume that Q has a sink s so that $Q - \{s\}$ and $Q - (N_s^{\text{in}}(Q) \cup \{s\})$ are sink-recurrent (by mutating if necessary). Consider the freezings $\mathcal{A}_1 = \mathcal{A}(\mathbf{x}, Q[s])$ and $\mathcal{A}_2 = \mathcal{A}(\mathbf{x}, Q[N_s^{\text{in}}(Q)])$. The mutable parts of $Q[s]$ and $Q[N_s^{\text{in}}(Q)]$ are $Q - \{s\}$ and $Q - N_s^{\text{in}}(Q)$, respectively, which are both sink-recurrent, the former by definition, and the latter because $Q - N_s^{\text{in}}(Q)$ differs from the sink-recurrent quiver $Q - (N_s^{\text{in}}(Q) \cup \{t\})$ by an isolated vertex. So \mathcal{A}_1 and \mathcal{A}_2 are locally acyclic by induction, and thus are cluster localizations.

Let t be any neighbor of s . Then the pair (s, t) forms a *covering pair* in the sense of [Mul13], and by [Mul13, Lemma 5.3] it follows that x_s and x_t cannot simultaneously vanish on $\mathcal{A}(\tilde{Q})$. It follows that \mathcal{A}_1 and \mathcal{A}_2 cover \mathcal{A} . The union of the covers of \mathcal{A}_1 and \mathcal{A}_2 by isolated cluster algebras is a cover of $\mathcal{A}(\mathbf{x}, Q)$ by isolated cluster algebras. \square

5.2. Local acyclicity. Our goal is to show the following result, which by Proposition 5.5 implies that the cluster algebra $\mathcal{A}(\mathbf{x}, \tilde{Q})$ is locally acyclic.

Theorem 5.6. *For any $u \leq \beta$, the ice quiver $\tilde{Q}_{u,\beta}$ is sink-recurrent.*

Proof. We proceed by induction on the number $\ell(\beta) - \ell(u)$ of vertices of $\tilde{Q}_{u,\beta}$. For the base case $\ell(\beta) = \ell(u)$, we see that β is a reduced word for u and all crossings are hollow, and thus $\tilde{Q}_{u,\beta}$ is an empty quiver. Let us now assume that $\ell(\beta) > \ell(u)$.

By Remark 3.3, it suffices to consider the case $u = w_0$. Applying the moves (B1) and (B4), we may assume that all indices in β are positive. Then, assuming $\beta = i\beta_0$, we can transform β into

$$(5.2) \quad \beta = i\beta_0 \xrightarrow{\text{(B5)}} (-i)\beta_0 \xrightarrow{\text{(B1)}} \cdots \xrightarrow{\text{(B1)}} \beta_0(-i) \xrightarrow{\text{(B4)}} \beta_0 i^*.$$

We call the operation (5.2) *the conjugation move*.

Since $u = w_0$ and $\ell(\beta) > \ell(u)$, the braid word β must be non-reduced. Then, after applying the moves (B2)–(B3), we may transform β into a word of the form $\beta_1 i i \beta_2$, for two

positive braid words β_1, β_2 . Applying conjugation moves (5.2), we may further transform it into the word $ii\beta_2\beta_1^*$, where β_1^* is obtained from β_1 by applying the map $i \mapsto i^*$ to each index. Applying one more move (B5), we obtain the word $(-i)i\beta_2\beta_1^*$ which we still denote by β .

By the same argument as in Section 4.4.1, we get that the crossing $i_1 = -i$ is solid. Let $\beta' := i\beta_2\beta_1^*$ be obtained by omitting $-i$ from β . Since i_1 is solid, we have $u \leq \beta'$, and by the induction hypothesis, the quiver $Q_{u,\beta'}$ is sink-recurrent.

Suppose first that the crossing $i_2 = i$ is hollow. It is easy to check from the propagation rules in Figure 8 that no mutable relative cycle passes through the bridge b_1 . In particular, we see that $Q_{u,\beta} = Q_{u,\beta'}$, which we know is sink-recurrent by induction.

Suppose now that both crossings $i_1 = -i$ and $i_2 = i$ are solid. The graph $G_{u,\beta}$ has a square $psrq$ formed by the two corresponding bridges as in Figure 15(left). The index $d := 2$ is mutable and the relative cycle C_d passes through the vertices of the square in the counterclockwise direction. Any other mutable relative cycle C_c satisfying $\langle C_c, C_d \rangle \neq 0$ must have signature sp (i.e., pass through the bridge b_2 in the direction opposite to C_d). In particular, we see that $\langle C_c, C_d \rangle = 1$ whenever c is mutable and $\langle C_c, C_d \rangle \neq 0$. It follows that d is a sink in $Q_{u,\beta}$.

Let $\beta'' := \beta_2\beta_1^*$ be obtained by omitting both $-i$ and i from β . We still have $u \leq \beta''$, and by the induction hypothesis, the quiver $Q_{u,\beta''}$ is sink-recurrent. We have $Q_{u,\beta'} = Q_{u,\beta} - \{d\}$. The quiver $Q_{u,\beta''}$ is obtained from $Q_{u,\beta}$ by deleting d together with all vertices that have an arrow pointing to d , since the corresponding cycles become frozen in $G_{u,\beta''}$. The result follows. \square

Remark 5.7. Similar reasoning has been recently used in [GL22a, Proposition 7.9] to study *plabic fences*, which are recovered as special cases of our construction when $u = \text{id}$.

From Theorem 5.6 and Proposition 5.5, we have the following immediate corollary.

Corollary 5.8. *For any $u \leq \beta$, the quiver $\tilde{Q}_{u,\beta}$ is locally acyclic.*

5.3. Really full rank. Our goal is to show the following result; cf. Definition 5.1.

Theorem 5.9. *The quiver $\tilde{Q}_{u,\beta}$ is really full rank.*

In order to give a proof, we study the marked surface $(\mathbf{S}_{u,\beta}, \mathbf{M})$ and the lattices $\Lambda_{u,\beta} = H_1(\mathbf{S}_{u,\beta}, \mathbf{M})$ and $\Lambda_{u,\beta}^* = H_1(\mathbf{S}_{u,\beta} \setminus \mathbf{M}, \partial\mathbf{S}_{u,\beta} \setminus \mathbf{M})$ in more detail. See Figure 6(d) for an example of a surface $\mathbf{S}_{u,\beta}$. We first construct an explicit basis of $\Lambda_{u,\beta}^*$. Recall from Section 3.3 that $\mathbf{S}_{u,\beta}$ is obtained by replacing every edge of $G_{u,\beta}$ with a thin rectangle and gluing them together at the vertices of $G_{u,\beta}$. For every edge e of $G_{u,\beta}$, let the *dual edge* $e^* \in \Lambda_{u,\beta}^*$ denote some orientation of a short line segment intersecting e connecting the opposite boundaries of the corresponding thin rectangle.

Lemma 5.10. *The elements $(b_c^*)_{c \in J_{u,\beta}}$ form a \mathbb{Z} -basis of $\Lambda_{u,\beta}^*$.*

Proof. Recall from (3.2) that the lattices $\Lambda_{u,\beta}$ and $\Lambda_{u,\beta}^*$ are dual to each other. Since $\mathbf{S}_{u,\beta}$ deformation retracts onto $G_{u,\beta}$, we see that $\Lambda_{u,\beta} \cong \mathbb{Z}^{|J_{u,\beta}|}$ is a free abelian group whose rank is the number of bridges in $G_{u,\beta}$. Thus, $\Lambda_{u,\beta}^* \cong \mathbb{Z}^{|J_{u,\beta}|}$, and it suffices to show that the elements $(b_c^*)_{c \in J_{u,\beta}}$ span $\Lambda_{u,\beta}^*$ over \mathbb{Z} .

It is clear that any element of $\Lambda_{u,\beta}^*$ can be written as a \mathbb{Z} -linear combination of the elements of the form e^* for the various edges e of $G_{u,\beta}$: this can be achieved by taking a curve inside

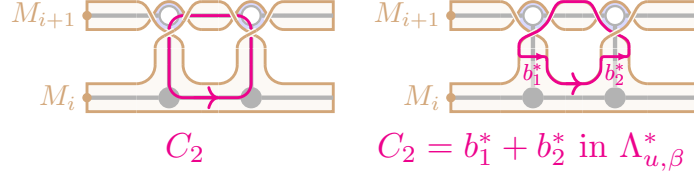


FIGURE 26. Pushing a relative cycle in $\Lambda_{u,\beta}^*$ to the boundary.

$\mathbf{S}_{u,\beta}$ and “pushing it to the boundary,” i.e., applying an isotopy so that the resulting curve is contained inside $\partial\mathbf{S}_{u,\beta}$ with the exception of several line segments of the form $\pm e^*$ for some edge e ; see Figure 26. It remains to explain how an arbitrary edge e^* can be expressed as a \mathbb{Z} -linear combination of the dual bridge edges.

For any vertex p of $G_{u,\beta}$ incident to edges e_1, e_2, e_3 , we have a linear relation $\epsilon_1 e_1^* + \epsilon_2 e_2^* + \epsilon_3 e_3^* = 0$ inside $\Lambda_{u,\beta}^*$, for some $\epsilon_1, \epsilon_2, \epsilon_3 \in \{\pm 1\}$. Every non-bridge edge of $G_{u,\beta}$ passes through a dot inside $\Gamma(u_{(c)})$ for some $c \in [0, m]$. We treat these edges from right to left, i.e., by induction on $c = m, m-1, \dots, 0$. For the induction base, if e is a non-bridge edge of $G_{u,\beta}$ whose right endpoint is a degree 1 vertex in $\Gamma(u_{(m)})$ then clearly $e^* = 0$ in $\Lambda_{u,\beta}^*$. For the induction step, consider the right endpoint p of e , and let e_2, e_3 be the other two edges incident to p . The above linear relation expresses e^* as a sum of $\pm e_2^*$ and $\pm e_3^*$, and by the induction hypothesis, each of them is a \mathbb{Z} -linear combination of dual bridge edges. \square

Corollary 5.11. *The relative cycles $(C_c)_{c \in J_{u,\beta}}$ form a \mathbb{Z} -basis of $\Lambda_{u,\beta}$.*

Proof. Each relative cycle C_c passes through the bridge edge b_c and possibly through some bridges to the left of it. We therefore get $\langle C_c, b_c^* \rangle = \pm 1$ and $\langle C_c, b_d^* \rangle = 0$ for $d > c$. Therefore the matrix $\langle C_c, b_d^* \rangle$ is lower triangular with ± 1 -s on the diagonal, which implies the result. \square

Proof of Theorem 5.9. Our goal is to show that the mutable relative cycles $(C_c)_{c \in J_{u,\beta}^{\text{mut}}}$ can be extended to a \mathbb{Z} -basis \mathcal{B} of $\Lambda_{u,\beta}^*$. Indeed, if this is true, then by Corollary 5.11, each element of the basis of $\Lambda_{u,\beta}$ dual to \mathcal{B} with respect to $\langle \cdot, \cdot \rangle$ can be expressed as a \mathbb{Z} -linear combination of $(C_c)_{c \in J_{u,\beta}}$. This is equivalent to expressing the standard basis vectors of \mathbb{Z}^k , where $k := |J_{u,\beta}^{\text{mut}}|$, as \mathbb{Z} -linear combinations of the rows of the exchange matrix $\tilde{B}(\tilde{Q}_{u,\beta})$.

We show that $(C_c)_{c \in J_{u,\beta}^{\text{mut}}}$ can be extended to a \mathbb{Z} -basis of $\Lambda_{u,\beta}^*$ by induction in the same way as we did in Theorem 5.6. The \mathbb{Z} -span of $(C_c)_{c \in J_{u,\beta}^{\text{mut}}}$ is invariant under mutation formulae (3.4). It is therefore unchanged under the moves (B1)–(B4). For the move (B5), we showed in Proposition 4.7 that the surface $\mathbf{S}_{u,\beta}$ is unchanged except that we swap the labels of two marked points. The collection $(C_c)_{c \in J_{u,\beta}^{\text{mut}}}$ is also unchanged under (B5). We may therefore apply the moves (B1)–(B5) and arrive at the case where β has a double bridge on the left:⁴ $\beta = ii\beta_0$ for some $\beta_0 \in (\pm I)^{m-2}$.

Let $\beta' := i\beta_0$. As in the proof of Theorem 5.6, we have $u \leq \beta'$. The graph $G_{u,\beta}$ has one more mutable cycle C_d with $d := 2$ and one more bridge b_1 than the graph $G_{u,\beta'}$. Let \mathcal{B}' be the \mathbb{Z} -basis of $\Lambda_{u,\beta'}^*$ containing $(C_c)_{c \in J_{u,\beta}^{\text{mut}} \setminus \{d\}}$. Then it is clear that $\{b_1\} \sqcup \mathcal{B}'$ is a \mathbb{Z} -basis of $\Lambda_{u,\beta}^*$. As shown in Figure 26, we have $C_d = \pm b_2^* \pm b_1^*$ in $\Lambda_{u,\beta}^*$. Thus, $\mathcal{B} := \{C_d\} \sqcup \mathcal{B}'$ is a \mathbb{Z} -basis of $\Lambda_{u,\beta}^*$ containing $(C_c)_{c \in J_{u,\beta}^{\text{mut}}}$. \square

⁴Unlike in the proof of Theorem 5.6, here we require the two bridges to be of the same color.

6. DOUBLE BRAID VARIETIES

6.1. Notation. Let $G = \mathrm{SL}_n$. Recall that $I := [n - 1]$ indexes the simple transpositions of the Weyl group $W = S_n$, and that for $i \in I$, we denote $i^* := n - i$. For $i \in I$, we set $(-i)^* := -i^*$. Let B_+ and B_- denote the subgroup of upper triangular and lower triangular matrices, respectively, and let U_+ and U_- denote the respective unipotent subgroups. We use H to denote the torus of diagonal matrices.

For $i \in I$, let $\phi_i : \mathrm{SL}_2 \rightarrow G$ denote the homomorphism where $\phi_i(g)$ is the matrix which has g as the 2×2 submatrix on rows and columns $i, i + 1$ and otherwise agrees with the identity matrix.

We use ϕ_i to lift S_n to G . Let

$$\dot{s}_i := \phi_i \begin{pmatrix} 0 & -1 \\ 1 & 0 \end{pmatrix}.$$

For $w \in S_n$, we define $\dot{w} := \dot{s}_{i_1} \dots \dot{s}_{i_n}$ where $s_{i_1} \dots s_{i_n}$ is a reduced expression for w . The map $w \mapsto \dot{w}$ is not a homomorphism, but if $\ell(vw) = \ell(v) + \ell(w)$, then $(vw)^\cdot = \dot{v}\dot{w}$. In particular, \dot{w} does not depend on the choice of reduced expression. Explicitly,

$$(\dot{w})_{i,j} = \begin{cases} 0 & \text{if } i \neq w(j), \\ (-1)^{|\{a < j : w(a) > w(j)\}|} & \text{if } i = w(j). \end{cases}$$

We omit the dot when the choice of the signs in the permutation matrix of w does not matter: e.g., we write B_+wB_+ and Hw in place of $B_+\dot{w}B_+$ and $H\dot{w}$.

We will also need the generators

$$(6.1) \quad x_i(t) := \phi_i \begin{pmatrix} 1 & t \\ 0 & 1 \end{pmatrix}, \quad y_i(t) := \phi_i \begin{pmatrix} 1 & 0 \\ t & 1 \end{pmatrix}, \quad \alpha_i^\vee(t) := \phi_i \begin{pmatrix} t & 0 \\ 0 & 1/t \end{pmatrix},$$

and the *braid matrices*

$$\begin{aligned} z_i(t) &:= \phi_i \begin{pmatrix} t & -1 \\ 1 & 0 \end{pmatrix} = x_i(t)\dot{s}_i = \dot{s}_iy_i(-t); \\ \bar{z}_i(t) &:= \phi_i \begin{pmatrix} t & 1 \\ -1 & 0 \end{pmatrix} = x_i(-t)\dot{s}_i^{-1} = \dot{s}_i^{-1}y_i(t). \end{aligned}$$

6.2. Weighted flags. A *weighted flag* is an element $F = gU_+ \in G/U_+$. Associated to a weighted flag F is the flag $\pi(F) = gB_+$, the image of F in G/B_+ .

Definition 6.1. Two weighted flags (F, F') are called (*weakly*) *w-related* if there exist $g \in G$ and $h \in H$ such that $(gF, gF') = (U_+, h\dot{w}U_+) \in G/U_+ \times G/U_+$. Equivalently, $F = g_1U_+$ and $F' = g_2U_+$ are weakly *w-related* if and only if $g_1^{-1}g_2 \in B_+\dot{w}B_+$. We write this as $F \xrightarrow{w} F'$.

Two weighted flags (F, F') are called *strictly w-related* if there exists $g \in G$ such that $(gF, gF') = (U_+, \dot{w}U_+) \in G/U_+ \times G/U_+$. Equivalently, $F = g_1U_+$ and $F' = g_2U_+$ are strictly *w-related* if and only if $g_1^{-1}g_2 \in U_+\dot{w}U_+$. We write this as $F \xrightarrow{w} F'$.

Let F, F' be two weighted flags and let B, B' be their images in G/B_+ . Then

$$(6.2) \quad F \xrightarrow{w} F' \text{ implies } F \xrightarrow{w} F', \text{ which in turn implies } B \xrightarrow{w} B' \text{ (see Section 2.7).}$$

We collect some elementary facts about relative position (see e.g. [SW21, Appendix]).

Lemma 6.2.

- (1) $F \xrightarrow{\text{id}} F'$ if and only if $F = F'$.
- (2) If $F \xrightarrow{v} F' \xrightarrow{w} F''$ and $\ell(vw) = \ell(v) + \ell(w)$, then $F \xrightarrow{vw} F''$.
- (3) Suppose $\ell(vw) = \ell(v) + \ell(w)$. If $F \xrightarrow{vw} F''$, then there exists a unique F' such that $F \xrightarrow{v} F'$ and $F' \xrightarrow{w} F''$.

Lemma 6.3. *Suppose $F \xrightarrow{s_i} F'$ and say $F = gU_+$. Then there exists a unique $t \in \mathbb{C}$ such that $F' = gz_i(t)U_+$. Similarly, if $F' = g'U_+$, there exists a unique $t' \in \mathbb{C}$ such that $F = g'\bar{z}_i(t')U_+$.*

Remark 6.4. The parameters t, t' in Lemma 6.3 depend on the choices of the representative matrices g, g' .

Lemma 6.5. *Suppose $F \xrightarrow{v} gU_+ \xrightarrow{s_i} gz_i(t)U_+$ and let w be such that $F \xrightarrow{w} gz_i(t)U_+$. If $vs_i > v$, then $w = vs_i$ for all $t \in \mathbb{C}$. If $vs_i < v$, then $w = vs_i$ for $t = 0$ and $w = v$ for $t \in \mathbb{C}^\times$. In particular, $w \in \{v, vs_i\}$.*

Lemma 6.6. *Suppose $F \xrightarrow{w} F''$.*

- (1) If $w > ws_i$, then there is a unique F' such that $F \xrightarrow{ws_i} F' \xrightarrow{s_i} F''$.
- (2) If $w > s_iw$, then there is a unique F' such that $F \xrightarrow{s_i} F' \xrightarrow{s_iw} F''$.

Proof. We show only (1). The images $\pi(F)$ and $\pi(F'')$ in G/B_+ uniquely determine a flag $L \in G/B_+$ satisfying $\pi(F) \xrightarrow{ws_i} L \xrightarrow{s_i} \pi(F'')$, and L has a unique lift F' to G/U_+ such that $F' \xrightarrow{s_i} F''$. \square

6.3. Double braid variety. For a pair $(u, \beta) \in S_n \times (\pm I)^m$ with $u \leq \beta$, let $\mathcal{Y}_{u, \beta}$ denote the space of tuples of weighted flags satisfying

$$(6.3) \quad \begin{array}{ccccccc} X_0 & \xleftarrow{s_{i_1}^+} & X_1 & \xleftarrow{s_{i_2}^+} & \cdots & \xleftarrow{s_{i_m}^+} & X_m \\ \uparrow_{w_0 \cdot \text{id}} & & & & & & \uparrow_{w_0 \cdot u} \\ Y_0 & \xrightarrow{s_{i_1}^-} & Y_1 & \xrightarrow{s_{i_2}^-} & \cdots & \xrightarrow{s_{i_m}^-} & Y_m \end{array}$$

Also define $\mathcal{Y}_{u, \beta}$ by omitting the condition that (X_0, Y_0) are weakly w_0 -related. Then $\mathcal{Y}_{u, \beta}$ is a \mathbb{C}^l -bundle over G/U_+ (where $l = m + \ell(w_0u)$), and $\mathring{\mathcal{Y}}_{u, \beta}$ is an open subset of $\mathcal{Y}_{u, \beta}$. We denote points in $\mathring{\mathcal{Y}}_{u, \beta}$ and $\mathcal{Y}_{u, \beta}$ by (X_\bullet, Y_\bullet) .

Remark 6.7. Intuitively, a point in $\mathcal{Y}_{u, \beta}$ is a walk in $G/U_+ \times G/U_+$ from a pair of weighted flags $X_m \xleftarrow{w_0u} Y_m$ to a pair of weighted flags $X_0 \xleftarrow{w_0} Y_0$. The ‘‘direction’’ of step c is dictated by the crossing i_c of β . A red crossing i in β means the step changes the i -dimensional subspace of the first flag in the pair. A blue crossing j means the step changes the $(n - |j|)$ -dimensional subspace of the second flag. Given an arbitrary pair (X_m, Y_m) satisfying $X_m \xleftarrow{w_0u} Y_m$, we can parametrize (X_{c-1}, Y_{c-1}) iteratively for $c = m, m-1, \dots, 1$ using Lemma 6.3: assuming $(X_c, Y_c) = (g_cU_+, g'_cU_+)$, we set

$$(6.4) \quad (X_{c-1}, Y_{c-1}) := \begin{cases} (g_c z_{i_c}(t_c)U_+, g'_c U_+), & \text{if } i_c > 0, \\ (g_c U_+, g'_c \bar{z}_{|i_c|}(t_c)U_+), & \text{if } i_c < 0, \end{cases}$$

for arbitrary parameters $\mathbf{t} := (t_1, t_2, \dots, t_m) \in \mathbb{C}^m$. For (X_\bullet, Y_\bullet) to be a point in $\mathring{\mathcal{Y}}_{u,\beta}$, we require further that $X_0 \xrightarrow{w_0} Y_0$, which is an extra open condition on the parameters (\mathbf{t}, X_m, Y_m) .

The group G acts on $\mathring{\mathcal{Y}}_{u,\beta}$ and $\mathcal{Y}_{u,\beta}$ by acting simultaneously on all the weighted flags by left multiplication.

Proposition 6.8. *The action of G on $\mathring{\mathcal{Y}}_{u,\beta}$ is free.*

Proof. G acts freely on pairs (X_0, Y_0) which are weakly w_0 -related. Indeed, it suffices to consider the case $(X_0, Y_0) = (U_+, h\dot{w}_0 U_+)$. The stabilizer of the pair $(U_+, h\dot{w}_0 U_+)$ is $U_+ \cap h\dot{w}_0 U_+ \dot{w}_0^{-1} h^{-1}$, which is contained in $U_+ \cap B_- = \{1\}$. \square

Definition 6.9. The *double braid variety* $\mathring{R}_{u,\beta} = G \backslash \mathring{\mathcal{Y}}_{u,\beta}$ is the quotient of $\mathring{\mathcal{Y}}_{u,\beta}$ by G .

Our notation is consistent with Section 2 due to the following.

Proposition 6.10. *Let $\beta \in I^m$ be a positive braid word. Then the double braid variety $\mathring{R}_{u,\beta}$ is isomorphic to the braid Richardson variety defined in (2.2).*

Proof. Write π for the natural map $G/U_+ \rightarrow G/B_+$. Let $(X_\bullet, Y_\bullet) \in \mathring{R}_{u,\beta}$. The G -action can be gauge-fixed by assuming $(X_0, Y_0) = (hU_+, \dot{w}_0 U_+)$, where $h \in H$. With this gauge-fix, we obtain a map $\pi^m : \mathring{R}_{u,\beta} \rightarrow (G/B_+)^m$ sending $(X_\bullet, Y_\bullet) \mapsto (\pi(X_1), \pi(X_2), \dots, \pi(X_m))$. We now show that this map is an isomorphism onto the braid Richardson variety of (2.2). Since $\pi(X_0) = B_+$ and $\pi(Y_0) = B_-$, (6.2) shows that π^m maps $\mathring{R}_{u,\beta}$ into the space (2.2).

For the inverse of π^m : Suppose we have two flags $B, B' \in G/B_+$ satisfying $B \xrightarrow{s_i} B'$ and a lift $F \in G/U_+$ of B is given. Then there is a unique $F' \in G/U_+$ that lifts B' and satisfies $F \xrightarrow{s_i} F'$. Now, given a point B_\bullet in the space (2.2), we set $Y_0 = \dots = Y_m = \dot{w}_0 U_+$ and set X_m to be the unique lift of B_m such that $Y_m \xrightarrow{w_0 u} X_m$. Lifting $B_{m-1}, B_{m-2}, \dots, B_1$ from right to left (using the observation at the beginning of the paragraph), we obtain a unique point in $\mathring{R}_{u,\beta}$ which π^m maps to B_\bullet . \square

Remark 6.11. When both blue and red subwords of β are reduced, the same argument as in the proof of Proposition 6.10 shows that our double braid varieties are isomorphic to the varieties considered by Webster and Yakimov [WY07]. When u is the identity, $\mathring{R}_{\text{id},\beta}$ is isomorphic to the double Bott–Samelson cells of Shen and Weng [SW21].

Remark 6.12. The isomorphism of Proposition 6.10 is not compatible with total positivity, in the sense that it does not send the totally positive part $R_{u,w}^{>0}$ of $\mathring{R}_{u,w}$ (introduced by Lusztig [Lus94]) to the subset of the braid variety $\mathring{R}_{u,w}$ where all cluster variables take positive value. In order to fix that, one must compose this isomorphism with an automorphism of $\mathring{R}_{u,w}$ discussed in Section 6.6.

Notation 6.13. For any object defined in terms of a pair (u, β) , we suppress the permutation u from the notation when $u = w_0$. For example, we write $\mathring{R}_\beta := \mathring{R}_{w_0,\beta}$.

Lemma 6.14. *Given $u \leq \beta$, let $\gamma^+ \in I^{\ell(w_0 u)}$ be a reduced word for $w_0 u$ using red letters and $\gamma^- \in (-I)^{\ell(uw_0)}$ be a reduced word for uw_0 in blue letters. Then*

$$\mathring{\mathcal{Y}}_{u,\beta} \cong \mathring{\mathcal{Y}}_{\beta\gamma^+} \cong \mathring{\mathcal{Y}}_{\beta\gamma^-} \quad \text{and} \quad \mathring{R}_{u,\beta} \cong \mathring{R}_{\beta\gamma^+} \cong \mathring{R}_{\beta\gamma^-}.$$

Proof. The isomorphisms

$$\mathring{\mathcal{Y}}_{\beta\gamma^+} \rightarrow \mathring{\mathcal{Y}}_{u,\beta} \quad \mathring{\mathcal{Y}}_{\beta\gamma^-} \rightarrow \mathring{\mathcal{Y}}_{u,\beta}$$

are given by truncating (X_\bullet, Y_\bullet) after the pair $(X_{\ell(\beta)}, Y_{\ell(\beta)})$. The choice of γ^+ and γ^- together with Lemma 6.2(2) ensures that the maps are well defined. Injectivity and surjectivity follow from Lemma 6.2(3). The isomorphisms are G -equivariant and so descend to the quotient. \square

6.4. Geometry of double braid varieties.

Proposition 6.15. *For $u \leq \beta$, the double braid variety $\mathring{R}_{u,\beta}$ is a smooth, affine, irreducible complex algebraic variety of dimension equal to $d(u, \beta) := \ell(\beta) - \ell(u)$.*

Proof. Using Lemma 6.14, we may assume $u = w_0$. Consider the space of tuples of weighted flags satisfying

$$(6.5) \quad \begin{array}{ccccccc} U_+ & \xleftarrow{s_{i_1}^+} & X_1 & \xleftarrow{s_{i_2}^+} & \cdots & \xleftarrow{s_{i_m}^+} & X_m \\ & & & & & & \uparrow \text{id} \\ Y_0 & \xrightarrow{s_{i_1}^-} & Y_1 & \xrightarrow{s_{i_2}^-} & \cdots & \xrightarrow{s_{i_m}^-} & Y_m \end{array}$$

This space is an iterated \mathbb{C}^1 -bundle and thus affine. Imposing the condition that U_+ and Y_0 are weakly w_0 -related (that is, $Y_0 \in B_+ \dot{w}_0 B_+ = B_+ \dot{w}_0 U_+$) cuts out a nonempty smooth affine open subset V of the iterated \mathbb{C}^1 -bundle. The braid variety \mathring{R}_β is the quotient of V by the diagonal action of $U_+ = \text{Stab}_G(U_+)$. The group U_+ acts freely on $B_+ \dot{w}_0 U_+$ and thus acts freely on V . It follows that the quotient \mathring{R}_β is also smooth and affine; it is also clearly irreducible.

For the dimension, note that

$$\dim(\mathring{\mathcal{Y}}_\beta) = \dim(G/U_+) + \ell(\beta) = \dim(G) - \ell(w_0) + \ell(\beta)$$

so $\dim(\mathring{R}_\beta) = \dim(\mathring{\mathcal{Y}}_\beta) - \dim(G) = \ell(\beta) - \ell(w_0)$. \square

Proposition 6.16. *Let $u \leq \beta$. Suppose that β' is related to β by any of the moves (B1)–(B5). Then $\mathring{R}_{u,\beta} \cong \mathring{R}_{u,\beta'}$.*

Proof. Using Lemma 6.14, we assume that $u = w_0$. We give an isomorphism $m : \mathring{\mathcal{Y}}_\beta \rightarrow \mathring{\mathcal{Y}}_{\beta'}$, which is G -equivariant and so descends to an isomorphism of double braid varieties. The map m changes only the weighted flags indexed by letters involved in the double braid or color-changing move, so we show only that snippet of the tuple. For moves involving letters of a single color, we give the isomorphism for the “red” move; the isomorphism is similar for the “blue” move. Without loss of generality, we may use the action of G to gauge-fix one of the weighted flags involved to be U_+ .

For (B1) ($ij \mapsto ji$ with i, j of opposite color), the map m is given by

$$\left(\begin{array}{ccccc} X & \xleftarrow{s_i} & X' & \xleftarrow{\text{id}} & X' \\ & & & & \\ Y & \xrightarrow{\text{id}} & Y & \xrightarrow{s_j^*} & Y' \end{array} \right) \mapsto \left(\begin{array}{ccccc} X & \xleftarrow{\text{id}} & X & \xleftarrow{s_i} & X' \\ & & & & \\ Y & \xrightarrow{s_j^*} & Y' & \xrightarrow{\text{id}} & Y' \end{array} \right).$$

For (B2) ($iji \mapsto jji$ with i, j of the same color, $|i - j| > 1$), we use the identity $z_i(t_1)z_j(t_2) = z_j(t_2)z_i(t_1)$. Supposing that the move is on red letters, the map m sends

$$(z_j(t_2)z_i(t_1)U_+ \xleftarrow{s_i} z_j(t_2)U_+ \xleftarrow{s_j} U_+) \mapsto (z_i(t_1)z_j(t_2)U_+ \xleftarrow{s_j} z_i(t_1)U_+ \xleftarrow{s_i} U_+)$$

and does not affect the weighted flags in the bottom row.

For (B3) ($iji \mapsto jij$ with i, j of the same sign, $j = i+1$), we use the identity $z_i(t_1)z_{i+1}(t_2)z_i(t_3) = z_{i+1}(t_3)z_i(t_1t_3 - t_2)z_{i+1}(t_1)$. Supposing that the move is on red letters, the map m sends

$$(z_i(t_1)z_{i+1}(t_2)z_i(t_3)U_+ \xleftarrow{s_i} z_i(t_1)z_{i+1}(t_2)U_+ \xleftarrow{s_{i+1}} z_i(t_1)U_+ \xleftarrow{s_i} U_+)$$

$$\mapsto (z_{i+1}(t_3)z_i(t_1t_3 - t_2)z_{i+1}(t_1)U_+ \xleftarrow{s_{i+1}} z_{i+1}(t_3)z_i(t_1t_3 - t_2)U_+ \xleftarrow{s_i} z_{i+1}(t_3)U_+ \xleftarrow{s_{i+1}} U_+)$$

and does not affect weighted flags in the bottom row.

For (B4) ($\beta i \mapsto \beta(-i^*)$ assuming $u = w_0$), we have $X_m = Y_m$. We note that $(i^*)^* = i$. The map m is given by

$$\left(\begin{array}{ccc} X & \xleftarrow{s_i} & X' \\ & & \parallel \\ X' & \xrightarrow{\text{id}} & X' \end{array} \right) \mapsto \left(\begin{array}{ccc} X & \xleftarrow{\text{id}} & X \\ & & \parallel \\ X' & \xrightarrow{s_i} & X \end{array} \right).$$

For (B5) ($(-i)\beta \mapsto i\beta$), we use the identity $z_{i^*}(t)^{-1}h\dot{w}_0 = h'\dot{w}_0\bar{z}_i(t')$, where $t' = th_{i^*+1}/h_{i^*}$ and $h'_{j,j} = h_{s_{i^*}(j), s_{i^*}(j)}$. Assuming $i \in I$, the map m sends

$$\left(\begin{array}{ccc} z_{i^*}(t)^{-1}h\dot{w}_0U_+ & \xleftarrow{\text{id}} & z_{i^*}(t)^{-1}h\dot{w}_0U_+ \\ w_0 \uparrow & & \\ z_{i^*}(t)^{-1}U_+ & \xrightarrow{s_{i^*}} & U_+ \end{array} \right) \mapsto \left(\begin{array}{ccc} h'\dot{w}_0U_+ & \xleftarrow{s_i} & h'\dot{w}_0\bar{z}_i(t')U_+ \\ w_0 \uparrow & & \\ U_+ & \xrightarrow{\text{id}} & U_+ \end{array} \right). \quad \square$$

From Lemma 6.14 and Proposition 6.16, we have an immediate corollary.

Corollary 6.17. *Any double braid variety $\mathring{R}_{u,\beta}$ with $u \leq \beta$ is isomorphic to a braid variety $\mathring{R}_{\beta'}$ where β' has only red letters.*

The purpose of defining double braid varieties is to obtain more seeds (or more Deodhar tori), one for each double braid word.

6.5. Grid and chamber minors. We next discuss regular functions on $\mathring{R}_{u,\beta}$. Given (X_\bullet, Y_\bullet) , let

$$(6.6) \quad Z_c := Y_c^{-1}X_c \in U_+ \backslash G / U_+.$$

It is clear that Z_c is well defined for a point in $\mathring{R}_{u,\beta}$, since it is unchanged by the action of G . We frequently abuse notation and use Z_c to denote both the double coset and a representative of this double coset. Our goal is to use the matrix Z_c to introduce certain regular functions on $\mathring{R}_{u,\beta}, \mathring{Y}_{u,\beta}, \mathcal{Y}_{u,\beta}$ which we refer to as *grid minors*. Recall from Section 3.1 the definition of the u -PDS $\mathbf{u} = (u_{(0)}, \dots, u_{(m)})$.

Definition 6.18. For $c \in J_{u,\beta}$ a crossing and $h \in I$, we define the *red grid minor* as

$$(6.7) \quad \Delta_{c,h}(X_\bullet, Y_\bullet) = \Delta_{w_0u_{(c)}[h],[h]}(Z_c),$$

and the *blue grid minor* as

$$(6.8) \quad \Delta_{c,-h}(X_\bullet, Y_\bullet) = \Delta_{[n+1-h,n],u_{(c)}^{-1}w_0[n+1-h,n]}(Z_c) = \Delta_{w_0[h],u_{(c)}^{-1}[h]}(Z_c),$$

where $Z_c = Y_c^{-1}X_c$.

Note that the color of a grid minor $\Delta_{c,h}$ is determined by the sign of h . It is not true in general that for $J \subset [n]$ of size $|J| = h$, a flag minor of the form $\Delta_{J,[h]}$ or $\Delta_{w_0[h],J}$ gives a well-defined function on $U_+ \backslash G/U_+$. However, for the particular varieties we are interested in, grid minors indeed give rise to well-defined functions.

Lemma 6.19. For each $c \in J_{u,\beta}$ and $h \in I$, the grid minors $\Delta_{c,\pm h}$ give rise to G -invariant regular functions on $\mathcal{Y}_{u,\beta}$ and $\mathring{\mathcal{Y}}_{u,\beta}$, and to regular functions on $\mathring{R}_{u,\beta}$. These regular functions are compatible with the quotient map $\mathring{\mathcal{Y}}_{u,\beta} \rightarrow \mathring{R}_{u,\beta}$ and the inclusion map $\mathring{\mathcal{Y}}_{u,\beta} \hookrightarrow \mathcal{Y}_{u,\beta}$.

Proof. As we will explain in Section 7, each of $\mathring{R}_{u,\beta}, \mathring{\mathcal{Y}}_{u,\beta}, \mathcal{Y}_{u,\beta}$ contains an open dense subset consisting of (X_\bullet, Y_\bullet) satisfying $X_c \xleftarrow{w_0u_{(c)}} Y_c$ for all $c \in [0, m] := \{0, 1, \dots, m\}$. In this case, Z_c is contained in a specific Bruhat cell $\mathring{\mathcal{X}}_{w_0u_{(c)}} := B_+w_0u_{(c)}B_+$ of G . Therefore for arbitrary (X_\bullet, Y_\bullet) , Z_c belongs to the closure $\mathcal{X}_{w_0u_{(c)}}$ of $\mathring{\mathcal{X}}_{w_0u_{(c)}}$ inside G . It is well known that the flag minors of the form (6.7)–(6.8) give rise to $U_+ \times U_+$ -invariant regular functions on $\mathcal{X}_{w_0u_{(c)}}$, which are moreover nonvanishing on $\mathring{\mathcal{X}}_{w_0u_{(c)}}$. Explicitly, each matrix in $\mathring{\mathcal{X}}_{w_0u_{(c)}}$ can be transformed by the $U_+ \times U_+$ -action into a unique matrix in the torus $w_0u_{(c)}H$, and the grid minors are characters of this torus. The fact that these functions are G -invariant and compatible with the quotient/inclusion maps is obvious from the definition of Z_c . \square

Lemma 6.20. Consider a crossing $c \in [m]$. Suppose $h \neq i_c$ is of the same sign as i_c . Then

$$\Delta_{c-1,h} = \Delta_{c,h}.$$

Proof. Let $i := i_c$. The result follows from the fact that $Z_{c-1} = Z_c x_i(t) \dot{s}_i$ or $Z_{c-1} = \dot{s}_i x_i(t) Z_c$ (as usual using Z_c also to denote a representative for the double coset) for some $t \in \mathbb{C}$, depending on whether c is red or blue. \square

We will be particularly interested in the following subclass of grid minors.

Definition 6.21. Define the *chamber minor* of c as

$$(6.9) \quad \Delta_c := \Delta_{c-1, i_c}.$$

Note that Δ_c is a minor of Z_{c-1} . In words, Lemma 6.20 shows that a crossing of color $x \in \{\text{red}, \text{blue}\}$ can change exactly one grid minor of color x (but may change many grid minors of the opposite color). The “changed” grid minor of color x to the left of the bridge b_c is exactly the chamber minor Δ_c .

Remark 6.22. We explain the relationship between grid minors and 3D plabic graphs; compare Figure 27 to Figure 6. Recall from Section 3.2 that for a 3D plabic graph $G_{u,\beta}$ with coordinates (i, j, t) , we consider its red projection $\pi_{\text{red}}(G_{u,\beta})$ with coordinates (t, j) and its blue projection $\pi_{\text{blue}}(G_{u,\beta})$ with coordinates (t, i) . For $c \in [0, m]$ and $h \in I$, let us place the red grid minor $\Delta_{c,h}$ at the point $(t = c, j = h + 0.5)$, lying in some face of $\pi_{\text{red}}(G_{u,\beta})$.

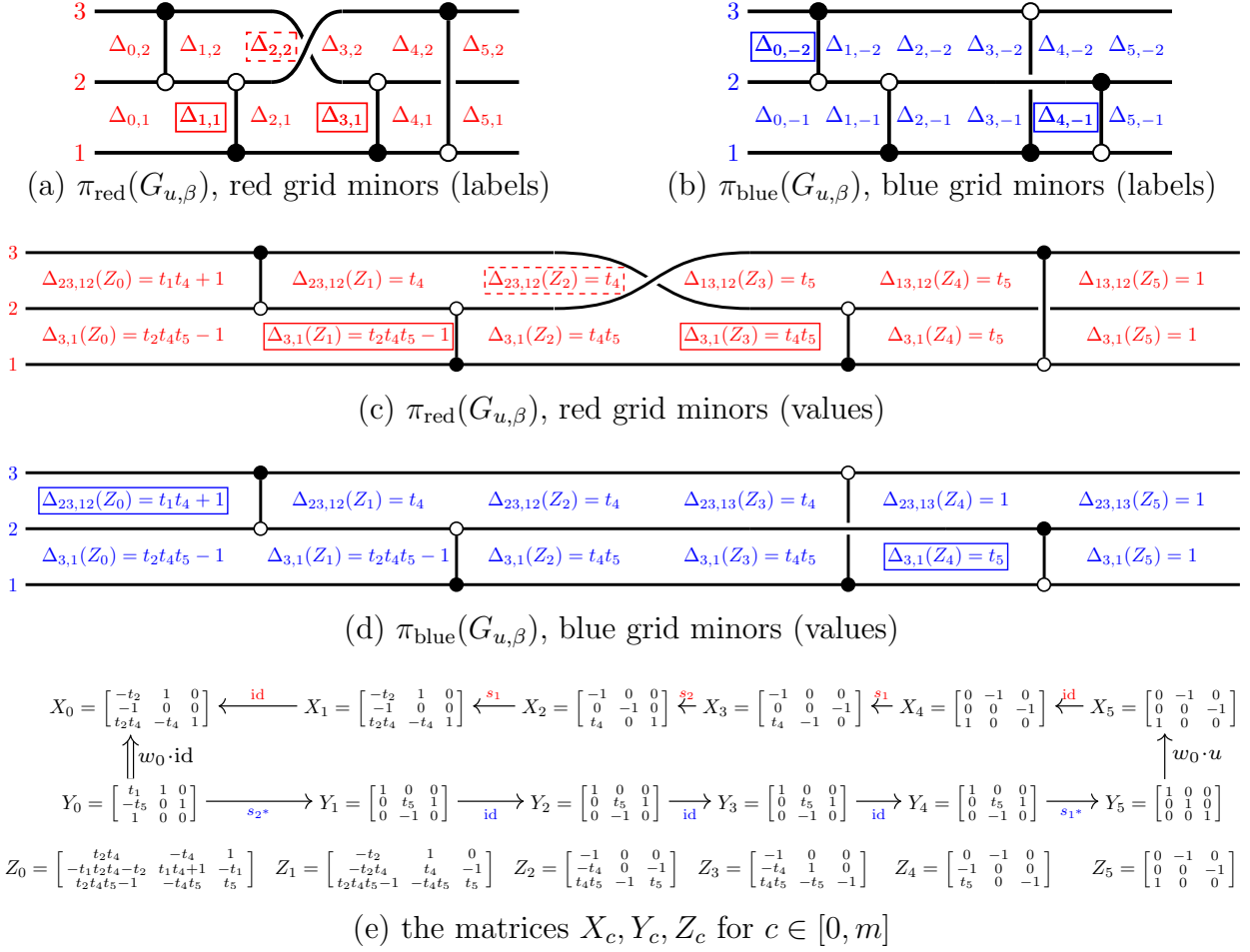


FIGURE 27. Grid minors for $u = s_2$ and $\beta = (-2, 1, 2, 1, -1)$; see Example 3.10, Figure 6, and Example 6.24. The chamber minors Δ_c , $c \in [m]$, are boxed.

Similarly, we place the blue grid minor $\Delta_{c,-h}$ at the point $(t = c, i = h + 0.5)$, lying in some face of $\pi_{\text{blue}}(G_{u,\beta})$. This labeling is shown in Figure 27(a,b). Each chamber minor Δ_c appears immediately to the left of the bridge b_c in the projection of the corresponding color; these minors are boxed in Figure 27.

Remark 6.23. Lemma 6.20 can be seen as a special case of the observation that any two red (resp., blue) grid minors that belong to the same face of $\pi_{\text{red}}(G_{u,\beta})$ (resp., $\pi_{\text{blue}}(G_{u,\beta})$) are equal.

Example 6.24. We continue Example 3.10; thus, $u = s_2$, $\beta = (-2, 1, 2, 1, -1)$, and $J_{u,\beta} = \{1, 2, 4, 5\}$. The matrices X_c, Y_c, Z_c are computed in Figure 27(e) from right to left using (6.4). The grid minors given by (6.7)–(6.8) are computed in Figure 27(c,d). The solid (resp., hollow) chamber minors are boxed in solid (resp., dashed) lines.

6.6. Comparison with chamber minors for Richardson's and double Bruhat cells. As we mentioned in the introduction, braid varieties include double Bruhat cells, open

positroid varieties, and open Richardson varieties, cluster structures on which have been studied previously in many works including [FZ99, GY20, Sco06, SSBW19, GL19, Lec16, Ing19]. We briefly explain how our chamber minors relate to chamber minors defined in some of these previous works.

Let $g \mapsto g^{-\iota}$ be the involutive automorphism of G defined by

$$x_i(t) \mapsto x_i(-t), \quad y_i(t) \mapsto y_i(-t), \quad \dot{s}_i \mapsto \dot{s}_i^{-1}, \quad h \mapsto h,$$

for all $i \in I$, $t \in \mathbb{C}$, and $h \in H$. This map is a composition of the involution $g \mapsto g^\iota$ studied in [FZ99, Section 2.1] with the involution $g \mapsto g^{-1}$ (these two involutions commute). The properties of the involution $g \mapsto g^{-\iota}$ in relation to total positivity were first studied in [GL22b, Section 6.2]. Since $G = \mathrm{SL}_n$, one can check that for a matrix $g = (g_{i,j})_{i,j \in [n]}$, we have $g^{-\iota} = ((-1)^{i+j} g_{i,j})_{i,j \in [n]}$.

We will use the following relations for relative positions of weighted flags:

$$(6.10) \quad U_+ \xleftarrow{\dot{s}_i} \dot{s}_i^{-1} U_+, \quad \alpha_i^\vee(1/t) U_+ \xleftarrow{\dot{s}_i} y_i(-t) U_+, \quad \alpha_{i^*}^\vee(t) \dot{w}_0^{-1} U_+ \xrightarrow{\dot{s}_{i^*}} x_{i^*}(-t) \dot{w}_0^{-1} U_+,$$

for all $t \in \mathbb{C}^\times$ and $i \in I$, where α_i^\vee was defined in (6.1).

6.6.1. Open Richardson varieties. Observe that the map $gB_+ \mapsto g^{-\iota}B_+$ preserves the subsets B_-uB_+ , B_+wB_+ , and therefore yields an involutive automorphism of $\mathring{R}_{u,w}$. Choose a reduced word⁵ β for w and consider the isomorphism between an open Richardson and a braid Richardson variety

$$(6.11) \quad \mathring{R}_{u,w} \xrightarrow{\sim} \mathring{R}_{u,\beta}, \quad gB_+ \mapsto (X_\bullet, Y_\bullet),$$

where (X_\bullet, Y_\bullet) satisfies the following conditions:

$$\pi(X_0) = B_+, \quad \pi(X_m) = g^{-\iota}B_+, \quad \text{and} \quad Y_0 = Y_1 = \cdots = Y_m = \dot{w}_0^{-1}U_+.$$

As explained in the proof of Proposition 6.10, these conditions determine the tuple $(X_\bullet, Y_\bullet) \in \mathring{R}_{u,\beta}$ uniquely. We explain how to do this explicitly when the element gB_+ is *MR-parametrized*; such parametrizations were introduced in [MR04] in relation to total positivity for flag varieties [Lus94]. Let

$$(6.12) \quad g := g_1 \cdots g_m, \quad \text{where} \quad g_c = \begin{cases} \dot{s}_{i_c} & \text{if } c \notin J_{u,\beta}, \\ y_{i_c}(t_c) & \text{if } c \in J_{u,\beta}. \end{cases}$$

Here $\mathbf{t} = (t_1, \dots, t_m)$ consists of some nonzero parameters. We get

$$g^{-\iota} = g_1^{-\iota} \cdots g_m^{-\iota}, \quad \text{where} \quad g_c^{-\iota} = \begin{cases} \dot{s}_{i_c}^{-1} & \text{if } c \notin J_{u,\beta}, \\ y_{i_c}(-t_c) & \text{if } c \in J_{u,\beta}. \end{cases}$$

We first check that we may set $X_m := g^{-\iota}U_+$, i.e., that $X_m \xleftarrow{w_0 u} Y_m$. Indeed, it is well known [GL22b, Equation (2.8)] that $g \in U_- \dot{u}$. Thus, $g^{-\iota} \in U_- \ddot{u}$, where for a reduced word $u = s_{j_1} \cdots s_{j_l}$, we set $\ddot{u} := \dot{u}^{-\iota} = ((u^{-1})^\vee)^{-1} = \dot{s}_{j_1}^{-1} \cdots \dot{s}_{j_l}^{-1}$. The element \ddot{u} satisfies $\dot{w}_0 \ddot{u} = (w_0 u)^\vee$. It follows that $\dot{w}_0 \cdot (X_m, Y_m) = (\dot{w}_0 g^{-\iota} U_+, U_+)$, where $\dot{w}_0 g^{-\iota} U_+ \in U_+(w_0 u)^\vee U_+$, and thus indeed $X_m \xleftarrow{w_0 u} Y_m$. We now may compute X_{m-1}, \dots, X_0 iteratively using $X_{c-1} \xleftarrow{\dot{s}_{i_c}} X_c$ together with the relations in (6.10). Comparing our chamber minors with the chamber minors of [Ing19], we arrive at the following result.

⁵We denote the reduced word for w by β as opposed to \mathbf{w} in order to make the visual differences between the varieties $\mathring{R}_{u,w}$ and $\mathring{R}_{u,\beta}$ more apparent.

Let $\beta = (i_1, i_2, \dots, i_m)$, where $m = \ell(w) + \ell(v)$, be a double reduced word for (w, v) ; that is, it is a shuffle of a reduced word for w on positive indices and a reduced word for v on negative indices. The following map is an isomorphism by an argument similar to [WY07, Proposition 2.1]:

$$(6.13) \quad L^{w,v} \xrightarrow{\sim} \mathring{R}_{\text{id},\beta}, \quad g \mapsto (X_\bullet, Y_\bullet),$$

where (X_\bullet, Y_\bullet) satisfies the following conditions:

$$\pi(X_0) = B_+, \quad X_m = g^{-\iota} U_+, \quad \pi(Y_0) = B_-, \quad \text{and} \quad Y_m = g^{-\iota} \dot{w}_0^{-1} U_+.$$

Applying the relations (6.10), we compute X_{m-1}, \dots, X_0 and Y_{m-1}, \dots, Y_0 iteratively. In order to compare our minors to the minors considered in [FZ99, BFZ05], let us choose a parametrization

$$g := g_1 \cdots g_m, \quad \text{where} \quad g_c = \begin{cases} y_{i_c}(t_c) & \text{if } i_c > 0, \\ x_{|i_c|}(t_c) & \text{if } i_c < 0. \end{cases}$$

The nonzero parameters t_1, \dots, t_m are expressed as monomials in the cluster variables of [FZ99, BFZ05] computed on the *twisted matrix* $\xi^{w,v}(g)$; see [FZ99, Definition 1.5]. Given a matrix $x \in B_- B_+$, let us denote by $([x]_-, [x]_0, [x]_+) \in U_- \times H \times U_+$ its LDU factorization. One can check that for any $g \in G^{w,v}$, the matrix $g_0 := [\dot{w}^{-1}g]_0$ is well defined.

It follows from the definition of the map (6.13) that we have $Z_c \in H \dot{w}_0$ for each $c \in [0, m]$. In particular, the red and the blue grid minors coincide: $\Delta_{c,h} = \Delta_{c,-h}$ for all c, h . We leave the verification of the following result to an interested reader.

Proposition 6.29. *Under the isomorphism (6.13), the grid minors $\Delta_{c,h}$ are equal to the chamber minors of [FZ99, Section 4.5] evaluated at $g_0 \xi^{w,v}(g)$. In particular, all chamber and grid minors from Definitions 6.18 and 6.21 take positive values on the image of the totally positive part $G_{>0}^{w,v} \subset G^{w,v}$ under (6.13).*

Example 6.30. We consider the running example of [FZ99, Section 4.5], except that we ignore the H -part factors in their decomposition (marked by green points in [FZ99, Figure 4]). Thus, we have

$$\beta = (2, -1, 3, -3, -2, 1, 2, -1, 1), \quad w = s_2 s_3 s_1 s_2 s_1, \quad v = s_1 s_3 s_2 s_1, \quad u = \text{id}.$$

The matrices g , g_0 , and $g_0 \xi^{w,v}(g)$ are given by

$$g = \begin{bmatrix} t_2 t_5 t_7 t_9 + t_2 t_6 t_8 t_9 + t_2 t_6 + t_2 t_9 + t_8 t_9 + 1 & t_2 t_5 t_7 + t_2 t_6 t_8 + t_2 + t_8 & t_2 t_5 & 0 \\ t_5 t_7 t_9 + t_6 t_8 t_9 + t_6 + t_9 & t_5 t_7 + t_6 t_8 + 1 & t_5 & 0 \\ t_1 t_5 t_7 t_9 + t_1 t_6 t_8 t_9 + t_1 t_6 + t_1 t_9 + t_7 t_9 & t_1 t_5 t_7 + t_1 t_6 t_8 + t_1 + t_7 & t_1 t_5 + 1 & t_4 \\ t_3 t_7 t_9 & t_3 t_7 & t_3 & t_3 t_4 + 1 \end{bmatrix}, \quad g_0 = \begin{bmatrix} t_3 t_7 t_9 & 0 & 0 & 0 \\ 0 & \frac{t_1 t_6}{t_9} & 0 & 0 \\ 0 & 0 & \frac{1}{t_6 t_7} & 0 \\ 0 & 0 & 0 & \frac{1}{t_1 t_3} \end{bmatrix}, \quad \text{and}$$

$$g_0 \xi^{w,v}(g) = \begin{bmatrix} \frac{t_2 t_5 t_7 t_9 + t_2 t_6 t_8 t_9 + t_2 t_6 + t_2 t_9 + t_8 t_9 + 1}{t_2 t_5} & \frac{t_8 t_9 + 1}{t_8} & \frac{1}{t_4 t_5 t_8} & 1 \\ \frac{t_2 t_6 + 1}{t_2 t_5 t_9} & \frac{1}{t_8 t_9} & \frac{1}{t_4 t_5 t_8 t_9} & \frac{1}{t_9} \\ \frac{1}{t_2 t_5 t_6 t_7} & \frac{1}{t_6 t_7 t_8} & \frac{t_4 t_5 t_6 t_7 t_8}{t_6 t_8 + 1} & \frac{t_6 t_8 + 1}{t_6 t_7} \\ 0 & \frac{t_2}{t_1 t_3 t_8} & \frac{t_1 t_5 t_8 + t_2 t_6 t_8 + t_2 + t_8}{t_1 t_3 t_4 t_5 t_8} & \frac{t_1 t_3 t_4 t_5 t_8 + t_1 t_5 t_8 + t_2 t_6 t_8 + t_2 + t_8}{t_1 t_3} \end{bmatrix}.$$

One can check that the chamber minors from [FZ99, Figure 6] computed on the matrix $g_0 \xi^{w,v}(g)$ coincide with the red grid minors computed in Figure 28(b).

Remark 6.31. The chamber minors of [FZ99] computed on the matrix $\xi^{w,v}(g)$ have a description in terms of strands in a double wiring diagram; see [FZ99, Theorem 4.11]. If one computes them on the matrix $g_0 \xi^{w,v}(g)$ instead, one gets a similar description: each chamber minor equals $(\prod t_k)^{-1}$, where the product is taken over *all* crossings which are to the right of

the chamber and such that the chamber is located vertically between the two strands participating in the crossing. In other words, the transformation $\xi^{w,v}(g) \mapsto g_0 \xi^{w,v}(g)$ gauge-fixes to 1 the chamber minors corresponding to the chambers open on the right.

7. DEODHAR GEOMETRY AND SEEDS

Let $u \leq \beta$. We will use the u -positive distinguished subexpression (cf. Section 3.1) to define a torus in $\mathring{R}_{u,\beta}$, which will ultimately be a cluster torus. We will then use (u, d) -almost positive sequences (cf. Section 3.6) to define hypersurfaces in $\mathring{R}_{u,\beta}$, and in turn to define cluster variables for $\mathring{R}_{u,\beta}$.

7.1. The Deodhar torus. We continue to denote the u -PDS by $\mathbf{u} = (u_{(0)}, \dots, u_{(m)})$.

Definition 7.1. The *Deodhar torus* $T_{u,\beta} \subset \mathring{R}_{u,\beta}$ is the subset of $\mathring{R}_{u,\beta}$ given by the conditions

$$(7.1) \quad X_c \xleftarrow{w_0 u_{(c)}} Y_c \quad \text{for } c = 0, 1, \dots, m.$$

Remark 7.2. Points in $T_{u,\beta}$ lift to walks of the sort described in Remark 6.7 where at each step, one greedily increases the relative position of X_c and Y_c .

Recall from the proof of Lemma 6.19 that all grid minors are nonvanishing on the Deodhar torus $T_{u,\beta}$.

Lemma 7.3.

- (1) For each solid $c \in J_{u,\beta}$, the grid minors $(\Delta_{c-1,j})_{j \in \pm I}$ are Laurent monomials in the grid minors $(\Delta_{c,h})_{h \in \pm I}$ and the chamber minor $\Delta_c = \Delta_{c-1, i_c}$.
- (2) For each hollow $c \in [m] \setminus J_{u,\beta}$, the grid minors $(\Delta_{c-1,j})_{j \in \pm I}$ are Laurent monomials in the grid minors $(\Delta_{c,h})_{h \in \pm I}$.
- (3) Every grid minor $\Delta_{c,j}$ is a Laurent monomial in solid chamber minors $(\Delta_d)_{d \in J_{u,\beta}}$.

Proof. It suffices to verify the statement on $T_{u,\beta}$.

(1) and (2): Set $i := i_c$. We assume c is red, as the other case is similar. By Lemma 6.20, we only need to check the statement for blue grid minors and, if c is hollow, additionally for $\Delta_{c-1,i}$. (For c solid, the statement is vacuously true for $\Delta_{c-1,i} = \Delta_c$.) Consider a point $(X_\bullet, Y_\bullet) \in T_{u,\beta}$. Following the proof of Lemma 6.19, let us choose representative matrices X_c, Y_c such that $Z_c = h(w_0 u_{(c)})$ for some $h \in H$. With this choice (cf. Remark 6.4), we find that for some $t \in \mathbb{C}$,

$$\begin{array}{ccc} X_{c-1} = gz_i(t)U_+ & \xleftarrow{s_i} & X_c = gU_+ \\ \uparrow w_0 u_{(c-1)} & & \uparrow w_0 u_{(c)} \\ Y_{c-1} & \xrightarrow{\text{id}} & Y_c. \end{array}$$

Set $Z := Z_c$, so $Z_{c-1} = Zz_i(t)$. We use the following elementary calculation to compare grid minors at $c-1$ to those at c .

$$(7.2) \quad \Delta_{A,B}(Zz_i(t)) = \begin{cases} \Delta_{A,B}(Z) & \text{if } s_i(B) = B, \\ -\Delta_{A,s_i(B)}(Z) & \text{if } s_i(B) < B, \\ t\Delta_{A,B}(Z) + \Delta_{A,s_i(B)}(Z) & \text{if } s_i(B) > B. \end{cases}$$

Recall that $Z = h(w_0u_{(c)})$, so many minors of Z vanish. If the crossing c is hollow (so $u_{(c-1)} < u_{(c)}$), then when in the third case of (7.2), the minor multiplying t is always zero. This is enough to show the blue grid minor $\Delta_{c-1,j}$ equals $\Delta_{c,j}$. One can check further that

$$\Delta_{c-1,i} = \frac{\Delta_{c,i-1}\Delta_{c,i+1}}{\Delta_{c,i}}.$$

If c is solid, then (7.2) implies $t = \Delta_c/\Delta_{c,i}$, and that a blue grid minor $\Delta_{c-1,j}$ is either equal to $\Delta_{c,j}$ or it is equal to $t\Delta_{c,j}$. Both of these are Laurent monomials in the desired set of grid minors.

(3): Gauge-fix so that $Y_m = U_+$ and $X_m = (w_0u)U_+$. All of the grid minors $\Delta_{m,j}$ are equal to 1, so by (1) and (2), the grid minors $\Delta_{m-1,j}$ are Laurent monomials in the chamber minor Δ_m , if m is solid, and are equal to 1 if m is hollow. Continuing from right to left, (1) implies that all grid minors $\Delta_{c,j}$ are Laurent monomials in the solid chamber minors $\{\Delta_d\}_{d \in J_{u,\beta} | d \geq c}$. \square

We now show that the Deodhar torus is in fact a torus.

Proposition 7.4.

- (1) The Deodhar torus $T_{u,\beta}$ is an open subset of $\mathring{R}_{u,\beta}$, isomorphic to an algebraic torus of dimension $d(u, \beta)$.
- (2) The character lattice of $T_{u,\beta}$ consists of Laurent monomials in the solid chamber minors Δ_c , $c \in J_{u,\beta}$. The ring of regular functions on $T_{u,\beta}$ is the ring of Laurent polynomials in the chamber minors.
- (3) The grid minors are characters of $T_{u,\beta}$.

Proof. We will show that the map $T_{u,\beta} \rightarrow (\mathbb{C}^\times)^{d(u,\beta)}$ sending a point to the tuple of its solid chamber minors is an isomorphism. This implies all three of the claims. Using Lemma 6.14, we assume that $u = w_0$. Following Notation 6.13, we set $T_\beta := T_{w_0,\beta}$ and $d(\beta) := d(w_0, \beta) = \ell(\beta) - \ell(w_0)$.

We first show how to uniquely recover a point in T_β from the nonzero values of Δ_c . That is, we show that the map is injective. By Lemma 7.3, it suffices to show that a point in T_β can be uniquely recovered from its grid minors. Throughout, we gauge-fix $Y_0 = U_+$ and $X_0 = hw_0U_+$, where $h \in H$.

First, we can recover X_0 and Y_0 , as h is uniquely determined by the grid minors $\Delta_{0,j}$.

Now we show for $c \in [m]$ that if X_{c-1}, Y_{c-1} are known, then X_c, Y_c are uniquely determined by the grid minors. There are two cases, depending on whether c is solid or hollow.

Case 1: Suppose the crossing c is solid, so $u_{(c-1)} = u_{(c)}$. Let $i := i_c$. If c is red, resp., blue, we have

$$\begin{array}{ccc} X_{c-1} = gz_i(t)U_+ \xleftarrow{s_i} X_c = gU_+ & & X_{c-1} \xleftarrow{\text{id}} X_c \\ w_0u_{(c-1)} \uparrow \uparrow & \text{resp.}, & w_0u_{(c-1)} \uparrow \uparrow \\ Y_{c-1} \xrightarrow{\text{id}} Y_c, & & Y_{c-1} = g\bar{z}_{|i|^*}(t)U_+ \xrightarrow{s_{|i|^*}} Y_c = gU_+, \end{array}$$

for a unique $t \in \mathbb{C}^\times$. So $Z_c = Z_{c-1}z_i(t)^{-1}$ if c is red, and $Z_c = \bar{z}_{|i|^*}(t)Z_{c-1}$ if c is blue. We would like to find t . By a formula analogous to (7.2), we have $t = \Delta_{c,i}/\Delta_{c-1,i}$. So X_c, Y_c can be recovered from the grid minors and thus from the chamber minors.

Case 2: Suppose the crossing c is hollow, so $u_{(c-1)} < u_{(c)}$. In this case, X_{c-1} and Y_{c-1} satisfy the conditions of Lemma 6.6(1) if c is red and Lemma 6.6(2) if c is blue. So X_c and Y_c are uniquely determined.

To show $T_\beta \rightarrow (\mathbb{C}^\times)^{d(\beta)}$ is also surjective, we must check that an arbitrary tuple in $(\mathbb{C}^\times)^{d(\beta)}$ is the list of chamber minors for a point of T_β . To see this, we define a point of T_β moving right to left. Set $Y_m = X_m = U_+$. Then, supposing we have defined $X_c = gU_+$ and $Y_c = fU_+$, let $t := \Delta_{c-1, i_c} / \Delta_{c, i_c}$ and define

$$X_{c-1} = \begin{cases} gz_{i_c}(t)U_+ & \text{if } i_c > 0, \\ X_c & \text{if } i_c < 0, \end{cases} \quad \text{and} \quad Y_{c-1} = \begin{cases} Y_c & \text{if } i_c > 0, \\ f\bar{z}_{i_c^*}(t)U_+ & \text{if } i_c < 0. \end{cases}$$

This produces a point in T_β by Lemma 6.5. Using (7.2) or similar formulas, one can also check that its chamber minors are equal to the desired tuple. \square

While the braid variety $\mathring{R}_{u,\beta}$ is unchanged by braid moves, the Deodhar torus $T_{u,\beta}$ may change. In particular, we will show later that non-mutation moves and color-changing moves preserve the Deodhar torus, while mutation moves change it.

7.2. Deodhar hypersurfaces. For $d \in J_{u,\beta}$, recall the notion of the (u, d) -almost positive sequence $(v_{(0)}^{(d)}, \dots, v_{(0)}^{(m)})$ from Definition 3.15. In this section, we use the (u, d) -APS for solid d to define Deodhar hypersurfaces for $\mathring{R}_{u,\beta}$.

Definition 7.5. Let $d \in J_{u,\beta}^{\text{mut}}$. Define the *mutable Deodhar hypersurface* $V_d \subset \mathring{R}_{u,\beta}$ to be the closure of the locus satisfying

$$(7.3) \quad X_c \xleftarrow{w_0 v_{(c)}^{(d)}} Y_c \quad \text{for all } c \in [0, m].$$

Abusing notation, also denote $V_d \subset \mathring{\mathcal{Y}}_{u,\beta} \subset \mathcal{Y}_{u,\beta}$.

Remark 7.6. Points in the locus satisfying (7.3) lift to walks of the sort described in Remark 6.7 where at every step besides step d , one greedily increases the relative position of X_c and Y_c . At step d , one makes a ‘‘mistake’’ and decreases the relative position of X_d and Y_d .

Proposition 7.7. *The closed subset $\mathring{R}_{u,\beta} \setminus T_{u,\beta}$ is the union of the mutable Deodhar hypersurfaces V_d for $d \in J_{u,\beta}^{\text{mut}}$. Each Deodhar hypersurface V_d is irreducible and has codimension 1 in $\mathring{R}_{u,\beta}$.*

Proof. Parametrizing $\mathcal{Y}_{u,\beta}$ using (6.4), the conditions (7.3) cut out an iterated fiber bundle over $G/U_+ \times G/U_+$, where each fiber is either \mathbb{C} , \mathbb{C}^\times , or (in the case of the crossing $c = d$) a point. This is an irreducible variety that is codimension one in $\mathcal{Y}_{u,\beta}$. The condition that $d \in J_{u,\beta}^{\text{mut}}$ implies that this locus belongs to $\mathring{\mathcal{Y}}_{u,\beta}$, and in particular, that the action of G is free. It follows that $V_d \subset \mathring{R}_{u,\beta}$ is a codimension 1 irreducible hypersurface.

Let $(X_\bullet, Y_\bullet) \in \mathring{R}_{u,\beta} \setminus T_{u,\beta}$ belong to the complement. Then one of the conditions (7.1) fails. Let $d \in [0, m]$ be equal to the largest value of c for which (7.1) fails. Let $V'_d \subset \mathring{R}_{u,\beta}$ be the locus of points where (7.1) holds for $c > d$ and fails for $c = d$. By Lemma 6.5 and the definition of the almost positive subexpression $(v_{(0)}^{(d)}, \dots, v_{(0)}^{(m)})$, an open dense subset V''_d of V'_d satisfies (7.3). Recall that when $d \in J_{u,\beta}$ is a frozen crossing, the 0-th term $v_{(0)}^{(d)}$ of the

(u, d) -APS is not equal to the identity. Thus, if $d \notin J_{u,\beta}^{\text{mut}}$ then V_d'' , and therefore V_d' itself, is empty, a contradiction. Thus, $d \in J_{u,\beta}^{\text{mut}}$ and (X_\bullet, Y_\bullet) belongs to the hypersurface V_d . \square

When $d \in J_{u,\beta}^{\text{fro}}$, elements (X_\bullet, Y_\bullet) satisfying (7.3) do not lie in $\mathring{R}_{u,\beta}$. In this case, we must define the corresponding Deodhar hypersurface inside $\mathcal{Y}_{u,\beta}$.

Definition 7.8. Let $d \in J_{u,\beta}^{\text{fro}}$. Define the *frozen Deodhar hypersurface* $V_d \subset \mathcal{Y}_{u,\beta}$ as the closure of the locus satisfying (7.3).

The following result follows from the same argument as in the proof of Proposition 7.7.

Lemma 7.9. For $d \in J_{u,\beta}^{\text{fro}}$, the subvariety $V_d \subset \mathcal{Y}_{u,\beta}$ is irreducible and codimension 1 in $\mathcal{Y}_{u,\beta}$.

Let $\text{ord}_V f \in \mathbb{Z}$ denote the order of vanishing of a rational function f on a hypersurface V . Note that if $f \in \mathbb{C}(\mathring{R}_{u,\beta})$ we can calculate $\text{ord}_V f$ in $\mathring{R}_{u,\beta}$ or pull it back to $\mathring{\mathcal{Y}}_{u,\beta}$ and calculate $\text{ord}_V f$ there. In the case that V is a frozen Deodhar hypersurface, we compute $\text{ord}_V f$ by pulling f back to $\mathring{\mathcal{Y}}_{u,\beta}$ and then viewing f as a rational function on $\mathcal{Y}_{u,\beta}$. When f is a grid minor, its pullback to $\mathring{\mathcal{Y}}_{u,\beta}$ and extension to $\mathcal{Y}_{u,\beta}$ are regular functions in view of Lemma 6.19.

Proposition 7.10. Fix $d \in J_{u,\beta}$. For $j \in I$,

$$\text{ord}_{V_d} \Delta_{c,j} = \begin{cases} 1 & \text{if } u_{(c)}[j] \neq v_{(c)}^{(d)}[j], \\ 0 & \text{otherwise,} \end{cases} \quad \text{and} \quad \text{ord}_{V_d} \Delta_{c,-j} = \begin{cases} 1 & \text{if } u_{(c)}^{-1}[j] \neq (v_{(c)}^{(d)})^{-1}[j], \\ 0 & \text{otherwise.} \end{cases}$$

Proof. We compute the order of vanishing inside the space $S \subset \mathcal{Y}_{u,\beta}$ of tuples (X_\bullet, Y_\bullet) of the form (6.5) (i.e., the space where X_0 has been gauge-fixed to U_+). This space S is an affine space with coordinates $\mathbf{t} = (t_1, t_2, \dots)$, as each X_i or Y_i is of the form $z_{i_{j_1}}(t_{j_1}) \cdots z_{i_{j_r}}(t_{j_r})$ or $\bar{z}_{i_{j_1}}(t_{j_1}) \cdots \bar{z}_{i_{j_r}}(t_{j_r})$ for some r . (These coordinates differ from those given by (6.4).) The Z_c are then also products of inverses of braid matrices in some subset of the parameters \mathbf{t} .

Let Z be any matrix that is a product of braid matrices or their inverses with parameters from \mathbf{t} , each parameter used at most once. Then it is easy to see that every minor of Z is linear or constant in each variable t_i . The Deodhar hypersurface V_d is cut out by a minor of Z_{d-1} , and this minor has degree one in some parameter $t = t_{i(d)}$. Any grid minor $\Delta_{c,j}$ is at most degree one in t , and thus vanishes to order at most one on V_d .

Suppose $j \in I$. Then $u_{(c)}[j] = v_{(c)}^{(d)}[j]$ if and only if for a generic point in V_d , the j -th subspace in the weighted flag X_c has the correct relative position (given by $u_{(c)}[j]$) with respect to Y_c . This holds if and only if $\Delta_{c,j}$ does not vanish on V_d . As we showed above, $\text{ord}_{V_d} \Delta_{c,j} \leq 1$, and thus we obtain the stated formula for $j \in I$. The argument for $j \in -I$ is identical. \square

Proposition 7.11. The map

$$(7.4) \quad f \mapsto (\text{ord}_{V_c} f)_{c \in J_{u,\beta}}$$

is an isomorphism from the character lattice of $T_{u,\beta}$ to $\mathbb{Z}^{d(u,\beta)}$.

Proof. Let $C \subset \mathbb{Z}^{d(u,\beta)}$ be the image of $\{\Delta_c\}_{c \in J_{u,\beta}}$. By Proposition 7.10, the chamber minor Δ_c vanishes to order 1 on V_c , and does not vanish on V_d for $d < c$. Thus, there is an upper unitriangular matrix taking the standard basis of $\mathbb{Z}^{d(u,\beta)}$ to C . In particular, the images of the chamber minors form a basis of $\mathbb{Z}^{d(u,\beta)}$. \square

7.3. Seeds. The isomorphism (7.4) allows us to define new distinguished characters on $T_{u,\beta}$, which will be the cluster variables.

Definition 7.12. For $c \in J_{u,\beta}$, we define the *cluster variable* x_c to be the unique character of $T_{u,\beta}$ that vanishes to order one on V_c and has neither a pole nor a zero on $V_{c'}$ for $c' \in J_{u,\beta} \setminus \{c\}$. We denote the cluster by $\mathbf{x}_{u,\beta} = \{x_c\}_{c \in J_{u,\beta}}$.

Example 7.13. Continuing Example 6.24, we see that in the notation of Figure 27, the cluster variables are given by

$$x_1 = t_1 t_4 + 1, \quad x_2 = t_2 t_4 t_5 - 1, \quad x_4 = t_4, \quad x_5 = t_5.$$

In particular, $\Delta_4 = t_4 t_5 = x_4 x_5$ factors as a product of two cluster variables.

It is immediate from the definition that each cluster variable is a regular function on $\mathring{R}_{u,\beta}$ and in particular each frozen variable is a unit in $\mathbb{C}[\mathring{R}_{u,\beta}]$. It is also immediate that the cluster variables in $\mathbf{x}_{u,\beta}$ are algebraically independent and irreducible.

Recall the definition of the ice quiver $\tilde{Q}_{u,\beta}$ from (3.3). The vertices of $\tilde{Q}_{u,\beta}$ are labeled by $c \in J_{u,\beta}$, as are the elements of $\mathbf{x}_{u,\beta}$. So we define the seed

$$(7.5) \quad \Sigma_{u,\beta} := (\mathbf{x}_{u,\beta}, \tilde{Q}_{u,\beta}).$$

We may now state our main result.

Theorem 7.14. *For all $u \leq \beta$, we have*

$$\mathbb{C}[\mathring{R}_{u,\beta}] = \mathcal{A}(\Sigma_{u,\beta})$$

as subrings of $\mathbb{C}[\mathring{R}_{u,\beta}]$. Moreover, the cluster algebra $\mathcal{A}(\Sigma_{u,\beta})$ is locally acyclic and really full rank.

The proof of the isomorphism will occupy Sections 8–9. The local acyclicity and the really full rank property of $\mathcal{A}(\Sigma_{u,\beta})$ are Corollary 5.8 and Theorem 5.9.

We say that a cluster variable x_c *appears* in a grid minor $\Delta_{d,h}$ if $\text{ord}_{V_c} \Delta_{d,h} = 1$. One characterization for when this happens is given by Proposition 7.10. We now relate it to the combinatorics of 3D plabic graphs; cf. Section 2.4. Recall from Section 3.4 that for each $d \in J_{u,\beta}$ we have a relative cycle C_d in $G_{u,\beta}$ which bounds a disk D_d . Recall also from Remark 6.22 that we decorate the faces of the projections of $G_{u,\beta}$ with grid minors.

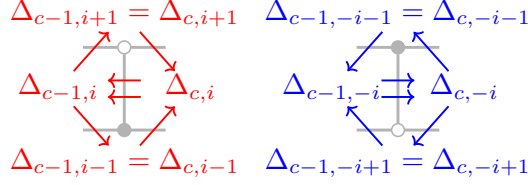
Lemma 7.15. *Let $d \in J_{u,\beta}$, $c \in [0, m]$, and $h \in I$ (resp., $h \in -I$). Then x_d appears in $\Delta_{c,h}$ if and only if $\Delta_{c,h}$ lies in the red (resp., blue) projection of the disk D_d .*

Proof. This follows from Propositions 7.10 and 3.16. Proposition 7.10 computes $\text{ord}_{V_d} \Delta_{c,h}$ by comparing certain subsets: $u_{(c)}[h]$ and $v_{(c)}^{(d)}[h]$ for the red minor, and $(u_{(c)})^{-1}[[h]]$ and $(v_{(c)}^{(d)})^{-1}[[h]]$ for the blue minor.

Proposition 3.16 shows that the permutation $v_{(c)}^{(d)}$ can be recovered from the monotone multicurve $\gamma^{d,c}$. From the details of this construction, one can conclude that $u_{(c)}[h] \neq v_{(c)}^{(d)}[h]$ if and only if one of the curves in $\gamma^{d,c}$ intersects the horizontal line $j = h + 0.5$ inside $\Gamma(u_{(c)})$. This is equivalent to the point $(c, h + 0.5)$ lying in the red projection of D_d . Similarly, $(u_{(c)})^{-1}[h] \neq (v_{(c)}^{(d)})^{-1}[h]$ if and only if one of the curves in $\gamma^{d,c}$ intersects the vertical line $i = h + 0.5$ in $\Gamma(u_{(c)})$ if and only if $(c, h + 0.5)$ lies in the blue projection of D_d . Comparing with Proposition 7.10 gives the result. \square

Example 7.16. Recall from Example 7.13 that in Figure 27, we have $\Delta_4 = x_4x_5$. This is consistent with the fact that the face of $\pi_{\text{red}}(G_{u,\beta})$ containing $\Delta_4 = \Delta_{3,1}$ lies inside the cycles C_4, C_5 shown in Figure 6(e).

We now give an alternate construction of $\tilde{Q}_{u,\beta}$ related to the half-arrow description in Section 3.7. First, consider a collection $P_{u,\beta}^+$ (resp., $P_{u,\beta}^-$) of half-arrows between the red (resp., blue) grid minors $\{\Delta_{c,h}\}_{c \in [0,m], h \in I}$ (resp., $\{\Delta_{c,h}\}_{c \in [0,m], h \in -I}$). It is obtained by placing the following configuration of half-arrows around each bridge b_c with $i_c > 0$ in $\pi_{\text{red}}(G_{u,\beta})$ (resp., each blue bridge b_c with $i_c < 0$ in $\pi_{\text{blue}}(G_{u,\beta})$), where $i := |i_c|$:



Proposition 7.17. Define a quiver with vertex set $\mathbf{x}_{u,\beta}$ as follows. Write each grid minor as

$$\Delta_{d,h} = \prod_{c \in J_{u,\beta}} x_c^{q_{d,h}^c},$$

where $q_{d,h}^c := \text{ord}_{V_c} \Delta_{d,h} \geq 0$. For every half-arrow $\Delta_{d,h} \rightarrow \Delta_{d',h'}$ in $P_{u,\beta}^+$ and $P_{u,\beta}^-$, draw $q_{d,h}^c q_{d',h'}^c$ arrows from x_c to x'_c . (In other words, for every x_c appearing in $\Delta_{d,h}$ and x'_c appearing in $\Delta_{d',h'}$, draw a half-arrow $x_c \rightarrow x'_c$.) Then delete loops and 2-cycles. The resulting collection of half-arrows agrees with the quiver $\tilde{Q}_{u,\beta}$. That is, the signed number of half-arrows between any two vertices is twice the number of arrows between the corresponding vertices of $\tilde{Q}_{u,\beta}$.

Proof. This follows directly from Lemma 7.15 and Proposition 3.18. \square

Remark 7.18. Let $\beta = \mathbf{w}$ be a reduced word for $w \in S_n$. Comparing the above half-arrow description to [Ing19, Definition VII.2] and applying Proposition 6.25, it follows that the isomorphism (6.11) sends Ingermanson's seed to our seed $\Sigma_{u,\beta}$. Thus, our cluster structure on the open Richardson variety $\mathring{R}_{u,w}$ recovers the upper cluster structure on $\mathring{R}_{u,w}$ constructed in [Ing19].

8. MOVES PRESERVE THE CLUSTER ALGEBRA

To each $u \leq \beta$, we have associated a seed $\Sigma_{u,\beta}$ and thus also a cluster algebra $\mathcal{A}_{u,\beta} := \mathcal{A}(\Sigma_{u,\beta}) \subset \mathbb{C}[\mathring{R}_{u,\beta}]$. Our ultimate goal is to show that $\mathbb{C}[\mathring{R}_{u,\beta}]$ is isomorphic to $\mathcal{A}_{u,\beta}$. As an intermediate step, we show the following.

Theorem 8.1. Suppose β and β' are related by one of the moves (B1)–(B5). Let $m : \mathring{R}_{u,\beta} \xrightarrow{\sim} \mathring{R}_{u,\beta'}$ be the corresponding isomorphism from Proposition 6.16. Then the isomorphism $m^* : \mathbb{C}[\mathring{R}_{u,\beta'}] \xrightarrow{\sim} \mathbb{C}[\mathring{R}_{u,\beta}]$ restricts to an isomorphism $\mathcal{A}_{u,\beta'} \xrightarrow{\sim} \mathcal{A}_{u,\beta}$.

Remark 8.2. If β and β' are related by moves (B1)–(B4), then the quivers $\tilde{Q}_{u,\beta}$ and $\tilde{Q}_{u,\beta'}$ are related either by relabeling the vertices or by mutation (cf. Theorem 4.3, Proposition 4.7). So in these cases, we have an isomorphism $\mathcal{A}_{u,\beta} \cong \mathcal{A}_{u,\beta'}$, and to prove Theorem 8.1, we

just need to check that the isomorphism is induced by the appropriate isomorphism of braid varieties.

Throughout the following three subsections, we assume that $u = w_0$ (cf. Notation 6.13 and Lemma 6.14), and that β and β' are related by a single move (B1)–(B5). We let $m : \mathring{R}_\beta \rightarrow \mathring{R}_{\beta'}$ denote the corresponding isomorphism, defined in Proposition 6.16. Any pullback mentioned is a pullback by m . We set $J_{\beta'}$ to be the set of solid crossings for β' . For $x_c \in \mathbf{x}_{\beta'}$, we denote $p_c := m^*(x_c)$ and $\mathbf{p}_{\beta'} := \{p_c\}_{c \in J_{\beta'}}$. The isomorphism m also induces a map on the double cosets Z_c ; we write Z'_c to denote the image of Z_c under this map. Pullbacks of grid minors are also denoted with primes.

8.1. Non-mutation moves and (B4) do not change the seed. In this section, we prove Theorem 8.1 for non-mutation moves and (B4). We show that in this case, Σ_β and $(\mathbf{p}_{\beta'}, \tilde{Q}_{\beta'})$ differ only by reindexing. As noted in Remark 8.2, it suffices to check this statement for cluster variables.

Proposition 8.3. *Suppose β and β' are related by a non-mutation move or (B4) and let α be the corresponding relabeling bijection $J_\beta \rightarrow J_{\beta'}$ from Section 4.4. Then $x_c = p_{\alpha(c)}$.*

Proof. For (B4), α is the identity. It is clear that $\Delta_{c,h} = \Delta'_{c,h}$ and x_d appears in $\Delta_{c,h}$ if and only if p_d appears in $\Delta'_{c,h}$. The claim follows. Indeed, suppose $d \in J_\beta^{\text{mut}}$ and for all solid $c > d$, we already know $x_c = p_{\alpha(c)}$. Then $\Delta_{d-1, i_d} = x_d M$ and $\Delta'_{d-1, i_d} = p_{\alpha(d)} M'$, where M (resp., M') is a product of cluster variables x_c (resp., $p_{\alpha(c)}$) with $c > d$. By above, the left-hand sides of these two equations are equal and $M = M'$. So e.g. by restricting to the Deodhar torus, we may conclude $x_d = p_{\alpha(d)}$.

Now, for non-mutation moves. Suppose the non-mutation move involves the indices in some interval $(l, r] \subset [m]$ of length 2 or 3. Let G^L (resp., G^R) denote the portion of G_β between $\Gamma(u_{(0)})$ and $\Gamma(u_{(l)})$ (resp., between $\Gamma(u_{(r)})$ and $\Gamma(u_{(m)})$). Note that G^L (resp., G^R) is also equal to the portion of $G_{u, \beta'}$ between $\Gamma(u'_{(0)})$ and $\Gamma(u'_{(l)})$ (resp., between $\Gamma(u'_{(r)})$ and $\Gamma(u'_{(m)})$). By Section 4.4, for all $c \in J_\beta$, the cycles C_c and $C'_{\alpha(c)}$ behave identically on G^L and G^R . This implies a point is contained in the red (resp., blue) projection of D_c if and only if it is contained in the red (resp., blue) projection of $D'_{\alpha(c)}$. Also, for $c \notin (l, r) := [l+1, r-1]$, we have $\Delta_{c,h} = \Delta'_{c,h}$ for all $h \in \pm I$. Using Lemma 7.15, we obtain the following.

Lemma 8.4. *Suppose $c \notin (l, r)$ and $d \in J_\beta$. Then x_d appears in $\Delta_{c,h}$ if and only if $p_{\alpha(d)}$ appears in $\Delta'_{c,h} = \Delta_{c,h}$.*

Note that α is the identity on $(r, m]$. The same argument as in the (B4) case shows $x_c = p_{\alpha(c)}$ for solid crossings $c > r$. For solid $c \in (l, r]$, to show $x_c = p_{\alpha(c)}$, it suffices to find a grid minor $\Delta_{d,h}$ with $d \leq l$ which is a product of x_c and other $x_{c'}$ which are already known to be equal to $p_{\alpha(c')}$. In fact, a grid minor $\Delta_{l,h}$ will always work; this can be seen from Figures 22–24 and the rules governing cycles. Now, α is also the identity on $[1, l]$, so the same argument as for (B4) shows $x_c = p_{\alpha(c)}$ for solid $c \leq l$. \square

8.2. Mutation moves mutate the seed. In this section, we prove Theorem 8.1 for mutation moves. We show that in this case, Σ_β and $(\mathbf{p}_{\beta'}, \tilde{Q}_{\beta'})$ are related by mutation. This statement has already been checked for the quivers, so we just check the cluster variables.

Lemma 8.5. *Suppose β and β' are related by the mutation move whose rightmost crossing is $c+1$. Then for $d \in J_\beta \setminus \{c+1\}$, we have $x_d = p_d$.*

Proof. This argument is similar to the proof of Proposition 8.3. Say the mutation move occurs on indices in the interval $(l, r) \in [m]$, with $r := c + 1$. Then for $h \in [0, l] \cup [r, m]$, the cluster variable x_{c+1} does not appear in grid minors $\Delta_{d,h}$ and $\Delta_{d,h} = \Delta'_{d,h}$. Moreover, a cluster variable $x_{c'} \neq x_{c+1}$ appears in $\Delta_{d,h}$ for $h \in [0, l] \cup [r, m]$ if and only if $p_{c'}$ appears in $\Delta'_{d,h}$. The desired equality now follows from a triangularity argument. \square

Now, we verify that the single new cluster variable in $\mathbf{p}_{\beta'}$ satisfies the exchange relation given by Σ_{β} . We will need some identities for grid minors, which we obtain from standard determinantal identities.

The following relations hold on G .

Proposition 8.6 (Desnanot–Jacobi identity). *Suppose $p, q \in S_n$ and $a \in I$ with $\ell(ps_a) = \ell(p) + 1$ and $\ell(qs_a) = \ell(q) + 1$. Then*

$$(8.1) \quad \Delta_{p[a],q[a]} \Delta_{ps_a[a],qs_a[a]} = \Delta_{ps_a[a],q[a]} \Delta_{p[a],qs_a[a]} + \Delta_{p[a-1],q[a-1]} \Delta_{p[a+1],q[a+1]}.$$

Proposition 8.7 ([FZ99, Theorem 1.16(1)]). *Let $p, q \in S_n$ and $a, b \in I$. Suppose $(s_a s_b)^3 = 1$ and $\ell(qs_a s_b s_a) = \ell(q) + 3$. Then*

$$(8.2) \quad \Delta_{p[a],qs_a[a]} \Delta_{p[b],qs_b[b]} = \Delta_{p[a],q[a]} \Delta_{p[b],qs_a s_b[b]} + \Delta_{p[a],qs_b s_a[a]} \Delta_{p[b],q[b]}.$$

Lemma 8.8. *Let $A, B \subset [n]$ with $|A| = |B|$, $a \in I$, and suppose $s_a(A) \geq A$ in the lexicographic order. Then*

$$\Delta_{s_a(A),B}(\dot{s}_a M) = \Delta_{A,B}(M) \quad \text{and} \quad \Delta_{B,s_a(A)}(M \dot{s}_a) = -\Delta_{B,A}(M).$$

Now, we use the determinantal identities above to obtain relations on grid minors before and after a mutation move.

Proposition 8.9.

(1) *Suppose β, β' are related by a (B1) special solid move $ji \rightarrow ij$ on crossings $c, c + 1$. Then the grid minors on \mathring{R}_{β} satisfy*

$$(8.3) \quad \Delta_{c,j} \Delta'_{c,j} = \Delta_{c+1,j} \Delta_{c-1,j} + \Delta_{c,j-1} \Delta_{c,j+1}.$$

(2) *Suppose β, β' are related by a (B3) fully solid move $iji \rightarrow jij$ on crossings $c-1, c, c+1$. Then the grid minors on \mathring{R}_{β} satisfy*

$$(8.4) \quad \Delta_{c,i} \Delta'_{c,j} = \Delta_{c+1,i} \Delta_{c-2,j} + \Delta_{c+1,j} \Delta_{c-2,i}.$$

Proof. Set $v := u_{(c+1)}$.

For (1): We will assume $j < 0$ and $i > 0$, as the other case is similar. Let $k = -j$. Note that we can write Z_{c-1}, Z_c and Z'_c in terms of Z_{c+1} :

$$Z_{c-1} = (\bar{z}_{k^*}(t'))^{-1} Z_{c+1} z_i(t) = \dot{s}_{k^*} x_{k^*}(t') Z_{c+1} x_i(t) \dot{s}_i$$

while $Z_c = Z_{c+1} x_i(t) \dot{s}_i$ and $Z'_c = \dot{s}_{k^*} x_{k^*}(t') Z_{c+1}$.

Now, apply (8.1) to Z_{c-1} with $p = w_0 s_k$, $q = v^{-1}$, and $a = k$. Using $vs_i = s_k v > v$, Lemma 8.8, Lemma 6.20, and the $U_+ \times U_+$ -invariance of the grid minors, we obtain the equation (8.3). For example,

$$\Delta_{p[a],qs_a[a]} = \Delta_{s_k^* w_0[k],s_i v^{-1}[k]}(Z_{c-1}) = -\Delta_{w_0[k],s_i v^{-1}[k]}(Z_c) = \Delta_{w_0[k],v^{-1}[k]}(Z_{c+1}) = \Delta_{c+1,j}.$$

For (2): Using the same strategy as above, we apply (8.2) to Z_{c-2} (or its transpose) to obtain (8.4). If $i > 0$ and $j = i + 1$, for example, we set $p = w_0 v$, $q = \text{id}$, $a = i$ and $b = i + 1$. \square

We need one additional identity on grid minors to show that p_{c+1} satisfies the correct exchange relation.

Lemma 8.10. *Choose a crossing c . Let $a \in [n]$ and let $b = -u_{(c)}(a)$. Then the relation*

$$\Delta_{c,a}\Delta_{c,b+1} = \Delta_{c,b}\Delta_{c,a-1}$$

holds on \mathring{R}_β , where we set $\Delta_{c,0} = \Delta_{c,\pm n} := 1$.

Proof. It suffices to show that this relation holds on the Deodhar torus T_β , which is dense. As in the proof of Lemma 7.3, we choose representatives X_c, Y_c so that the matrix Z_c is of the form

$$g := Z_c = h(w_0 u_{(c)})$$

for some $h \in H$. Only the entries $g_{w_0 u_{(c)}(i),i}$ are nonzero. So for $i > 0$, $\Delta_{c,i}$ is (up to sign) the product of the nonzero entries of g in columns $1, \dots, i$. For $i < 0$, $\Delta_{c,i}$ is (up to sign) the product of the nonzero entries of g in rows $w_0(|i|), w_0(|i|) + 1, \dots, n$. Using this, we find

$$\frac{\Delta_{c,a}}{\Delta_{c,a-1}} = \frac{\Delta_{c,b}}{\Delta_{c,b+1}} = (-1)^q g_{w_0(|b|),a}$$

where q is the number of nonzero entries of g southwest of $g_{w_0(|b|),a}$. \square

Proposition 8.11. *Let β and β' be related by a mutation move whose rightmost crossing is $c + 1$. Then $(\mathbf{p}_{\beta'}, \mathring{Q}_{\beta'}) = \mu_{c+1}(\Sigma_\beta)$.*

Proof. Case 1: Suppose the mutation move is a (B1) special solid move $ji \rightarrow ij$ on crossings $c, c+1$. Without loss of generality, we may assume $j < 0$ and $i > 0$. We see from Figure 19(a) and Lemma 7.15 that x_{c+1} appears only in grid minors $\Delta_{c,i}$ and $\Delta_{c,j}$. Using Proposition 7.17, we find that the cluster variable x'_{c+1} in $\mu_{c+1}(\Sigma_\beta)$ satisfies the exchange relation

$$(8.5) \quad x_{c+1}x'_{c+1} = (\Delta_{c+1,i}\Delta_{c-1,j} + (\Delta_{c,i-1}\Delta_{c,i+1}\Delta_{c,j-1}\Delta_{c,j+1})^{1/2})/f$$

$$(8.6) \quad = (\Delta_{c+1,i}\Delta_{c-1,j} + \Delta_{c,i-1}\Delta_{c,j-1})/f$$

where f is the cluster monomial

$$f = \prod_{d \neq c+1} x_d^{\min(\text{ord}_{V_d}(\Delta_{c+1,i}\Delta_{c-1,j}), \text{ord}_{V_d}(\Delta_{c,i-1}\Delta_{c,j-1}))}$$

The equality in (8.6) follows from Lemma 8.10: since $j = -u_{(c)}(i)$ and $j - 1 = -u_{(c)}(i + 1)$, we get $\Delta_{c,j+1} = \Delta_{c,i-1}\Delta_{c,j}/\Delta_{c,i}$ and $\Delta_{c,i+1} = \Delta_{c,j-1}\Delta_{c,i}/\Delta_{c,j}$.

On the other hand, using (8.3) and Lemma 8.10 together, we have that

$$(8.7) \quad \Delta'_{c,j}\Delta_{c,i} = \Delta_{c+1,i}\Delta_{c-1,j} + \Delta_{c,i-1}\Delta_{c,j-1}$$

on \mathring{R}_β , where $\Delta'_{c,j}$ is the grid minor evaluated after the braid move. This can be seen by working on the Deodhar torus and multiplying (8.3) by $\Delta_{c+1,i-1}/\Delta_{c+1,j+1}$; one must also use $\Delta_{c+1,j+1} = \Delta_{c,j+1}$, which follows from the move being special solid.

To show that p_{c+1} obeys the exchange relation, we will prove that the left-hand side of (8.7) is equal to $f x_{c+1} p_{c+1}$. It is easy to check that x_{c+1} appears in $\Delta_{c,i}$ and p_{c+1} appears in $\Delta'_{c,j}$. So all that remains is to show that for $d \neq c + 1$,

$$\text{ord}_{V_d}(\Delta'_{c,j}\Delta_{c,i}) = \min(\text{ord}_{V_d}(\Delta_{c+1,i}\Delta_{c-1,j}), \text{ord}_{V_d}(\Delta_{c,i-1}\Delta_{c,j-1})).$$

Eq. (4.1) implies an analogous statement for (8.3); that is, the order of vanishing of the left-hand side on V_d is the minimum of the orders of vanishing of the two terms on the

right. Since (8.7) differs from (8.3) by a Laurent monomial in cluster variables, we obtain the desired equality for (8.7).

Case 2: Suppose the mutation move is a (B3) fully solid move $iji \rightarrow jij$ on crossings $c-1, c, c+1$. We assume $i > 0$; the $i < 0$ case is similar. The proof strategy is similar to Case 1, so we will be brief. By Proposition 7.10, the only red grid minors x_{c+1} appears in are $\Delta_{c,i} = \Delta_{c-1,i}$. So by Proposition 7.17, the exchange relation for x'_{c+1} is

$$x_{c+1}x'_{c+1} = (\Delta_{c+1,i}\Delta_{c-2,j} + \Delta_{c+1,j}\Delta_{c-2,i})/f$$

where f is the cluster monomial

$$f = \prod_{d \neq c+1} x_d^{\min(\text{ord}_{V_d}(\Delta_{c+1,i}\Delta_{c-2,j}), \text{ord}_{V_d}(\Delta_{c+1,j}\Delta_{c-2,i}))}.$$

On the other hand, (8.4) and (4.1) together imply that the right-hand side of the exchange relation is equal to $x_{c+1}p_{c+1}$. \square

8.3. Move (B5) rescales the seed. In this section, we prove Theorem 8.1 for (B5). If the first crossing is hollow, this is straightforward (Lemma 8.12). If the first crossing is solid, we show that Σ_β and $(\mathbf{p}_{\beta'}, \tilde{Q}_{\beta'})$ differ only in a single frozen variable and arrows involving that frozen variable, in a way that preserves the cluster algebra (Proposition 8.13).

Lemma 8.12. *Suppose $\beta = (-i)\gamma$ and $\beta' = i\gamma$ for some positive double braid γ . If the first crossing is hollow, then $\Sigma_\beta = (\mathbf{p}_{\beta'}, \tilde{Q}_{\beta'})$.*

Proof. Note that the first crossing is hollow in β if and only if it is hollow in β' . The color of the hollow crossing does not matter in the definition of the surface $\mathbf{S}_{u,\beta}$ and does not affect the interaction of any mutable cycle with any other cycle, so $\mathbf{S}_{u,\beta} = \mathbf{S}_{u,\beta'}$ and $\tilde{Q}_\beta = \tilde{Q}_{\beta'}$. Further, the upper triangular matrix relating chamber minors and cluster variables is the same for both seeds, and all chamber minors pull back to chamber minors. This implies $x_c = p_c$ for all $c \in J_\beta$. \square

We now assume that the first crossings of β and β' are solid. We would like to apply the following proposition to the two seeds at hand.

Proposition 8.13 ([Fra16], cf. [LS16, Proposition 5.11]). *Suppose (\mathbf{x}, \tilde{Q}) and $(\mathbf{x}', \tilde{Q}')$ are two seeds in \mathcal{F} such that*

- \tilde{Q} and \tilde{Q}' are ice quivers on the same set of vertices, whose mutable parts coincide,
- the mutable variables in \mathbf{x} and \mathbf{x}' are the same, and the two sets of frozen variables are related by an invertible monomial transformation, and
- for each mutable vertex c ,

$$\prod_{v \in \tilde{Q}} x_v^{\#\text{arrows } v \rightarrow c \text{ in } \tilde{Q}} = \prod_{v \in \tilde{Q}'} (x'_v)^{\#\text{arrows } v \rightarrow c \text{ in } \tilde{Q}'}$$

Then $\mathcal{A}(\mathbf{x}, \tilde{Q}) = \mathcal{A}(\mathbf{x}', \tilde{Q}')$.

We first analyze the relationship between the clusters \mathbf{x}_β and $\mathbf{p}_{\beta'}$.

Lemma 8.14. *Suppose $\beta = (-i)\gamma$ and $\beta' = i\gamma$ and the first crossing is solid. Then for $(c, h) \neq (0, \pm i)$, x_d appears in $\Delta_{c,h}$ if and only if p_d appears in $\Delta_{c,h}$. Further, $x_c = p_c$ for $c \neq 1$.*

Proof. Note that for $(c, h) \neq (0, \pm i)$, $\Delta_{c,h} = \Delta'_{c,h}$.

For the first claim: by Proposition 7.10, the appearance of a cluster variable x_d in a grid minor $\Delta_{c,h}$ depends only on d and the suffix $i_{c+1} \dots i_m$ of β . The same statement holds for p_d , $\Delta'_{c,h} = \Delta_{c,h}$ and β' . Since for $c > 0$, the suffixes of β and β' coincide, this implies the first claim for all grid minors with $c > 0$. For $c = 0$, by Lemma 6.20, each blue grid minor for $c = 0$ besides $\Delta_{0,-|i|}$ is equal to a blue grid minor for $c = 1$. It follows from the definition that $\Delta_{0,h} = \Delta_{0,-h}$, so this gives the first claim for grid minors with $(c, h) \neq (0, \pm i)$.

The second claim follows from the first, since cluster variables are unitriangularly related to chamber minors, and the first claim implies the unitriangular matrices for the two seeds differ only in the first row (or column). \square

Lemma 8.15. *Suppose $\beta = (-i)\gamma$ and $\beta' = i\gamma$ and the first crossing is solid. Then $p_1 = x_1^{-1}M$ where M is a Laurent monomial in the frozen variables of \mathbf{x}_β other than x_1 .*

Proof. Suppose $i > 0$. For $h \in H$, let $h_j := h_{j,j}$.

Gauge-fix as in the proof of Proposition 6.16, so $Z_0 = hw_0$ and $Z'_0 = h'\dot{w}_0$, where h' is obtained from h by swapping the positions of h_{n-i+1} and h_{n-i} . It is easy to see that $\Delta_{0,a} = \Delta_{0,-a} = h_n \cdots h_{n-|a|+1}$, and similarly for $\Delta'_{0,a}$. Now, because x_1 appears in $\Delta_{0,-i}$ but not $\Delta_{0,-(i+1)}$, we have $h_{n-i} = x_1^{-1}N$ where N is a Laurent monomial in the other frozen variables of \mathbf{x}_β . Similarly, because p_1 appears in $\Delta'_{0,i}$ and not $\Delta'_{0,i-1}$, we have $h'_{n-i+1} = h_{n-i} = p_1 N'$ where N' is a Laurent monomial in the other frozen variables of $\mathbf{p}_{\beta'}$. So $p_1 = x_1^{-1}N/N'$. Since all frozen variables in $\mathbf{p}_{\beta'} \setminus \{p_1\}$ are equal to frozen variables of \mathbf{x}_β , we have proved the claim. \square

Lemma 8.16. *Suppose $\beta = (-i)\gamma$ and $\beta' = i\gamma$ and the first crossing is solid. For each mutable crossing $c \in J_\beta^{\text{mut}}$, we have*

$$(8.8) \quad \prod_{d \in \tilde{Q}_\beta} x_d^{\#\text{arrows } d \rightarrow c \text{ in } \tilde{Q}_\beta} = \prod_{d \in \tilde{Q}_{\beta'}} p_d^{\#\text{arrows } d \rightarrow c \text{ in } \tilde{Q}_{\beta'}}.$$

Proof. The result follows straightforwardly from Proposition 7.17. Suppose $i > 0$. The quiver P_β^+ is obtained from $P_{\beta'}^+$ by adding the half-arrows coming from the leftmost red bridge of $\pi_{\text{red}}(G_\beta)$; the quiver $P_{\beta'}^-$ is obtained from P_β^- by adding the half-arrows coming from the leftmost blue bridge of $\pi_{\text{blue}}(G_{u,\beta'})$. Together with Lemma 8.14, this implies that the quivers \tilde{Q}_β and $\tilde{Q}_{\beta'}$ can be obtained from a third quiver \tilde{Q} by adding a vertex x_1 or p_1 and adding the half-arrows contributed by the leftmost bridge.

As before, for $h \in H$, let $h_j := h_{j,j}$. Gauge-fix as in Proposition 6.16, so $Z_0 = hw_0$ and $Z'_0 = h'\dot{w}_0$, where h' is obtained from h by swapping the positions of h_{n-i+1} and h_{n-i} .

Fix $c \in J_\beta^{\text{mut}}$, and let L and R denote the left- and right-hand sides of (8.8). If x_c does not appear in $\Delta_{1,i}$, then there are no arrows between x_c and x_1 and the arrows $x_d \rightarrow x_c$ in \tilde{Q}_β are in bijection with arrows $p_d \rightarrow p_c$ in $\tilde{Q}_{\beta'}$. We find that (8.8) follows from Lemma 8.14.

If x_c does appear in $\Delta_{1,i}$, then the arrows in P_β^+ around the leftmost red bridge contribute

$$\frac{(\Delta_{0,i+1}\Delta_{0,i-1})^{1/2}}{\Delta_{0,i}} = \frac{h_{n-i}^{1/2}}{h_{n-i+1}^{1/2}}$$

to L .

From Lemma 8.14, we know p_c appears in $\Delta'_{1,-i} = \Delta_{1,i}$. The half-arrows in $P_{\beta'}^-$ around the leftmost blue bridge contribute

$$\frac{\Delta'_{0,-i}}{(\Delta_{0,-(i+1)}\Delta_{0,-(i-1)})^{1/2}} = \frac{h_{n-i}^{1/2}}{h_{n-i+1}^{1/2}}$$

to R .

Now, if we divide L and R by $(h_{n+i-1}/h_{n-i})^{1/2}$, we obtain two expressions that are equal. Indeed, the expressions are monomials in $\mathbf{x}_\beta \setminus \{x_1\}$ and $\mathbf{p}_{\beta'} \setminus \{p_1\}$, respectively, and exponents in both expressions are determined by arrows in \tilde{Q} . \square

9. PROOF OF THEOREM 7.14

In this section, we continue to assume $u = w_0$. Recall that to each double braid word $\beta \geq w_0$, we have associated a cluster algebra $\mathcal{A}_\beta \subset \mathbb{C}[\mathring{R}_\beta]$. By Theorem 8.1, this cluster algebra is invariant under (B1)–(B5). We prove that $\mathbb{C}[\mathring{R}_\beta]$ is equal to \mathcal{A}_β by induction on the length $\ell = \ell(\beta)$.

9.1. Reduction to $ii\beta'$. Using Theorem 8.1 and arguing as in the beginning of Theorem 5.6, we may assume $\beta = ii\beta'$ is a double braid in positive letters starting with ii . Note that the index $1 \in J_\beta$ is solid and the cluster variable x_1 is frozen.

We first deal with the case that the second i is hollow, i.e., $2 \notin J_\beta$.

Proposition 9.1. *If $2 \notin J_\beta$, then we have an isomorphism $r : \mathring{R}_\beta \xrightarrow{\sim} \mathring{R}_{i\beta'} \times \mathbb{C}^\times$ which induces an isomorphism $r^* : \mathcal{A}_{i\beta'}[x_1^\pm] \xrightarrow{\sim} \mathcal{A}_\beta$. This implies the statement of Theorem 7.14 in the case $2 \notin J_\beta$.*

Proof. Before defining the map r , we need the following facts. First, since all letters of β are positive and $u = w_0$, we have $Y_0 = Y_1 = \dots = Y_m = X_m$. If $X_0 \xleftarrow{s_i} X_1 \xleftarrow{s_i} \dots \xleftarrow{s_{im}} X_m$ represents a point in \mathring{R}_β , then we claim that $X_1 \xleftarrow{w_0} X_m$. Indeed, $X_2 \xleftarrow{w} X_m$ where $w \leq w_0 s_i$, since $w_0 s_i$ is the Demazure product of $i_3 i_4 \dots i_m$. We must in fact have $w = w_0 s_i$, as otherwise it would be impossible to have $X_0 \xleftarrow{w_0} X_m$. Since $X_1 \xleftarrow{s_i} X_2 \xleftarrow{w_0 s_i} X_m$ and $w_0 \geq w_0 s_i$, it follows from Lemma 6.5 that $X_1 \xleftarrow{w_0} X_m$. Also, since Z_0, Z_1 are contained in $B_+ w_0 B_+$, the grid minors $\Delta_{0,h}$ and $\Delta_{1,h}$ are units in $\mathbb{C}[\mathring{R}_\beta]$.

Second, $x_1 = \Delta_{0,i}/\Delta_{1,i}$ and the vertex 1 of \tilde{Q}_β is an isolated frozen vertex. Indeed, an almost positive sequence $v_{(c)}^{(d)}$ greedily decreases at each crossing besides d , going right to left through β . From this and Proposition 7.10, it follows that a cluster variable $x_c \neq x_1$ appears in $\Delta_{1,i}$ if and only if it appears in $\Delta_{0,i}$. Since x_1 appears in $\Delta_{0,i}$, this proves that $x_1 = \Delta_{0,i}/\Delta_{1,i}$. It also proves that the frozen vertex 1 is isolated: x_1 appears only in the grid minor $\Delta_{0,i}$, so by Proposition 7.17 there can only be arrows from x_1 to cluster variables appearing in $\Delta_{0,i-1}, \Delta_{0,i+1}$ and $\Delta_{1,i} = x_1^{-1} \Delta_{0,i}$. All of these cluster variables are frozen.

The map r is defined as

$$r : (X_0 \xleftarrow{s_i} X_1 \xleftarrow{s_i} \dots \xleftarrow{s_{im}} X_m) \mapsto \left((X_1 \xleftarrow{s_i} \dots \xleftarrow{s_{im}} X_m), x_1 \right).$$

It is well defined by the previous paragraph. It is straightforward to check that the inverse map is

$$q : \left((X_1 = gU_+ \xleftarrow{s_i} \dots \xleftarrow{s_{im}} X_m), t \right) \mapsto (gz_i(t)U_+ \xleftarrow{s_i} X_1 \xleftarrow{s_i} \dots \xleftarrow{s_{im}} X_m).$$

By induction, $\mathbb{C}[\mathring{R}_{i\beta'}] = \mathcal{A}_{i\beta'}$. So $\mathbb{C}[\mathring{R}_{i\beta'} \times \mathbb{C}^\times]$ is also equal to some cluster algebra which we denote \mathcal{A} . One quiver \tilde{Q} for \mathcal{A} is the disjoint union of $\tilde{Q}_{i\beta'}$ and a frozen vertex; the cluster is $\mathbf{x}_{i\beta'}$ together with the generator of the character lattice of \mathbb{C}^\times , which is frozen.

We claim that $\mathcal{A} = q^*(\mathcal{A}_\beta)$. The cluster \mathbf{x}_β pulls back to the cluster of \mathcal{A} mentioned above, as the grid minors pull back to grid minors and the combinatorics of Proposition 7.10 is identical for β and $i\beta'$ away from the first crossing. And it is easy to see that $\tilde{Q} = \tilde{Q}_\beta$, which shows the claim.

The statement of Theorem 7.14 in the case $2 \notin J_\beta$ is now immediate, as $q^*(\mathbb{C}[\mathring{R}_\beta]) = \mathbb{C}[\mathring{R}_{i\beta'} \times \mathbb{C}^\times] = \mathcal{A} = q^*(\mathcal{A}_\beta)$. \square

Henceforth, we assume that the first two crossings are solid, i.e., $1, 2 \in J_\beta$.

9.2. Open-closed covering. Let $x := x_2$ be the ‘‘leftmost’’ mutable cluster variable in \tilde{Q}_β . Let

$$W := \{x_2 \neq 0\} \quad V := V_2 = \{x_2 = 0\}$$

be the open-closed covering of \mathring{R}_β coming from x_2 . Thus V is a Deodhar hypersurface and W is its complement. By the proof of Theorem 5.6, vertex 2 is a sink in Q_β , the mutable part of \tilde{Q}_β .

Lemma 9.2. *The open subset W is isomorphic to $\mathring{R}_{i\beta'} \times \mathbb{C}^\times$, and V is isomorphic to $\mathring{R}_{\beta'} \times \mathbb{C}$.*

Proof. The isomorphism $W \cong \mathring{R}_{i\beta'} \times \mathbb{C}^\times$ is identical to the map r in the proof of Proposition 9.1 (using the ratio $\Delta_{0,i}/\Delta_{1,i}$ rather than x_1). The condition that $x_2 \neq 0$ is equivalent to the condition that $X_1 \xleftarrow{w_0} X_m$, so W is precisely the subset of \mathring{R}_β on which the map r is well defined.

The isomorphism $V \xrightarrow{\sim} \mathring{R}_{\beta'} \times \mathbb{C}$ is similar. If $X_0 \xleftarrow{s_i} X_1 \xleftarrow{s_i} \dots \xleftarrow{s_{i_m}} X_m$ represents a point in V , then X_m is not weakly w_0 -related to X_1 . Because $X_0 \xleftarrow{w_0} X_m$, we have in fact $X_1 \xleftarrow{w_0 s_i} X_m$. By Lemma 6.5, this means $X_2 \xleftarrow{w_0} X_m$. So we may define a map $V \xrightarrow{\sim} \mathring{R}_{\beta'} \times \mathbb{C}$ by

$$(g s_i z_i(t) U_+ = X_0 \xleftarrow{s_i} g s_i U_+ = X_1 \xleftarrow{s_i} g U_+ = X_2 \leftarrow \dots \xleftarrow{s_{i_m}} X_m) \mapsto \left((X_2 \xleftarrow{s_{i_2}} \dots \xleftarrow{s_{i_m}} X_m), t \right).$$

(The fact that all points in V are represented by a tuple of the form written above follows from Lemma 6.5 as well.) The inverse of this map is clear. \square

9.3. Triangularity. The grid minors $\Delta_{c,j}$ on \mathring{R}_β restrict to the corresponding grid minors on $\mathring{R}_{i\beta'}$ (resp., $\mathring{R}_{\beta'}$), except for grid minors for the leftmost (resp., the leftmost two) crossings.

Functions on $\mathring{R}_{i\beta'}$ (resp., $\mathring{R}_{\beta'}$) can be pulled back to W (resp., V) under the projection $\pi_{i\beta'} : \mathring{R}_{i\beta'} \times \mathbb{C}^\times \rightarrow \mathring{R}_{i\beta'}$ (resp., $\pi_{\beta'} : \mathring{R}_{\beta'} \times \mathbb{C} \rightarrow \mathring{R}_{\beta'}$).

By induction, we have shown that $\mathbb{C}[\mathring{R}_{i\beta'}] = \mathcal{A}_{i\beta'}$ and $\mathbb{C}[\mathring{R}_{\beta'}] = \mathcal{A}_{\beta'}$. These equalities are compatible with the one that we want to prove, as the following result demonstrates.

Proposition 9.3. *Let x_c be a cluster variable of \mathbf{x}_β , not equal to x_1 (resp., x_1 or x_2). Then x_c restricts to the pullback under $\pi_{i\beta'}$ (resp., $\pi_{\beta'}$) of similarly denoted cluster variable on $\mathring{R}_{i\beta'}$ (resp., $\mathring{R}_{\beta'}$). That is, $x_c \in \mathcal{A}_\beta$ and $x'_c \in \mathcal{A}_{i\beta'}$ (resp., $x'_c \in \mathcal{A}_{\beta'}$) have the same image in the following diagrams:*

$$\mathcal{A}_\beta \hookrightarrow \text{Frac}(\mathbb{C}[\mathring{R}_\beta]) \xrightarrow{\text{restriction}} \text{Frac}(\mathbb{C}[W]) \xleftarrow{\text{pullback}} \mathbb{C}[\mathring{R}_{i\beta'}] = \mathcal{A}_{i\beta'},$$

$$\mathcal{A}_\beta \hookrightarrow \text{Frac}(\mathbb{C}[\mathring{R}_\beta]) \xrightarrow{\text{restriction}} \text{Frac}(\mathbb{C}[V]) \xleftarrow{\text{pullback}} \mathbb{C}[\mathring{R}_{\beta'}] = \mathcal{A}_{\beta'}.$$

Proof. The claimed compatibility is true for grid minors, and the Laurent monomial expressions for x_c and x'_c in terms of grid minors are the same. \square

9.4. Regularity of mutated cluster variables. The results of Section 8 show that the mutation of x_2 is a regular function on \mathring{R}_β . Indeed, applying (B5) rescales a single frozen variable by a Laurent monomial in frozen variables and applying (B1) mutates at x_2 . The resulting seed is $\mathbf{x}_{i(-i)\beta'}$ and it consists of regular functions on \mathring{R}_β . The cluster variable \tilde{x}_2 in this seed differs from the mutation of x_2 by a unit, hence the mutation of x_2 is also a regular function.

For all other mutated cluster variables \tilde{x}_c , we note that the formula for the mutation is the same in $\Sigma_\beta, \Sigma_{i\beta'}$ and $\Sigma_{\beta'}$. Now, either (a) x_c is mutable in both $\Sigma_{i\beta'}$ and $\Sigma_{\beta'}$ or (b) x_c is mutable in $\Sigma_{i\beta'}$ and frozen in $\Sigma_{\beta'}$. If (a), then by induction \tilde{x}_c is regular on both W and V and thus on \mathring{R}_β . If (b), then by induction \tilde{x}_c is regular on W . Since x_c is a unit on V and $\tilde{x}_c = (M + M')/x_c$ where M, M' are monomials in the other cluster variables, \tilde{x}_c is also regular on V .

9.5. Tori in the braid variety. For $c \in J_\beta^{\text{mut}}$, let $\tilde{\mathbf{x}}_c$ be the cluster of the mutated seed $\mu_c(\Sigma_\beta)$. Since we have shown all the cluster variables and their mutations are regular, we have maps

$$\begin{aligned} \varphi : \mathring{R}_\beta &\rightarrow \mathbb{C}^d, & g &\mapsto (x_1(g), x_2(g), \dots, x_d(g)) = \mathbf{x}(g); \\ \varphi_c : \mathring{R}_\beta &\rightarrow \mathbb{C}^d, & g &\mapsto (x_1(g), x_2(g), \dots, x_d(g)) = \tilde{\mathbf{x}}_c(g). \end{aligned}$$

Let T_c be the Deodhar torus associated to the cluster $\tilde{\mathbf{x}}_c$.

Proposition 9.4. *There are inclusions of cluster tori $T \hookrightarrow \mathring{R}_\beta$ and $T_c \hookrightarrow \mathring{R}_\beta$ which are partial inverses to φ, φ_c . In other words, we have inclusions $\mathbb{C}[\mathring{R}_\beta] \subset \mathbb{C}[\mathbf{x}^{\pm 1}]$ and $\mathbb{C}[\mathring{R}_\beta] \subset \mathbb{C}[\tilde{\mathbf{x}}_c^{\pm 1}]$.*

Proof. For $T = T_\beta$, this statement is Proposition 7.4. For T_2 , this follows from Proposition 7.4 applied to the isomorphic braid variety $\mathring{R}_{i(-i)\beta}$, whose Deodhar torus pulls back to T_2 . For $c \neq 2$, by the inductive hypothesis T_c includes into W , so also includes into \mathring{R}_β . \square

9.6. Finishing. We proceed by following the argument in [BFZ05, proof of Theorem 2.10].

Lemma 9.5. *A Laurent monomial $M = \mathbf{x}^\mathbf{a}$ is regular on \mathring{R}_β if and only if the exponents of mutable cluster variables are nonnegative.*

Proof. The “if” part is trivial. For the “only if” part, consider the restriction of M to the torus T_c . Then $x_c^{a_c}$ is a regular function on T_c and must be a Laurent polynomial in $\tilde{\mathbf{x}}_c$. It follows from the exchange relation that $a_c \geq 0$. \square

Lemma 9.6. *For $c \in J_\beta^{\text{mut}}$, x_c is irreducible in $\mathbb{C}[\mathring{R}_\beta]$.*

Proof. Every regular function on \mathring{R}_β is a Laurent polynomial in \mathbf{x} . If $x_c = PQ$ is the product of two regular functions P and Q then both P and Q must be Laurent monomials in \mathbf{x} . By Lemma 9.5, one of the factors must be a Laurent monomial in only the frozen variables, and thus invertible. Therefore x_c is irreducible. \square

Lemma 9.7. *Every mutation \tilde{x}_c of a cluster variable x_c is the product of an irreducible element f_c in $\mathbb{C}[\mathring{R}_\beta]$ with a Laurent monomial in $x_d, d \neq c$.*

Proof. Let $P \in \mathbb{C}[\mathring{R}_\beta]$ be an irreducible factor of \tilde{x}_c . Restricting to T_c , the same argument as in the proof of Lemma 9.6 implies that P is a Laurent monomial in $\tilde{\mathbf{x}}_c$. Restricting to T , we see that P is a Laurent polynomial in \mathbf{x} . Substituting the exchange relation, we deduce that the exponent of \tilde{x}_c in P , as a Laurent polynomial in $\tilde{\mathbf{x}}_c$, must be nonnegative. We see that one of the irreducible factors of \tilde{x}_c is equal to \tilde{x}_c times a Laurent monomial in $x_d, d \neq c$ and the remaining irreducible factors are Laurent monomials in $x_d, d \neq c$. \square

Lemma 9.8. *The complement of*

$$T \cup \bigcup_{c \in J_\beta^{\text{mut}}} T_c$$

has codimension at least 2 in \mathring{R}_β .

Proof. Let g be a point in the complement. Then either $x_c(g) = x_d(g) = 0$ for distinct mutable indices c, d , or $f_c(g) = x_d(g) = 0$ for distinct mutable indices c, d . The codimension two statement follows from Lemmas 9.6 and 9.7. \square

9.7. Proof of Theorem 7.14. Since \mathring{R}_β contains $T \cup \bigcup_c T_c$, the coordinate ring $\mathbb{C}[\mathring{R}_\beta]$ is contained in the upper bound of Σ_β given by

$$\mathbb{C}[\mathbf{x}^{\pm 1}] \cap \bigcap_{c \in J_\beta^{\text{mut}}} \mathbb{C}[\tilde{\mathbf{x}}_c^{\pm 1}].$$

Since \mathring{R}_β is smooth and thus normal, Lemma 9.8 implies that this inclusion is an equality. By [BFZ05, Corollary 1.7] the upper bound is equal to the upper cluster algebra. By [Mul13] and Corollary 5.8, the upper cluster algebra is equal to the cluster algebra. \square

10. APPLICATIONS

10.1. Curious Lefschetz. Let X be a smooth, affine, complex algebraic variety of dimension d . Then the cohomology $H^*(X) = H^*(X, \mathbb{C})$ has a mixed Hodge structure, which gives a Deligne (weak) splitting $H^k(X) = \bigoplus_{p,q} H^{k,(p,q)}(X)$. We say that X is of *mixed Tate type* if $H^k(X) = \bigoplus_p H^{k,(p,p)}(X)$. We say that X satisfies the *curious Lefschetz property* if X is of mixed Tate type and there is a class $[\gamma] \in H^{2,(2,2)}(X)$ such that cup product induces isomorphisms

$$[\gamma]^{d-p} : H^{p+s,(p,p)}(X) \xrightarrow{\sim} H^{2d-p+s,(2d-p,2d-p)}(X)$$

for all p and s . Curious Lefschetz implies the *curious Poincaré symmetry*

$$\dim H^{p+s,(p,p)}(X) = \dim H^{2d-p+s,(2d-p,2d-p)}(X).$$

In [LS16] it is shown that a large class of cluster varieties satisfy curious Lefschetz, and the following result is a consequence.

Theorem 10.1. *Suppose that \tilde{Q} is an ice quiver that is sink-recurrent, full rank, and has an even number of vertices. Then the cluster variety $X(\tilde{Q})$ satisfies curious Lefschetz.*

The even-dimensional hypothesis is not a significant restriction since we can always add an extra isolated frozen vertex. See also [LS16, Theorem 8.3].

Proof. Let X be a smooth, affine complex algebraic variety, and $X = U \cup V$ be an open covering of X , and $[\gamma] \in H^{2,(2,2)}(X)$. By [LS16, Theorem 3.5], if all three $(U, [\gamma])$, $(V, [\gamma])$, $(U \cap V, [\gamma])$ satisfy curious Lefschetz then so does $(X, [\gamma])$.

By [LS16, Proposition 8.2], full rank isolated cluster varieties satisfy the curious Lefschetz property with respect to a (nearly canonical) *GSV form* $[\gamma]$; cf. [GSV10].

Let $X = \text{Spec } \mathcal{A}(\tilde{Q})$ be a sink-recurrent, full rank cluster variety and let $X_1 = \text{Spec } \mathcal{A}_1$ and $X_2 = \text{Spec } \mathcal{A}_2$ give an open cover of X , as in the proof of Proposition 5.5. Both X_1 and X_2 are sink-recurrent, and $X_1 \cap X_2$ is also a cluster localization with mutable quiver $Q - (N_s^{\text{in}}(Q) \cup \{s\})$, which is sink recurrent. Thus, by induction we may assume that $X_1, X_2, X_1 \cap X_2$ all satisfy curious Lefschetz with respect to (the respective restriction of) the GSV form $[\gamma]$ of X . Thus $(X, [\gamma])$ satisfies curious Lefschetz as well. \square

We do not know whether the Louise condition [LS16] is satisfied for the quivers in this work. The cohomology of open Richardson varieties are particularly interesting because of the relations to both Category \mathcal{O} and to knot homology [GL20]; see also [GHM21].

Corollary 10.2. *Even-dimensional braid Richardson varieties $\mathring{R}_{u,\beta}$ satisfy the curious Lefschetz property and thus the curious Poincaré symmetry. Odd-dimensional braid varieties satisfy the curious Poincaré symmetry.*

10.2. Braid Richardson links. By applying Remark 3.3 and the moves (B1)–(B4), we reduce to considering pairs $u \leq \beta$ such that β has only positive indices. Then we can consider a *braid Richardson link* $L_{u,\beta}$ obtained as the braid closure of $\beta \cdot \beta(u)^{-1}$, where β is viewed as a positive braid, and $\beta(u)$ is the positive braid lift of u . This construction generalizes the *Richardson links* of [GL20]. At the same time, a link L_G inside \mathbb{R}^3 can be constructed from a plabic graph G ; see [STWZ19, FPST22, GL22a]. The construction can be extended to give a link $L_{G_{u,\beta}}$ for our 3D plabic graphs $G_{u,\beta}$, using the following convention for bridges and for hollow crossings:



The construction in [GL22a, Section 4.1] can be extended to our setting to show that the braid Richardson link $L_{u,\beta}$ agrees with the plabic graph link $L_{G_{u,\beta}}$.

If we treat the strands of $L_{G_{u,\beta}}$ as the boundaries of ribbons, as suggested in the figure above, the convention for hollow crossings forces the ribbons to intersect in \mathbb{R}^3 . There is a natural way to alter the surface $\mathbf{S}_{u,\beta}$ locally at hollow crossings to obtain a Seifert surface $S(L_{u,\beta})$ for $L_{u,\beta}$. However, $\mathbf{S}_{u,\beta}$ and $S(L_{u,\beta})$ are different as abstract surfaces. Nevertheless, one can draw versions of the relative cycles $(C_c)_{c \in J_{u,\beta}}$ on $S(L_{u,\beta})$ rather than on $\mathbf{S}_{u,\beta}$, preserving their intersection numbers.

The surface $S(L_{u,\beta})$ has the “wrong” homology, so an alternative is to consider a different embedding $\mathbf{S}'_{u,\beta}$ of the surface $\mathbf{S}_{u,\beta}$ in \mathbb{R}^4 , defined so that there are no intersections of ribbons at hollow crossings. The surface $\mathbf{S}'_{u,\beta}$ is diffeomorphic to $\mathbf{S}_{u,\beta}$, but it will now have the “correct” link $L_{u,\beta}$ as its boundary in \mathbb{R}^3 .

10.3. Point count. Let Q be a mutable quiver. Following [GL22a], define the *point count rational function* $R(Q; q)$ to be the function $q \mapsto \#X(\tilde{Q})(\mathbb{F}_q)/(q-1)^a$ where \mathbb{F}_q denotes a

finite field with q elements and \tilde{Q} is a really full rank ice quiver with mutable part Q and a frozen vertices.

Suppose Q is sink-recurrent. Then the covering considered in the proof of Proposition 5.5 shows that $R(Q; q)$ is a rational function not depending on the choice of \tilde{Q} ; see [GL22a, Section 5.3]. We obtain the following variant of [GL22a, Conjecture 2.8].

Theorem 10.3. *Let $u \leq \beta$, and suppose that the 3D plabic graph $G_{u,\beta}$ has $c(G_{u,\beta})$ connected components. Then we have*

$$R(Q_{u,\beta}; q) = (q - 1)^{c(G_{u,\beta})-1} P^{\text{top}}(L_{u,\beta}; q),$$

where $P^{\text{top}}(L_{u,\beta}; q)$ is obtained from the top a -degree term of the HOMFLY polynomial $P(L_{u,\beta}; a, z)$ by substituting $a := q^{-\frac{1}{2}}$ and $z := q^{\frac{1}{2}} - q^{-\frac{1}{2}}$.

Proof. By Theorems 5.6 and 5.9 and our main result Theorem 7.14, it follows that $R(Q_{u,\beta}; q)$ is equal to $(q - 1)^{-a} \# \mathring{R}_{u,\beta}(\mathbb{F}_q)$, where a is the number of frozen variables in $\tilde{Q}_{u,\beta}$. A recursion for the point count of $\mathring{R}_{u,\beta}$ is given in [GLTW22, Section 5]. The comparison with the top a -degree term of the HOMFLY polynomial proceeds in the same way as the proof of [GL20, Theorem 2.1]. \square

The special case of Theorem 10.3 when β is a reduced word for some permutation $w \in S_n$ follows from our main results combined with [GL20, Theorem 1.11]. See [GL20, GL21, GL22a] for further details and examples.

REFERENCES

- [BFZ05] Arkady Berenstein, Sergey Fomin, and Andrei Zelevinsky. Cluster algebras. III. Upper bounds and double Bruhat cells. *Duke Math. J.*, 126(1):1–52, 2005.
- [BGY06] K. A. Brown, K. R. Goodearl, and M. Yakimov. Poisson structures on affine spaces and flag varieties. I. Matrix affine Poisson space. *Adv. Math.*, 206(2):567–629, 2006.
- [CGG⁺22] Roger Casals, Eugene Gorsky, Mikhail Gorsky, Ian Le, Linhui Shen, and José Simental. Cluster structures on braid varieties. [arXiv:2207.11607v1](https://arxiv.org/abs/2207.11607v1), 2022.
- [CGGS20] Roger Casals, Eugene Gorsky, Mikhail Gorsky, and José Simental. Algebraic Weaves and Braid Varieties. [arXiv:2012.06931v1](https://arxiv.org/abs/2012.06931v1), 2020.
- [CGGS21] Roger Casals, Eugene Gorsky, Mikhail Gorsky, and José Simental. Positroid Links and Braid varieties. [arXiv:2105.13948v1](https://arxiv.org/abs/2105.13948v1), 2021.
- [CK22] Peigen Cao and Bernhard Keller. On Leclerc’s conjectural cluster structures for open Richardson varieties. [arXiv:2207.10184v1](https://arxiv.org/abs/2207.10184v1), 2022.
- [CW22] Roger Casals and Daping Weng. Microlocal Theory of Legendrian Links and Cluster Algebras. [arXiv:2204.13244v2](https://arxiv.org/abs/2204.13244v2), 2022.
- [Deo85] Vinay V. Deodhar. On some geometric aspects of Bruhat orderings. I. A finer decomposition of Bruhat cells. *Invent. Math.*, 79(3):499–511, 1985.
- [FG06] Vladimir Fock and Alexander Goncharov. Moduli spaces of local systems and higher Teichmüller theory. *Publ. Math. Inst. Hautes Études Sci.*, (103):1–211, 2006.
- [FG09] Vladimir V. Fock and Alexander B. Goncharov. Cluster ensembles, quantization and the dilogarithm. *Ann. Sci. Éc. Norm. Supér. (4)*, 42(6):865–930, 2009.
- [FPST22] Sergey Fomin, Pavlo Pylyavskyy, Eugeni Shustin, and Dylan Thurston. Morsifications and mutations. *J. Lond. Math. Soc. (2)*, 105(4):2478–2554, 2022.
- [Fra16] Chris Fraser. Quasi-homomorphisms of cluster algebras. *Adv. in Appl. Math.*, 81:40–77, 2016.
- [FZ99] Sergey Fomin and Andrei Zelevinsky. Double Bruhat cells and total positivity. *J. Amer. Math. Soc.*, 12(2):335–380, 1999.
- [FZ02] Sergey Fomin and Andrei Zelevinsky. Cluster algebras. I. Foundations. *J. Amer. Math. Soc.*, 15(2):497–529 (electronic), 2002.

- [GHM21] Eugene Gorsky, Matthew Hogancamp, and Anton Mellit. Tautological classes and symmetry in Khovanov–Rozansky homology. [arXiv:2103.01212v1](https://arxiv.org/abs/2103.01212v1), 2021.
- [GK13] Alexander B. Goncharov and Richard Kenyon. Dimers and cluster integrable systems. *Ann. Sci. Éc. Norm. Supér. (4)*, 46(5):747–813, 2013.
- [GL19] Pavel Galashin and Thomas Lam. Positroid varieties and cluster algebras. *Ann. Sci. Éc. Norm. Supér.*, to appear. [arXiv:1906.03501v2](https://arxiv.org/abs/1906.03501v2), 2019.
- [GL20] Pavel Galashin and Thomas Lam. Positroids, knots, and q, t -Catalan numbers. [arXiv:2012.09745v2](https://arxiv.org/abs/2012.09745v2), 2020.
- [GL21] Pavel Galashin and Thomas Lam. Positroid Catalan numbers. [arXiv:2104.05701v1](https://arxiv.org/abs/2104.05701v1), 2021.
- [GL22a] Pavel Galashin and Thomas Lam. Plabic links, quivers, and skein relations. [arXiv:2208.01175v1](https://arxiv.org/abs/2208.01175v1), 2022.
- [GL22b] Pavel Galashin and Thomas Lam. The twist for Richardson varieties. [arXiv:2204.05935v1](https://arxiv.org/abs/2204.05935v1), 2022.
- [GLSBS] Pavel Galashin, Thomas Lam, Melissa Sherman-Bennett, and David Speyer. Braid variety cluster structures, II: general type. *In preparation*.
- [GLTW22] Pavel Galashin, Thomas Lam, Minh-Tam Quang Trinh, and Nathan Williams. Rational Non-crossing Coxeter-Catalan Combinatorics. [arXiv:2208.00121v1](https://arxiv.org/abs/2208.00121v1), 2022.
- [GSV10] Michael Gekhtman, Michael Shapiro, and Alek Vainshtein. *Cluster algebras and Poisson geometry*, volume 167 of *Mathematical Surveys and Monographs*. American Mathematical Society, Providence, RI, 2010.
- [GY20] K. R. Goodearl and M. T. Yakimov. The Berenstein–Zelevinsky quantum cluster algebra conjecture. *J. Eur. Math. Soc. (JEMS)*, 22(8):2453–2509, 2020.
- [Ing19] Grace Ingermanson. *Cluster Algebras of Open Richardson Varieties*. ProQuest LLC, Ann Arbor, MI, 2019. Thesis (Ph.D.)—University of Michigan.
- [Kar16] Rachel Karpman. Bridge graphs and Deodhar parametrizations for positroid varieties. *J. Combin. Theory Ser. A*, 142:113–146, 2016.
- [Kar17] Steven N. Karp. Sign variation, the Grassmannian, and total positivity. *J. Combin. Theory Ser. A*, 145:308–339, 2017.
- [KLS13] Allen Knutson, Thomas Lam, and David E. Speyer. Positroid varieties: juggling and geometry. *Compos. Math.*, 149(10):1710–1752, 2013.
- [Lec16] B. Leclerc. Cluster structures on strata of flag varieties. *Adv. Math.*, 300:190–228, 2016.
- [LS16] Thomas Lam and David E. Speyer. Cohomology of cluster varieties. I. Locally acyclic case. [arXiv:1604.06843v1](https://arxiv.org/abs/1604.06843v1), 2016.
- [Lus94] G. Lusztig. Total positivity in reductive groups. In *Lie theory and geometry*, volume 123 of *Progr. Math.*, pages 531–568. Birkhäuser Boston, Boston, MA, 1994.
- [Lus98] G. Lusztig. Total positivity in partial flag manifolds. *Represent. Theory*, 2:70–78, 1998.
- [Mel19] Anton Mellit. Cell decompositions of character varieties. [arXiv:1905.10685v1](https://arxiv.org/abs/1905.10685v1), 2019.
- [MR04] R. J. Marsh and K. Rietsch. Parametrizations of flag varieties. *Represent. Theory*, 8:212–242, 2004.
- [MS16] Greg Muller and David E. Speyer. Cluster algebras of Grassmannians are locally acyclic. *Proc. Amer. Math. Soc.*, 144(8):3267–3281, 2016.
- [Mul13] Greg Muller. Locally acyclic cluster algebras. *Adv. Math.*, 233:207–247, 2013.
- [Mul14] Greg Muller. $\mathcal{A} = \mathcal{U}$ for locally acyclic cluster algebras. *SIGMA Symmetry Integrability Geom. Methods Appl.*, 10:Paper 094, 8, 2014.
- [Mé22] Etienne Ménard. Cluster algebras associated with open Richardson varieties: an algorithm to compute initial seeds. [arXiv:2201.10292v1](https://arxiv.org/abs/2201.10292v1), 2022.
- [Pos06] Alexander Postnikov. Total positivity, Grassmannians, and networks. Preprint, <http://math.mit.edu/~apost/papers/tpgrass.pdf>, 2006.
- [Sco06] J. S. Scott. Grassmannians and cluster algebras. *Proc. London Math. Soc. (3)*, 92(2):345–380, 2006.
- [SSB] Khrystyna Serhiyenko and Melissa Sherman-Bennett. Leclerc’s conjecture on a cluster structure for type A Richardson varieties. *In preparation*.
- [SSBW19] K. Serhiyenko, M. Sherman-Bennett, and L. Williams. Cluster structures in Schubert varieties in the Grassmannian. *Proc. Lond. Math. Soc. (3)*, 119(6):1694–1744, 2019.

- [STWZ19] Vivek Shende, David Treumann, Harold Williams, and Eric Zaslow. Cluster varieties from Legendrian knots. *Duke Math. J.*, 168(15):2801–2871, 2019.
- [SW21] Linhui Shen and Daping Weng. Cluster structures on double Bott-Samelson cells. *Forum Math. Sigma*, 9:Paper No. e66, 89, 2021.
- [WY07] Ben Webster and Milen Yakimov. A Deodhar-type stratification on the double flag variety. *Transform. Groups*, 12(4):769–785, 2007.

DEPARTMENT OF MATHEMATICS, UNIVERSITY OF CALIFORNIA, LOS ANGELES, 520 PORTOLA PLAZA,
LOS ANGELES, CA 90025, USA

Email address: galashin@math.ucla.edu

DEPARTMENT OF MATHEMATICS, UNIVERSITY OF MICHIGAN, 2074 EAST HALL, 530 CHURCH STREET,
ANN ARBOR, MI 48109-1043, USA

Email address: tfylam@umich.edu

MASSACHUSETTS INSTITUTE OF TECHNOLOGY, 77 MASSACHUSETTS AVENUE, CAMBRIDGE, MA 02139

Email address: msherben@mit.edu

DEPARTMENT OF MATHEMATICS, UNIVERSITY OF MICHIGAN, 2844 EAST HALL, 530 CHURCH STREET,
ANN ARBOR, MI 48109-1043, USA

Email address: speyer@umich.edu